DRA/LANGLEY





# A DURABILITY STUDY OF PERICARDIAL BIOPROSTHESES

P. R. Schuster
Materials Science and Engineering Department
The Johns Hopkins University
Baltimore, MD 21218

TECHNICAL REPORT

NASA GRANT NAG 1-211

Ultrasonic and Optical Evaluation of Surgical Implant Materials and Devices

May 1984

Prepared for

National Aeronautics and Space Administration

Langley Research Center

Hampton, VA 23665

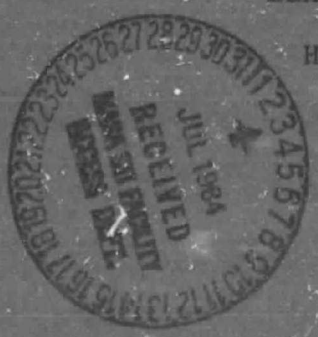

# A DURABILITY STUDY OF PERICARDIAL BIOPROSTHESES

P. R. Schuster
Materials Science and Engineering Department
The Johns Hopkins University
Baltimore, MD 21218

TECHNICAL REPORT

NASA GRANT NAG 1-211

Ultrasonic and Optical Evaluation of Surgical Implant Materials and Devices

May 1984

Prepared for

National Aeronautics and Space Administration

Langley Research Center

Hampton, VA 23665

## ABSTRACT

Bioprostheses have been in use since the early 1950's. However, it has been the different fixation and stabilization techniques for biological tissue that have increased the reliability of heart valve replacement surgery. The bioprostheses are preferred over the totally artificial valves because of certain very important advantages that are present. The bioprostheses are less thromboembolic, cause a lower incidence of hemolysis, and fail in a slow progressive manner.

This research project used both Laser Doppler Anemometry (L.D.A.) and accelerated fatigue testing in an attempt to assess the durability of certain bioprostheses. The L.D.A. system was made up of a number of different complex components, each with its own function fully described in the text. L.D.A., a non-invasive fluid flow measurement technique, was utilized to monitor the function of the cardiac valves over time. This was done through flow characterization in an aortic flow chamber, designed to closely simulate in vivo conditions, both in the near vicinity (sinuses of valsalva region) and also somewhat downstream (aortic region) from the valves. The flow characteristics were made up of various velocity profiles taken through the central plane of the channel after the required accelerated test intervals. The accelerated fatigue tester operated by opening and closing the valves at a rate of 1300 R.P.M., about 18x the normal rate. The accelerated tester continuously maintained physiologic conditions in terms of both the closing pressures and the environmental temperature.

The tri-leaflet Ionescu-Shiley Low Profile Mitral Valve and the tri-leaflet Carpentier-Edwards Low Profile Aortic Valve were chosen as the test valves for this study. Both are pericardial valves mounted on a flexible stent and chemically treated in a glutaraldehyde solution. The pericardial valves show an improved hemodynamic response and indicate a lower rate of thromboembolic complications in comparison with the porcine bioprostheses.

The results from the two test valves indicate a definite change in the flow characteristics downstream from the valve after certain accelerated test intervals. The high velocity cross-sectional flow area seems to increase over time in use, causing a decrease in the peak velocity. The tissue became more flaccid in certain areas, and tears were apparent at about 9.4 million cycles for the Ionescu-Shiley valve and at 24 million cycles for the Carpentier-Edwards valve. This corresponds to approximately 2 and 5 years of implantation for the Ionescu-Shiley and Carpentier-Edwards valves respectively.

Doppler Ultrasound is a technique currently used in vivo for the measurement of peak blood flow velocities in stenotic vessels. From the present research results, it appears that there would be a characteristic peak blood flow velocity change in the near vicinity of the bioprostheses due to fatigue of the valve, if calcification were not present. Therefore Doppler Ultrasound may become a feasible technique for monitoring the function of bioprostheses over time in vivo.

ACKNOWLEDGMENTS

The author wishes to thank Dr. Robert E. Green, Jr. and Mr. Edward P. Mueller for their continued support and guidance throughout this research project, Mr. Allen Fine for his assistance in the schematic drawing of the aortic chamber, Miss Kirsten Green for her excellent photography work, Dr. Ajit Yoganathan for his help in all areas, and last but not least my wife, Carol, for her continued support, understanding, and assistance in typing this manuscript.

This research was sponsored by the National Aeronautics and Space Administration, Langley Research Center, in providing support to the Bureau of Medical Devices of the Food and Drug Administration in evaluating the materials and devices used for surgical prostheses. A special note of thanks in this regard is due Dr. Joseph S. Heyman, Head, Materials Characterization Instrumentation Section, NASA Langley Research Center.

This report is based on the Master's Essay of Mr. Paul Robert Schuster accepted by The Johns Hopkins University in conformity with the requirements for the degree of Master of Science in Engineering.

TABLE OF CONTENTS


| | |
|---|---|
| ABSTRACT | ii |
| ACKNOWLEDGEMENTS | iv |
| TABLE OF ILLUSTRATIONS | vi |
| INTRODUCTION | 1 |
| EXPERIMENTAL SET UP | 10 |
| L.D.A. Theory | 10 |
| Signal Generation (Optical System) | 11 |
| Signal Processing (Electronic System) | 16 |
| Input Conditioner | 17 |
| Timer | 19 |
| Readout | 21 |
| Analog Output | 23 |
| Aortic Flow Chamber | 24 |
| Test Valves | 26 |
| EXPERIMENTAL PROCEDURES | 29 |
| L.D.A. Methods | 29 |
| Accelerated Testing | 34 |
| RESULTS AND DISCUSSION | 37 |
| CONCLUSIONS | 88 |
| BIBLIOGRAPHY | 90 |

TABLE OF ILLUSTRATIONS


| | | |
|---|---|---|
| Fig. 1. | The Laser Doppler Anemometry System (T.S.I. 9100 Series) | 12 |
| Fig. 2. | The Aortic Flow Chamber | 25 |
| Fig. 3. | Shelhigh Fatigue Test System #2 (Taken from Manual) | 35 |
| Fig. 4. | Valve Test Chamber for Fatigue Tester (Taken from Manual) | 36 |
| Fig. 5. | L.D.A. - 1.5" Upstream from Valve Location | 38 |
| Fig. 6. | L.D.A. - 0.75" Upstream from Valve Location | 38 |
| Fig. 7. | L.D.A. - Overlay Upstream from Valve Location | 39 |
| Fig. 8. | L.D.A. - 1)Sinus Region with no Valve Present | 40 |
| Fig. 9. | L.D.A. - 2)Sinus Region with no Valve Present | 40 |
| Fig. 10. | L.D.A. - Overlay Sinus Region with no Valve Present | 41 |
| Fig. 11. | L.D.A. - 1)Aortic Region with no Valve Present | 42 |
| Fig. 12. | L.D.A. - 2)Aortic Region with no Valve Present | 42 |
| Fig. 13. | L.D.A. - Overlay Aortic Region with no Valve Present | 43 |
| Fig. 14. | L.D.A. - 1)I-S prior to Accelerated Testing (Sinus) | 44 |
| Fig. 15. | L.D.A. - 2)I-S prior to Accelerated Testing (Sinus) | 44 |
| Fig. 16. | L.D.A. - 3)I-S prior to Accelerated Testing (Sinus) | 45 |
| Fig. 17. | L.D.A. - 1)I-S prior to Accelerated Testing (Aorta) | 45 |
| Fig. 18. | L.D.A. - 2)I-S prior to Accelerated Testing (Aorta) | 46 |
| Fig. 19a. | L.D.A. - Overlay I-S prior to Accelerated Testing (Sinus) | 47 |
| Fig. 19b. | L.D.A. - Overlay I-S prior to Accelerated Testing (Aorta) | 48 |

Fig. 20. L.D.A. - Sinus Region with and without Valve Present 49

Fig. 21. L.D.A. - 1)C-E prior to Accelerated Testing (Sinus) 51

Fig. 22. L.D.A. - 2)C-E prior to Accelerated Testing (Sinus) 51

Fig. 23. L.D.A. - 3)C-E prior to Accelerated Testing (Sinus) 52

Fig. 24. L.D.A. - 1)C-E prior to Accelerated Testing (Aorta) 53

Fig. 25. L.D.A. - 2)C-E prior to Accelerated Testing (Aorta) 53

Fig. 26. L.D.A. - Overlay C-E prior to Accelerated Testing (Sinus) 54

Fig. 27. L.D.A. - Overlay C-E prior to Accelerated Testing (Aorta) 55

Fig. 28. I-S Valve prior to Accelerated Testing (Inflow and Outflow Sides) 58

Fig. 29. C-E Valve prior to Accelerated Testing (Inflow and Outflow Sides) 58

Fig. 30. Closing Pressure on the I-S Valve at the Beginning of the First Accelerated Test Interval 59

Fig. 31. Closing Pressure on the C-E Valve at the Beginning of the First Accelerated Test Interval 59

Fig. 32. Closing Pressure on the I-S Valve at the End of the First Accelerated Test Interval 61

Fig. 33. Closing Pressure on the C-E Valve at the End of the First Accelerated Test Interval 61

Fig. 34. I-S Valve after the First Accelerated Test Interval (Inflow Side) 62

Fig. 35. I-S Valve after the First Accelerated Test Interval (Outflow Side) 62

Fig. 36. C-E Valve after the First Accelerated Test Interval (Inflow Side) 63

Fig. 37. C-E Valve after the First Accelerated Test Interval (Outflow Side) 63

Fig. 38. L.D.A. - 1)I-S after One Accelerated Test Interval (Sinus) 64

Fig. 39. L.D.A. - 2)I-S after One Accelerated Test Interval (Sinus) 64

Fig. 40. L.D.A. - 1)I-S after One Accelerated Test Interval (Aorta) 65

Fig. 41. L.D.A. - 2)I-S after One Accelerated Test Interval (Aorta) 65

Fig. 42. L.D.A. - Overlay I-S after One Accelerated Test Interval (Sinus) 66

Fig. 43. L.D.A. - Overlay I-S after One Accelerated Test Interval (Aorta) 67

Fig. 44. L.D.A. - 1)C-E after One Accelerated Test Interval (Sinus) 69

Fig. 45. L.D.A. - 2)C-E after One Accelerated Test Interval (Sinus) 69

Fig. 46. L.D.A. - 1)C-E after One Accelerated Test Interval (Aorta) 70

Fig. 47. L.D.A. - 2)C-E after One Accelerated Test Interval (Aorta) 70

Fig. 48. L.D.A. - Overlay C-E after One Accelerated Test Interval (Sinus) 71

Fig. 49. L.D.A. - Overlay C-E after One Accelerated Test Interval (Aorta) 72

Fig. 50. Closing Pressure on the C-E Valve at the Beginning of the Second Accelerated Test Interval 74

Fig. 51. Closing Pressure on the C-E Valve at the Beginning of the Second Accelerated Test Interval 74

Fig. 52. Closing Pressure on the C-E Valve at the Beginning of the Second Accelerated Test Interval 75

Fig. 53. Closing Pressure on the C-E Valve at the End of the Second Accelerated Test Interval 75

Fig. 54. C-E Valve after the Second Accelerated Test Interval (Inflow Side) 77

Fig. 55. C-E Valve After the Second Accelerated Test Interval (Outflow Side) 77

Fig. 56. Schematic Drawing of the Initial Failure of the C-E Valve (1A) and Predicted Complete Rupture (1B); (S. Gabbay, et al., J. Thorac. Cardiovasc. Surg., In Press) 77

fig. 57. L.D.A. - 1)C-E after Two Accelerated Test Intervals (Sinus) 78

Fig. 58. L.D.A. - 2)C-E after Two Accelerated Test Intervals (Sinus) 78

Fig. 59. L.D.A. - 1)C-E after Two Accelerated Test Intervals (Aorta) 79

Fig. 60. L.D.A. - 2)C-E after Two Accelerated Test Intervals (Aorta) 79

Fig. 61. L.D.A. - Overlay C-E after Two Accelerated Test Intervals (Sinus) 80

Fig. 62. L.D.A. - Overlay C-E after Two Accelerated Test Intervals (Aorta) 81

Fig. 63. L.D.A. - Composite I-S at Various Accelerated Test Intervals (Sinus) 82

Fig. 64. L.D.A. - Composite I-S at Various Accelerated Test Intervals (Aorta) 83

Fig. 65. L.D.A. - Composite C-E at various Accelerated Test Intervals (Sinus) 84

Fig. 66. L.D.A. - Composite C-E at various Accelerated Test Intervals (Aorta) 85

# INTRODUCTION

The history of prosthetic heart valves began primarily in the early 1950's. Bioprostheses, which are those prosthetic devices that are mainly composed of biological tissue, were successfully implanted by Lem, Aram, and Munnell in the descending thoracic aorta of dogs in 1952.[1] These valves were actually fresh aortic valves taken from human cadavers. At around the same time Hufnagel and Campbell independently developed the ball and cage artificial mechanical valve.[2,3] Interestingly enough, this design was most likely taken from the ball and cage bottle stopper which was invented and patented by J. B. Williams in 1858.[4] These mechanical valves were also implanted into the descending thoracic aorta of dogs to correct for aortic valve incompetence.[2,3,5]

As technology progressed different designs for prosthestic heart valves began to appear and also different materials became applicable. In terms of bioprostheses, interest began to develop in heterografts or animal grafts. One reason for this was the work of Dr. Alain Carpentier in France. French regulations did not permit the removal from a cadaver of any tissue within the first 48 hours of death. At that point the cardiac valves were infected and therefore useless.[6] Hence Dr. Carpentier decided to study animal tissue for use in bioprostheses. After intense research it was found that the porcine or pig's heart most closely matched the size of the human heart.[6] Therefore the porcine valves themselves could be used directly as valve implants. Initially direct

valve transplants were attempted with little success; then the stent was invented onto which the valves could be mounted. This improvement increased the success rate for valve replacement drastically.[7,8] Also a number of different tissues were investigated for use as cardiac valves: pericardium, aortic wall, veins, fascia lata, and dura mater; the pericardial valves being the most successful.[6,9,10]

Preparation and fixation methods for the biological tissue also improved over time. Initially after valve replacement host response was desired; it was thought that the host cells would grow and regenerate the valve.[11,12] Either a buffered mercurial solution or formalin solution was used for preservation in the mid 1960's. However, for long term durability these methods proved ineffective. Regeneration by host cells did not occur, in fact these cells were harmful to the tissue. Thus the tissue had to be chemically treated to protect it from cellular attack and prevent collagen degeneration.[6] The number of cross linkages between collagen molecules has been found to be an excellent indication of the stability of the tissue. Mechanically the cross linking decreases the compliance of the tissue structure where relative movement between fibers takes place.[13,14] Different chemical treatments were tested to either introduce cross linkages or to reinforce the existing ones. Of those tested, glutaraldehyde proved to be the best for increasing stability and decreasing host cellular response.[6,13-15] It was at this point in the late

1960's that the term bioprostheses came into use, in order to differentiate between a non treated graft and the glutaraldehyde fixed tissue.[7,12,16]

The stent, which was mentioned earlier, was developed with the idea in mind that the bioprostheses could be standardized, while alleviating certain failure modes.[17] Another major factor in the invention of the stent was the realization that with the valve mounted on a more rigid structure a fairly complete pre-operative analysis of the valve function could be accomplished. Initially the stent was designed with a circular shape, but this proved to be inappropriate. The stent must conform to the shape of the valve, so as not to inhibit its operation.[18] Also there is a musculature problem with animal valves in comparison with human valves. In animals, the interventricular wall extends to the base of the right coronary cusp, in essence supporting the cusp. If this support were to be cut it could lead to weakening and finally early failure of the valve.[6,9,18] Therefore the stent had to take on some asymmetrical configuration.

Prosthetic valves, whether primarily made up of biological materials or whether totally artificial, must meet certain criteria for their applicability in vivo. Dwight E. Harken in 1962, who had established the first intensive care unit at Peter Bent Brigham Hospital in 1950-51 and also helped to develop the ball and cage valve in 1960, stated that the criteria which must be meet for desirable prosthetic heart

valves are as follows: 1) The valve must have lasting physical and geometric features and be capable of permanent fixation in the normal anatomic state. 2) The valve should be chemically inert, nonthrombogenic, and harmless to blood elements and must not annoy the patient. 3) The valve must open and close promptly during the appropriate phase of the cardiac cycle and should offer no resistance to the physiologic flows.[19] A more recent version of the required criteria reads as follows: 1) a necessity for proven structural durability over a period of ten to twenty years, readily available and ease of surgical implantation, 2) absence of host reactivity harmful to valve function, nonthrombogenicity without the use of anticoagulants, and resistance to infective endocarditis, and 3) central flow orifice without transvalvular gradient.[20]

Mechanical or totally artificial valves were mentioned previously in this paper, but will not be a major topic. This research project, which will be discussed later, dealt only with biological valves for a few different reasons. One reason is that there are a number of critical advantages that biological valves have over artificial ones. These advantages allow the bioprostheses to adhere more closely to the required criteria. The most important of these advantages are the following: 1) The chances for thromboembolic complications are much lower, which means usually no long term anticoagulation therapy is necessary. 2) The more central flow better simulates the natural valves, leading to an improved hemodynamic

response when jetting does not occur. 3) Hemolysis or the damage to blood cells is reduced. 4) Failure usually progresses slowly, thereby reducing the risk of sudden death and allowing the time necessary to make corrections.[6,21]

Historically, prosthetic heart valves have been tested to obtain information on flow patterns created by the valves, on their resistance to fatigue failure, and on the thrombogenicity of the materials used in the prostheses.[22] These are three areas of primary importance when estimating effectiveness of prosthetic valves. In terms of biological valves, it is known that due to the glutaraldehyde fixation treatment the tissue is stabilized, therefore it should not degrade biologically. In fact, the tissue is encapsulated in the body immediately after implantation with a fibrous coating.[11,13] Thus with respect to thrombogenicity, the bioprostheses perform very well; the incidence of thrombosis is extremely low. So the durability of the tissue in bioprostheses is mainly a function of its capacity to withstand millions upon millions of repeated mechanical loading events.[23] The loading events are the opening and closing of the valve, due to the existing pressure gradients, for regulation of blood flow. The flow characteristics immediately downstream from the valve indicate the degree of competence of the valve itself.

This research project dealt with a combination of the fatigue properties and the flow characteristics of bioprostheses. The response of the biological tissue, in these

valves, to fatigue or cyclic loading was measured by its hydrodynamic performance. In essence, a research project was done, which combined accelerated testing and flow characterization, using Laser Doppler Anemometry, as a means of assessing the durability of bioprostheses. Separate studies have been done on accelerated testing of bioprostheses and also on valve flow characterization, however there has never been a correlation between the two. It seems likely that much pertinent information would be obtained through this combined study, since the two areas of study are of critical importance and have a definite relationship to one another. If it is actually possible to monitor the flow characteristics of a replacement valve over its lifespan, one may gain a better understanding of the failure modes that occur in vivo.

Many accelerated tests have been performed on bioprostheses with the results being somewhat difficult to interpret. The relationship between in vitro accelerated testing and in vivo clinical studies is somewhat undefined at this point.[11,24] The durability or lifespan of these bioprostheses for in vitro accelerated testing seems to be less, in terms of the number of working cycles, then what is usually found in vivo, but the failure modes and the failure locations are identical in both cases.[11,14,24-26] Accelerated testing is exactly what it sounds like. Prosthetic valves are placed in a tester which forces the opening and closing of the valve at rates much greater than those possible in the body. The average resting

adult has a heart rate of 72 beats per minute, so the heart beats approximately between 35 and 40 million times a year.[27] Most accelerated testers are frequency adjustable and have a range of between 600 and 2500 cycles per minute (beats/minute). In essence, the valves in the accelerated tester can be operated at between 9 and 35 times their normal rate. This allowed the mechanical loading of the prosthesis a great number of times in a very short duration, so as to simulate a long period of time in the body with a short period of time in the accelerated tester.[28] When using an accelerated tester, it must be keep in mind that even though the pressure differential across the valve during the closed phase can be adjusted to within the physiologic range, dynamic loads in the tissue may still be significantly different then those normally found in the body.[14,23,24,26] The important point that is of interest, is not a one to one correspondence between the failure time in accelerated testing with the failure time in clinical studies, but is the response of bioprostheses to repeated cyclic loading in terms of hemo- and hydrodynamics. This is in order to assess the direct effects that fatigue has on the function of the prosthetic valve, which is the regulation of blood flow in a manner that closely simulates the operation of the natural valve.

Laser Doppler Anemometry (L.D.A.) is an excellent technique for making a quantitative analysis of the flow characteristics of prosthetic heart valves. The L.D.A. system was the major tool used in this research project, hence it will be described

in great detail. This type of system has been used previously for determining flow characteristics downstream from prosthetic heart valves.[29,30] Dr. Ajit Yoganathan has done the most work in this field, and would definitely be considered the expert. He has been a tremendous help in previous studies utilizing the L.D.A. In looking through the literature, it becomes quite evident that almost all of this L.D.A. research has been done on artificial or mechanical valves; very few cases of L.D.A. flow characterization of a bioprosthesis have been performed.[31] The bioprostheses for the most part have a much more simplified flow profile indicative of their close simulation to the natural valve. The cusps open outward allowing for a more central flow with minimal resistance. This is in contrast to almost every type of mechanical valve. The mechanical valves such as the ball and cage, the tilting disk, the bi-leaflet, etc., all have an obstruction (an occluder) that the fluid must flow around. This naturally causes a deviation from the central flow profile, and also introduces a number of other problems, including stagnation zones, flow reversals, jetting, and excessive shear forces on endothelial cells due to high velocity flows near the wall.[29,32,33] There is, however, one type of mechanical valve that is still under investigation, which has been modeled after the natural valve, and thus has a large central flow orifice. This mechanical prosthetic heart valve is the trileaflet polyurethane.[34] To assure quality in the flow characteristics, L.D.A. can be used for the determination of velocity profiles both in

the immediate vicinity and also somewhat downstream of any type of prosthetic heart valve.

# EXPERIMENTAL SET UP

## L.D.A. Theory

Laser Doppler Anemometry is a non-invasive fluid flow measurement technique. The actual measurements taken are velocity measurements on particulate matter contained within the test fluid. If done correctly these velocity measurements can be directly correlated to the fluid velocity itself, in order to obtain flow characteristics.

The signal necessary for data acquisition is obtained through use of a high intensity coherent light source (laser), which is optically manipulated to produce a pattern of parallel fringes within an ellipsoidal shaped measuring volume. This probe volume is produced as a result of the intersection of two coherent laser beams. The laser beams have a Gaussian intensity distribution based on $e^{-2}$ intensity points of the beams. A beam that is Gaussian, has the characteristic of being a plane wave at its waist (cross section of minimum diameter), but everywhere else the beam is converging or diverging.[35,36] The waist is also called the Rayleigh range and is considered the region of maximum beam convergence. The intersection of the two beams occurs within the Rayleigh range of each beam, and this produces a parallel fringe pattern at the cross over region. These fringes appear due to the interference of the planar wavefronts of the two coherent beams. The planar wavefronts are the alternating electric fields of each beam, which constructively and destructively interfere.[35] It is known that the intensity of the radiation is proportional to the square of the amplitude of the

alternating electric field, therefore at regions of constructive interference a bright fringe is produced and at regions of destructive interference a dark fringe is produced. As particles in the fluid cross the fringes by passing through the probe volume, they scatter light which is picked up by a stationary receiving optics and photodetector system. The frequency of the scattered light is Doppler shifted proportional to the velocity of the particles which are flowing through the probe volume.[37] Natural particles contained within the fluid are often adequate seed for obtaining usable signals. However, artificial spherical seed particles can improve the signal to noise ratio immensely, when used correctly. If artificial particles are used three basic guidelines should be followed for accurate measurements: 1) The particles should have minimal drag; that is they should follow the flow without lagging behind, to give an accurate representation of the actual fluid velocity; 2) The particles must scatter a sufficient quantity of light to produce measureable signals, and 3) Particle concentration should be high enough for somewhat continous signal, but not too high as to flood the signal processor thereby reducing the accuracy of one's results.[35-37]

## Signal Generation (Optical System)

The L.D.A. system which was used in this research project is a rather complex one (Fig. 1). Its many components will be explained somewhat extensively. First, there is a Helium-Neon

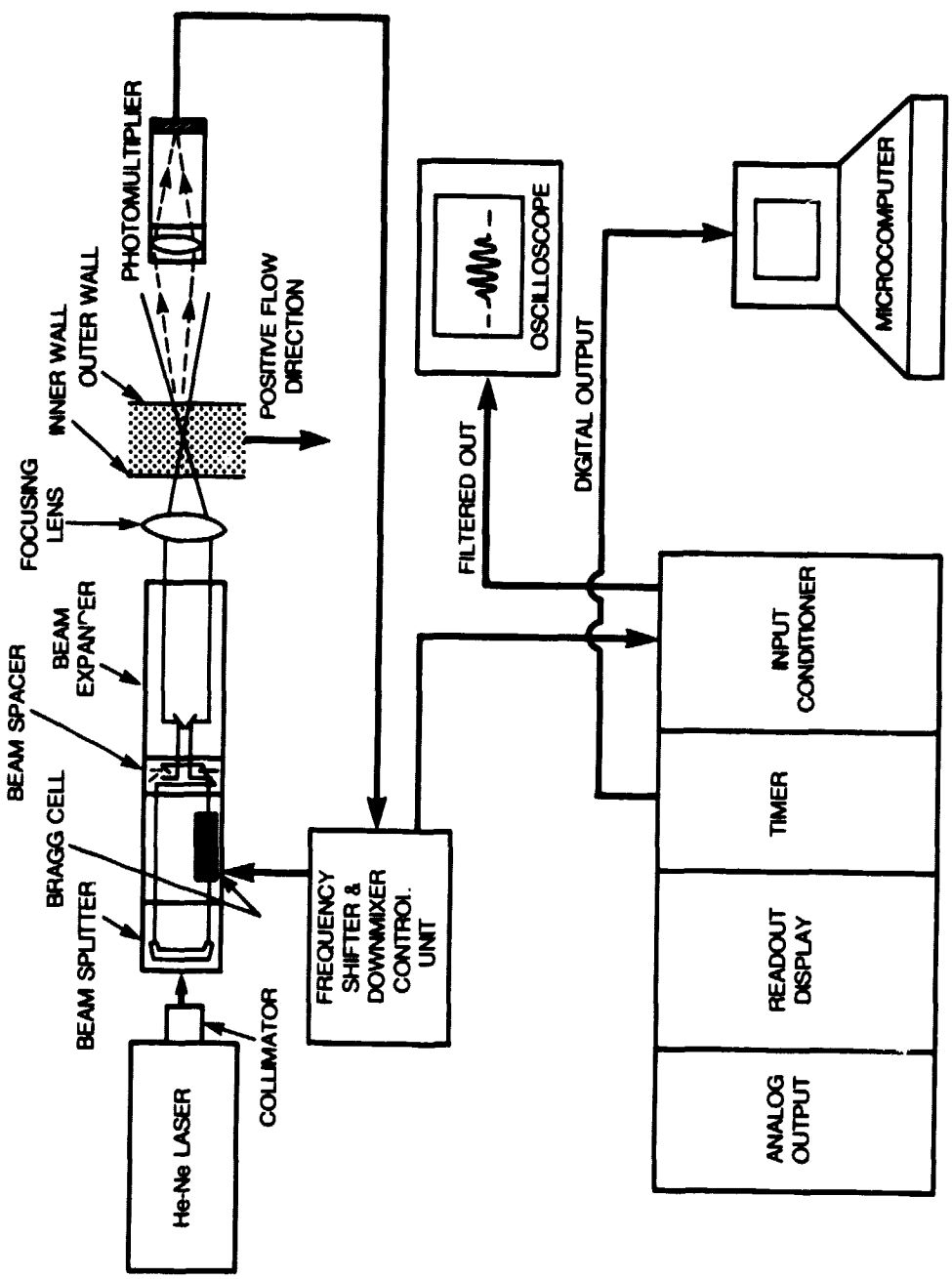


FIG. 1. THE LASER DOPPLER ANEMOMETRY SYSTEM (T.S.I. 9100 SERIES).

laser which produces intense monochromatic light, power rated at 15 milliwatts. The beam exiting the laser is collimated to control beam divergence, which in turn assures that after the beam is split the intersection point of the two focused gaussian beams will be at the waist of both beams. Intersection at the waist guarantees parallel fringes within the probe volume, thereby enhancing overall signal quality and the signal to noise ratio.[35-37]

The collimated beam is then split into two beams of equal intensity. The two beams are parallel and leave the beamsplitter 50 mm apart, both 25 mm from the position of the incident beam or optical axis. The plane of polarity of the two exiting beams is perpendicular to the plane of polarity of the incident beam. The reason for this is that the plane of polarization dictates the direction of propagation of the alternating electric fields for each beam. To obtain good fringe contrast and desirable fringe placement, it is necessary that the polarization planes of the exiting beams be in the horizontal plane. This insures that the propagating electric fields will have maximum interference, both constructively and destructively, at their intersection point further down the optical axis.[36] This also guarantees that the fringes will be positioned such that they are perpendicular to the mean flow direction, which is desirable in this case.

As one continues down the optical axis, the next component is the Bragg cell, which is driven by a frequency shifter power

supply and downmixer. The Bragg cell uses the interaction of one of the laser beams and high frequency ultrasound in a glass medium to shift the frequency of that beam.[35] The other beam is allowed to pass with no interaction or frequency change. The downmixer has an effective frequency shift range of 2 KHz to 10 MHz in a 1, 2, 5 sequence. The Bragg cell automatically causes an effective 40 MHz frequency shift which the downmixer reduces before the signal is sent on to be analyzed. The Bragg cell is a very useful component due to its many applications, which include correction for directional ambiguity, removal of pedestal frequency or D.C. component of the signal, optimization of signal frequency range for effective use of the signal processor, and many others.[35-36] In essence, through frequency shifting one of the laser beams relative to the other, the fringe pattern created within the probe volume is given a specific velocity of its own proportional to the shift frequency. This reduces the problem of directional ambiguity by causing the detected Doppler signals to differ, not only when the magnitude of the velocity of the particles going through the probe volume differs, but also when the direction of the particles going through the probe volume changes. For most applications, the pedestal (low frequency D.C. component of intensity variation) removal is accomplished by a high pass filter built into the downmix circuit. Also the input conditioner in the signal processor has its own effective frequency ranges in which analyzation of signal is most efficient and accurate. The

Doppler signal can be appointed a frequency within one of these effective ranges through the use of both the Bragg cell and the downmixer.

When making on-axis backscatter measurements, the receiving optics and photomultiplier system are the next components in line. If however work is being done in the forwardscatter mode, then the beam spacer and expander immediately follow the Bragg cell, and the receiving optics and photomultiplier system, including a collecting lens, are placed on the other side of the test fixture. The receiving assembly is comprised of a lens and mirror system which focuses the signal from the collecting lens onto the photodetector aperture. The photomultiplier detects the light signals and sends the information obtained, in the form of analog signals, to the signal processor to be analyzed.

Optimization of the probe volume is accomplished by adjustment o ..e beam spacing. At this point both beams are parallel and spaced 50 mm apart with one beam frequency shifted relative to the other. In order to minimize the probe volume, thus enabling measurements in very small flow regions and maximizing the resolution, it is necessary to expand the beam. However, the maximum allowable beam spacing for the beam expander entrance is 35 mm or less. Therefore a beam spacer is used. The beam spacer reduces the spacing from 50 mm to 13 mm. This reduction to 13 mm allows the use of a smaller transmitting lens along with the beam expander. After the beams have been spaced down to 13 mm, they enter the beam expander, which expands both the beam

spacing and the beam diameter by 3.75x. This expansion allows the focusing (transmitting) lens to focus the beams down to a reduced intersection point, which yields a smaller probe volume diameter and probe volume length. This greatly increases the accuracy and efficiency of the whole system and improves the signal to noise ratio.

If the system is correctly aligned, then there will exist a perfect intersection of the two laser beams at their waists. As mentioned earlier, this intersection region is called the probe volume or measuring volume and has an ellipsoidal shape. The probe volume will contain within it, a pattern of parallel fringes through which the fluid will flow and measurements will be taken.

## Signal Processing (Electronic System)

Now that the optical set up is complete, and particles within the fluid are passing through the probe volume, light signals begin to be picked up by the photodetector. At this point it is necessary to analyze the information obtained by the photodetector, which is now in the form of analog signals. A signal processor is used to receive this information from the photodetector and to make the decision either to accept the signal and analyze it, or reject it. The signal processor consists of four modularized electronic functions. The modules are the following: the input conditioner, the timer, the readout, and the analog output.

Input Conditioner:

The input conditioner allows one to set certain criteria which must be met for acceptance of a signal. When a signal is accepted, it is converted into the form of two intervals which are quantified by the timer. One interval is a representation of the time necessary for a specific number of Doppler cycles to be produced by a particle passing through the light and dark fringes; the second interval represents the time taken for half that number of Doppler cycles to be generated, within that same burst. This second interval is used to eliminate poor signals, and will be explained later when discussing the timer. The input conditioner contains a high and a low pass filter, which filters out a large percentage of noise collected by the photodetector, while allowing the signal to pass through. To further facilitate signal to noise improvement a Schmitt trigger circuit is included in the input conditioner. The Schmitt trigger threshold level of 50 mV or 100 mV peak to peak must be exceeded for signals to be sent ahead for analyzation. If the threshold is not exceeded, there will be no signal sent on to the timer. This is the purpose of the adjustable gain and amplifier in the input conditioner. The signal processor will accept signal amplitudes of 10 mV to 2 V peak to peak. If a signal comes in with too large an amplitude, a red indicator light on the panel illuminates; if the signal is below the Schmitt trigger threshold then no indicator light will come on and the gain can be set accordingly. The gain should be set such that a green indicator light just

comes on or flickers on and off. This means that the signal is exceeding the Schmitt trigger threshold without saturating it. Sufficient time must be allowed between each signal for analyzation and signal processing to be done accurately. The filtered signal which goes to the Schmitt trigger is available at the filtered analog output jack on the input conditioner front panel. Broad band noise levels at this output must be kept below 50 mV, so as not to exceed the Schmitt trigger threshold. If the noise level is too great, then the signal processor will be inhibited and will provide inaccurate results. The next criteria which must be met is the minimum cycles per burst setting. The minimum cycles per burst mode is indicated on the front panel of the input conditioner by the white numerals which vary from 1 to 5. The red numerals, which immediately follow the white ones, indicate that the total burst mode is in operation. These are the two modes which dictate the length of the interval to be timed. In the minimum cycles per burst mode an incoming signal must contain at least an equal number of cycles in comparison to that which is set; but only the set number of cycles will be quantified by the timer. However, in the total burst mode even when the minimum number of cycles is exceeded, the whole interval is quantified by the timer. When using the Apple microcomputer interface for automated data collection, one must work in the minimum cycles per burst mode. The software package for the microcomputer requires one to set the number of cycles contained in each signal burst which are to be quantified by the timer.

The Apple receives this information in digital form from the timer, but it can not differentiate the total number of cycles in each burst that were quantified. The cycle settings vary from $2^1$ or 2 up to $2^5$ or 32. Depending on the number of fringes in the probe volume and the frequency shift used, one can be very selective as to what signals will be accepted, through the use of the minimum cycles per burst criteria. Finally, there is an added amplitude limiter on the input conditioner which is rarely used. If the fluid contains very large particles whose erroneous signal cannot be filtered out, then the amplitude limit comes into play. It sets the maximum D.C. component amplitude that will be accepted. This is sufficient since larger particles generally give a higher amplitude D.C. component then do smaller particles.

Timer:

The function of the timer is obviously to measure the intervals generated by the input conditioner. The timer is made up of a high speed clock with 2 nanosecond resolution. The leading edge of an interval gates the clock into a counter, and the trailing edge turns the counter off. The size of the interval is therefore recorded in the counter for the set number of cycles on the input conditioner. The timer also makes a measurement on the size of the interval for half the set number of cycles in that same signal burst. This allows a comparison to be made on the cycle times between the two intervals. The signal will be

rejected, if symmetry or accuracy of the burst is off by an amount greater than that comparison percentage which one sets on the timer module. The compared cycle times should be very close for a good symmetrical signal, assuming the probe volume has, as it should, a symmetrical fringe pattern. If noise is disrupting the signal, but the signal has been able to pass through the input conditioner criteria, this comparison analysis will cause it to be rejected. Usually the only problem with signals that reach this comparison point is something called shot noise. Shot noise is the result of more than one particle passing through the probe volume at the same instant. Because of the constructive and destructive interference of the scattered light given off by each particle, the final signal received by the photodetector, and therefore the signal processor, is asymmetrical and thereby erroneous. This is one reason why particle concentration is of importance. The readout provisions in the timer module include a 12 bit digital output with a 4 bit exponent. There are two modes in which the exponent can be used (manual or auto-range). In the manual mode the exponent setting fixes a timing range, no matter what the actual timer measurement is. If the timer measurement exceeds the fixed range of the set exponent, then a red indicator overrange light will appear, and the signal information will be discarded. Also if the actual timer measurement is too small in comparison with the fixed range, then the timer output will be very close to zero, and therefore neither accurate nor useful. In the auto-range mode, the range will automatically fix

itself for times smaller than the exponent set. Again, if the timer measurement exceeds the limit that can be auto-ranged due to the exponent setting, the red overrange light will appear and the data will be foregone. In essence a digital filter, to filter excessive interval times, is produced. Also present on the timer panel are a data ready output jack, a monitor output jack, and a digital output 37 pin plug-in data connector. Whenever a Doppler burst is accepted, a 0.61 microsecond pulse is generated at the data ready jack output and is on the data ready line which is a part of the digital output. The data rate results from the counting of these pulses by a frequency counter, or in this case the readout module. The monitor output jack gives an analog version of the upper 10 bits of the 12 bit mantissa, in other words an analog voltage proportional to the interval time is given off. Finally, the digital output connector is used for interfacing the signal processor with a computer containing the appropriate hardware and software packages.

Readout:

The readout module is next in line. Here the display of the analog voltage proportional to the interval time or proportional to the Doppler frequency is given, depending on where the signal is generated. The analog signal can be obtained from the timer module and is equivalent to the signal generated at the monitor output jack. The timer module and readout module are internally wired for this. However, a more accurate signal can be obtained

externally, using the analog output module. As stated earlier, the signal produced at the monitor output jack is an analog version of the upper 10 bits of the 12 bit mantissa, but the signal provided by both output jacks on the analog output panel is an analog version of the whole 12 bit mantissa, thereby an improvement on the accuracy of ones results is obtained. The display of the analog signal is done through a digital voltmeter with the heading "OUTPUT (volts)". Also the time constant can be set from the three choices available. This output display can even be converted to read direct frequencies and velocities by the appropriate calibration factor. The data rate display, as stated earlier, operates as a frequency counter and records the data ready pulses from the timer module through internal wiring. Also there exists different resolution settings, and underneath that, there are available two input jacks which allow for external signals to be displayed. If an external signal source is used, then obviously the switch above the jack must be set to external, and if signals used are taken from the timer module and are therefore internally wired, the switch must be set to internal. The voltage input used to receive a signal from an external analog voltage source can be hooked up to either of the two outputs on the analog output module for increased accuracy. The input for the external data ready source is generally not used, but can be an effective tool if more than one frequency counter or pulse rate accumulator is employed.

Analog Output:

The last module in the signal processor cabinet is the analog output module, which has already been discussed somewhat in the previous paragraph. One output jack gives an accurate analog voltage signal proportional to the time required for the specific number of Doppler cycles (minimum cycles per burst mode), while the other output jack gives an accurate analog voltage proportional to the Doppler frequency, by inverting the analog time signal. The accuracy for the Doppler frequency can then be maximized by setting the frequency range through use of either the 10:1 or 100:1 setting, which ever appropriately encompasses the pertinent frequencies.

## The Aortic Flow Chamber

The aortic flow chamber (Fig. 2), which was used in the L.D.A. section of this study, was primarily designed by Dr. Ajit Yoganathan of the Georgia Institute of Technology. Permission was received from Dr. Yoganathan, who is considered an expert in the field of L.D.A. used for flow characterization of replacement heart valves, to take his design and improve on it when building the aortic chamber for this project. The chamber is made up of two parts, the inflow section which extends up until the valve housing, and the outflow section which begins at the valve housing and continues into the sinuses of valsalva and out to the aorta. The inflow section has an entry region that extends 6" in length and is made out of 1" (25.4 mm) internal diameter plastic tube. The entry region allows for the flow to fully develop prior to coming in contact with the valve. The [33] outflow tract from the left ventricle into the aorta is next. It is a 1" in diameter hole bored out of a 2"x 2.5"x 2.5" solid piece of plexiglas. One outflow section consists of the sinuses which measures approximately 1 and 3/8 inches in length. This area corresponds to a bulbous region at the root of the aorta into which the leaflets or cusps of the aortic valve fall back when the valve is completely open, allowing uninterrupted blood flow. The first 0.75" of the sinuses is a hole of 1.25" diameter bored out of a 8"x 2.5"x 2.5" solid piece of plexiglas. This region then tapers down into the 1" in diameter aorta. These dimensions were utilized in an effort to simulate in vivo condi-

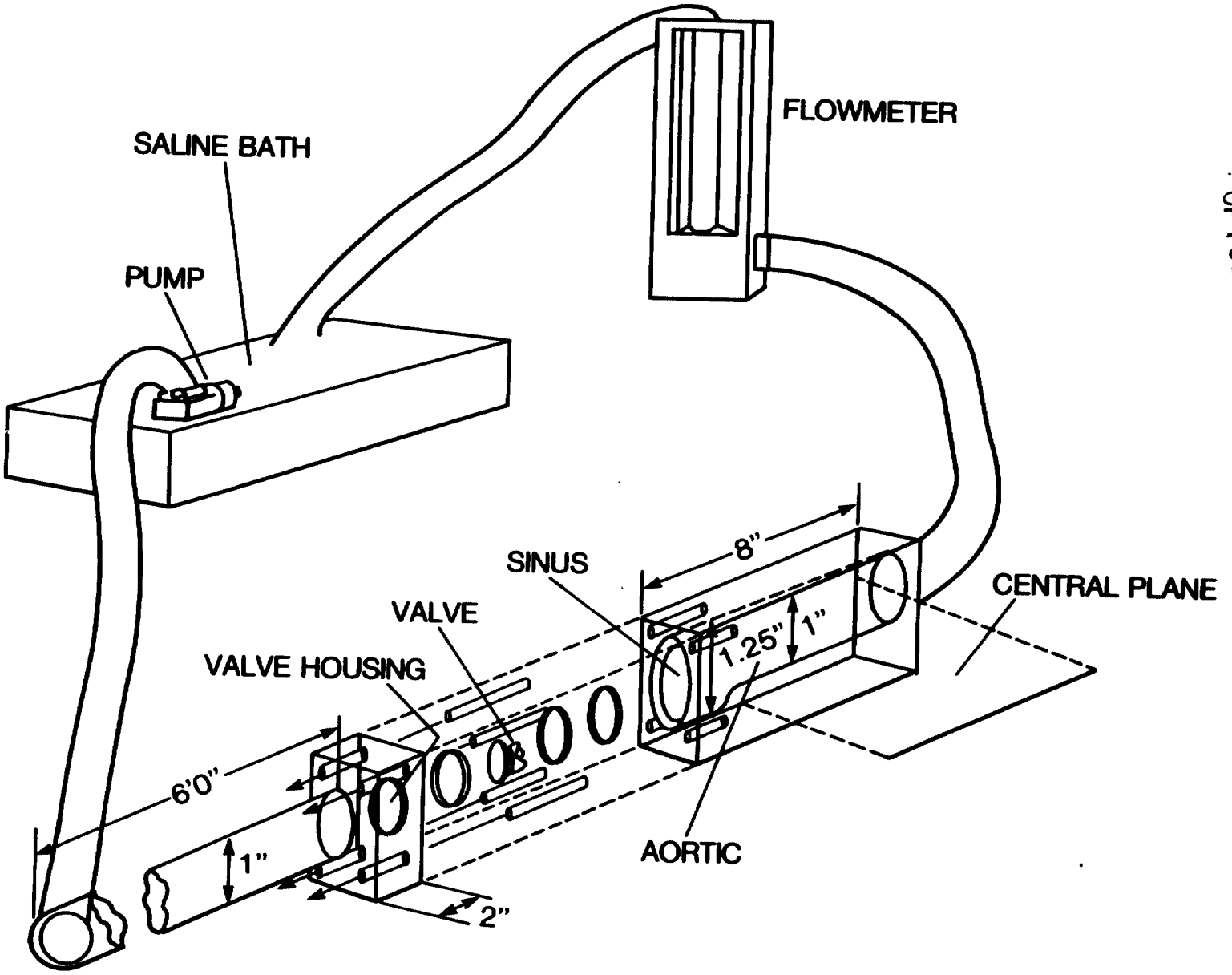


FIG. 2. THE AORTIC FLOW CHAMBER

tions and were obtained through autopsy reports and fluoroscopic movies made of patients with bioprostheses by Dr. Yoganathan.[33] The inflow entry region is connected to a Little Giant pump set in a 0.86% NaCl saline bath with an output of 25 l/min steady flow rate. This flow rate corresponds to the peak systolic flow at cardiac outputs of about 4.5 to 5 l/min.[29,32,33,38] In other words, the worst conditions that the valve would be subjected to in the heart of a normal human being at rest (not exerting oneself physically) were addressed.[39] The outflow portion is connected to a flowmeter (Brooks Instruments 1110) which allowed monitoring the pump's output. Finally, the flowmeter dumps the fluid back into the recirculating bath. The bath was maintained at temperatures approximating that of the body, in order to more closely simulate in vivo conditions.

## Test Valves

The decision as to the types of valves that were to be tested in the chamber was based on the fact that, in terms of the bioprostheses, the pericardial valves hold some distinct advantages over the porcine ones. One obvious advantage is that there exists no size limitation with the pericardial valves. These valves can be custom designed to meet any specifications. This is due to the fact that the bovine pericardium, the fibroserous membrane surrounding the heart of the cow, can be cut and shaped into any size leaflets or cusps.[13] However, with the porcine valves this limitation is quite apparent; no size variation

is possible since the valve is taken, as is, directly from the pig's heart. Another very important advantage of the pericardial over the porcine valves is an improved hemodynamic performance due to the design of the valve itself and to the relative alignment of the leaflets.[40-44] It has also been speculated that the pericardial valves have a lower rate of thromboembolic complication in comparison with the porcine valves.[44] This led to an investigation of two pericardial valve designs, one manufactured by Shiley Inc. and the other manufactured by Edwards Labs.

The two specific valves which were used in this study are the tri-cuspid Ionescu-Shiley Low Profile Mitral Valve and the tri-cuspid Carpentier-Edwards Low Profile Aortic Valve. Both are comprised of bovine pericardium mounted on a flexible stent and have been chemically treated in a glutaraldehyde solution. Throughout the rest of this paper the Ionescu-Shiley and the Carpentier-Edwards valves will be referred to as the I-S and C-E valves respectively.

The I-S valve has a flexible stent made out of Delrin, which is covered with porous Dacron. The stent or orifice diameter is listed as 23 mm., while the mounting diameter (annulus) is 27 mm.[20,45] The C-E valve on the other hand, has a flexible stent made out of Elgiloy, an alloy of Co. and Ni., chosen for its corrosion and fatigue resistance along with its high strength and biocompatibility, which is covered with porous polytetrafluoroethylene. Its orifice diameter is listed as 26 mm., while the mounting diameter is also 27 mm.[20] The

flexibility of the frame and the porosity of the cloth covering are critical. The frame acts as a shock absorber reducing the loading shock to the rest of the valve, and the porosity of the cloth facilitates desired tissue ingrowth and encapsulation.[18,46]

# EXPERIMENTAL PROCEDURES

## L.D.A. Methods

After careful and thorough rinsing of each valve with saline solution, the valves were placed in the aortic flow chamber for the initial L.D.A. measurements prior to accelerated testing. Distinct points on each valve were noted, so that when the valves were again placed in the aortic chamber the positioning would be the same. Flow characterization was done by mapping out the velocity profile across the central plane of the chamber. Measurements were taken at positions of 0.75" into the sinus region, just beyond the open leaflets, and at 1.5" from the valve housing, just into the aortic region. At the location of 0.75" into the sinus region, the ability to measure a full profile, while staying in the very near vicinity of the valve, existed. At 1.5" downstream, there were indications as to the type of flow going into the aorta, and also as to the extent that residual effects existed due to the fluid flowing through the valves. Multiple channel traversings were made until at least two or three acceptable full profiles were acquired at each location. In mapping out one profile, three to six mean velocity measurements were made at each point in the channel. These mean velocity measurements were each composed of 400 unique data points obtained due to the crossing of the fringes in the probe volume by the seed particles, 0.45 microns in diameter microspheres, in the saline solution. This large accumulation of data greatly increased the accuracy of the results and gave an indication as to its reproducibility. The

aortic flow chamber was placed on top of a vertical jack which was fastened onto a milling table. This set up procured the three degrees of freedom that were necessary for positioning the chamber and allowed for incremental movements of as small as 25.4 microns. The increments across the channel, at which point data was taken, varied depending on the location in the channel. Increments were made as small as 0.25 mm. when close to the wall and at critical regions, and as large as 2.5 mm. when in the center of the channel. Usually a total of 15 to 20 average velocities (average of the mean values) were accumulated per profile. Flow characterization was also done on the aortic flow chamber with no valve present. This demonstrated the inherent flow characteristics due to the design of the chamber itself. Thus, when analyzing the data, the ability existed to differentiate those inherent characteristics from the ones resulting from the flow through the valve. Profiles were mapped out at the same locations as when a valve was present, 0.75" and 1.5" downstream from the valve housing. Also profiles were determined at the locations of 1.5" and 0.75" upstream from the valve housing as a verification to the existence of fully developed flow. If fully developed flow exists, then the velocity profile will remain unchanged from then on, in the direction of motion.[47]

When assessing the L.D.A. data a few things must be kept in mind. The identification of the exact location in the flow channel was rather difficult if not impossible. The use of a solid piece of plexiglas alleviated the index of refraction

problem as the laser beams propagated through one medium to another, however, it did not correct the problem entirely. There still existed the problem of a focal length change as the beams propagated through other mediums besides air. This focal length continued to change with movement across the channel. Thus, it was necessary to determine the number of units needed to turn the micrometer dials on the milling table for each given increment of distance, taking into account these focal length changes. A simple computer program was written in Basic for the Apple to do this for any given desired movement (Table I). It worked well, however it was based on the fact that the outer wall of the chamber could be accurately located, and that the chamber dimensions were precise. Focusing on the outer wall was not easily done. At times, what appeared to be wall signal (shift frequency signal) was picked up at various locations, spaced out as far as a few hundred microns. An attempt to be as consistent as possible was made. Also the solid piece of plexiglas showed some variations in width which were not easily corrected, because of the most important highly polished surface finish. When building the aortic flow chamber at the F.D.A., sections were bored out as close to the desired dimensions as possible, however, many days had to be spent on the lathe polishing the inner surface of the chamber to achieve the essential transparency. This also altered the dimensions slightly. Therefore, even though the spacing between velocity profile points was known, the exact location of each point in the flow

```
100 TEXT : HOME
110 UO = 0
120 PRINT : PRINT
130 PRINT "INPUT DISTANCE DESIRED TO MOVE IN CHANNEL (mm.)"
140 INPUT DD
150 PRINT : PRINT
160 PRINT "INPUT WINDOW THICKNESS DT; IF IN THE SINUS REGION
    THEN DT=15.875, BUT IF IN THE AORTIC REGION THEN DT=19.05"
170 INPUT DT
180 DA = (163.39 - DT - DD)/(1.331)
190 U = (121.1 - DA)/(0.0254)
200 U1 = U - UO
210 PRINT "UNITS REQUIRED TO MOVE : "U1
220 PRINT : PRINT
230 UO = U
240 PRINT "INPUT Y TO CONTINUE":INPUT A$
250 IF A$ = "Y" GOTO 115
260 END
```

Table I. Basic Program for the Determination of Required Units

chamber was not. For the most part, this problem did not greatly affect any of the results, however, when viewing certain velocity profile overlays, one may notice a slight shift in the "X" or the distance direction as a result of it. Nevertheless, what really is of interest is the shape of the profiles, and how that shape changes after successive accelerated test intervals.

## Accelerated Testing

The accelerated tester (Shelhigh Fatigue Test System #2) is somewhat easier to understand and operate than the L.D.A. system (Figs.3 & 4). The motor and motor arm, with variable stroke settings, are connected to a linear platform which oscillates back and forth as the motor turns. On the linear platform is the vibrating plate with six vibrating bars running horizontally. While the motor turns, the motor arm drives the linear platform forwards and backwards, which causes the vibrating bars to compress the rubber hose on each side of the test chamber alternately. This compression of the hose causes an external pressure to be imposed on the incompressible fluid. The internal pressure inside each chamber must be zero. To accomodate the external pressure the fluid is displaced in the chambers, which causes the opening and closing of the valves. There are a total of three test chambers assemblies; each is actually made up of two valve housings. Therefore a total of six valves can be tested at one time in the system. Each valve housing has two pressure ports so that pressure drops across the valves can be measured, and physiologic conditions maintained. Also a heating element sits between the chambers, and the chambers are encased allowing regulation of the temperature inside the system. On the control console the temperature and speed controls are found, along with a timer, a digital temperature readout, and an R.P.M. meter.

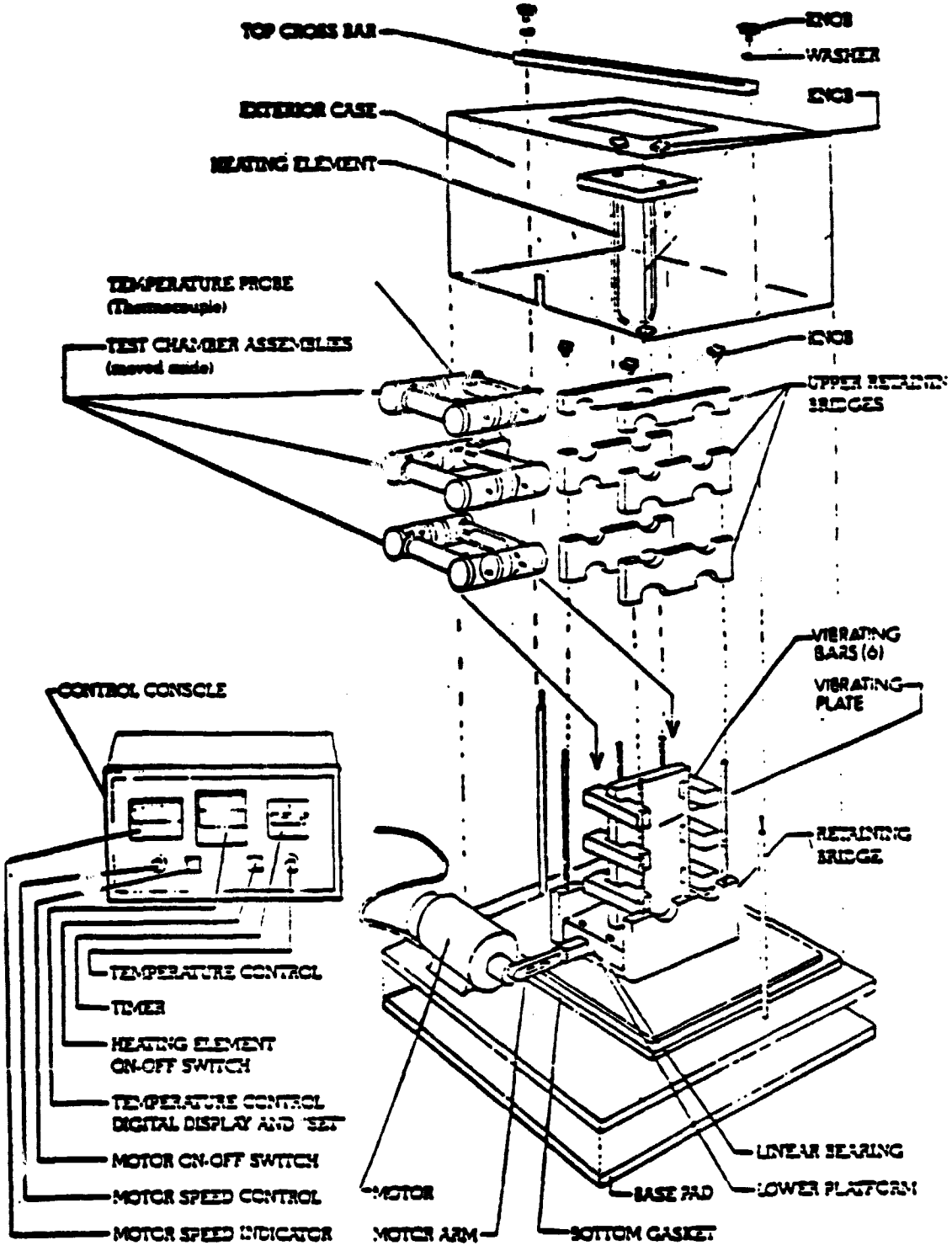


Fig. 3. Shelhigh Fatigue Test System #2. (Taken from Manual)

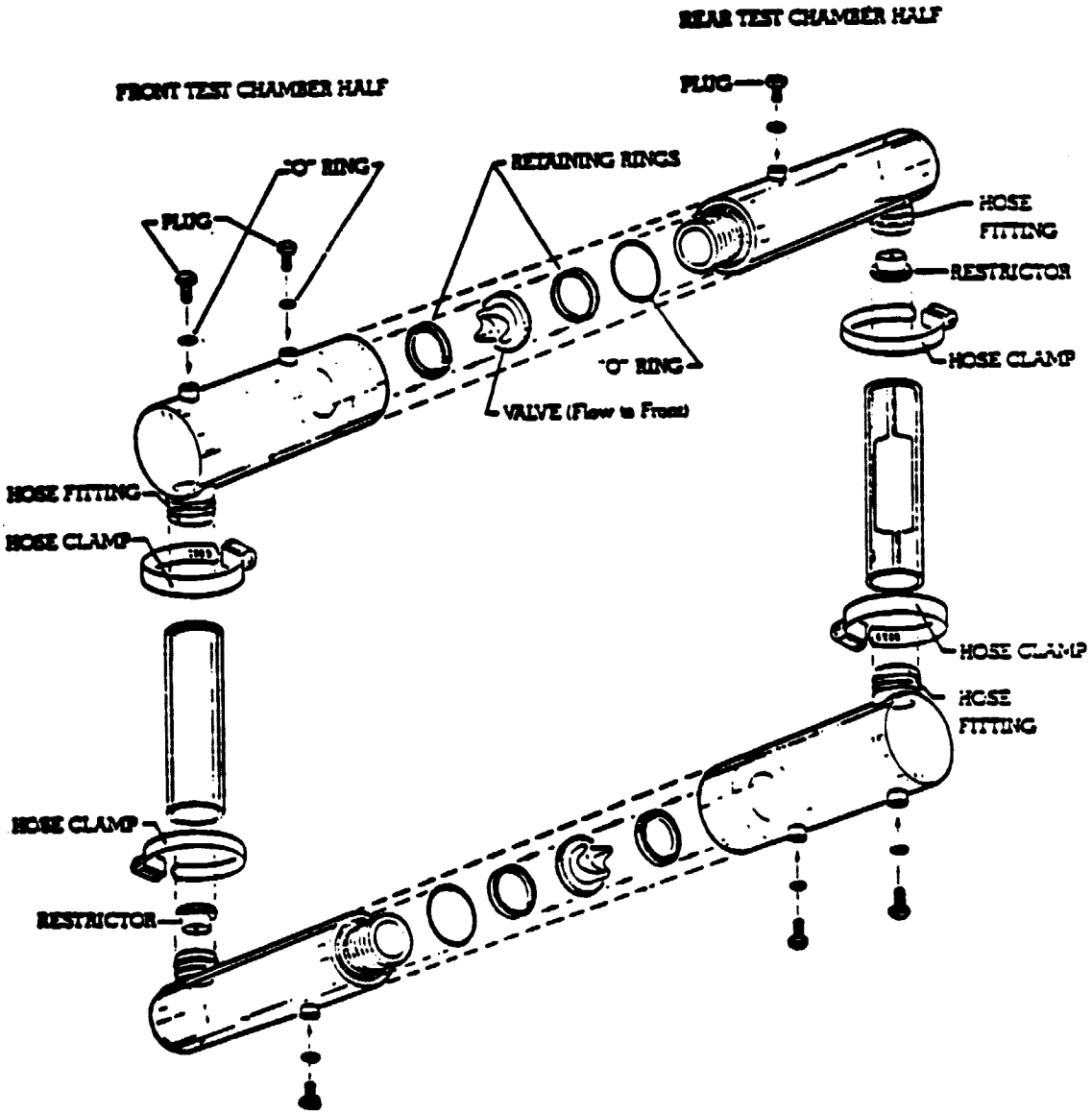


Fig. 4. Valve Test Chamber for Fatigue Tester. (Taken from Manual)

## RESULTS AND DISCUSSION

The existence of fully developed flow was verified by the L.D.A. measurements made at 1.5" and 0.75" upstream from the valve housing (Figs. 5 & 6). As seen in Fig. 7 the overlay of these profiles demonstrates a good match. The peak velocities and the shape of the profiles are the same at different locations in the chamber, a good indication of fully developed flow.[47]

As mentioned previously, the possibility existed that the design of the chamber could, in itself, alter the flow patterns. Therefore profiles in the sinus and aortic regions were obtained with no valve present (Figs. 8-13). In Figs. 10 & 13 it can be observed that these seem to be parabolic velocity profiles with no flow reversals present in both the sinus and aortic regions. The sinus region is synonymous with the location of 0.75" downstream from the valve housing, while the aortic region is synonymous with the location of 1.5" downstream from the valve housing.

After the chamber's inherent flow characteristics were determined, the I-S valve was placed into the aortic flow chamber. At this point the valve had not been subjected to any cyclic loading. Figs. 14-18 show the results in both the sinus and aortic regions, Figs. 19a & 19b show the overlays for each. Fig. 20 (composite of Figs. 10 & 19a) shows a tremendous change in the flow characteristics that takes place due to the presence of the I-S valve. In Fig. 10 the profiles indicate the existence of a symmetrical flow pattern that almost appears laminar, how-

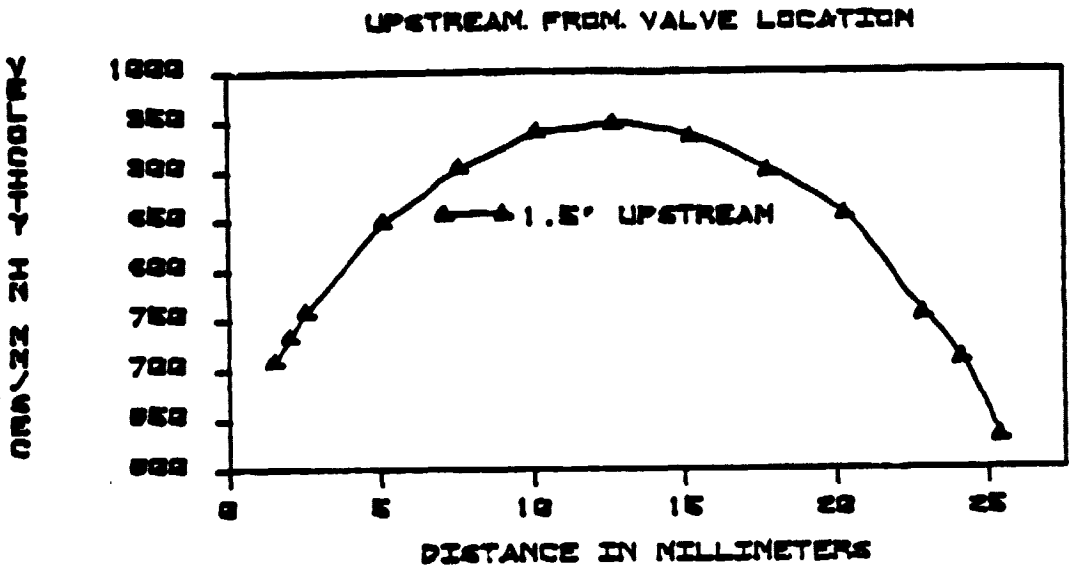


Fig. 5.

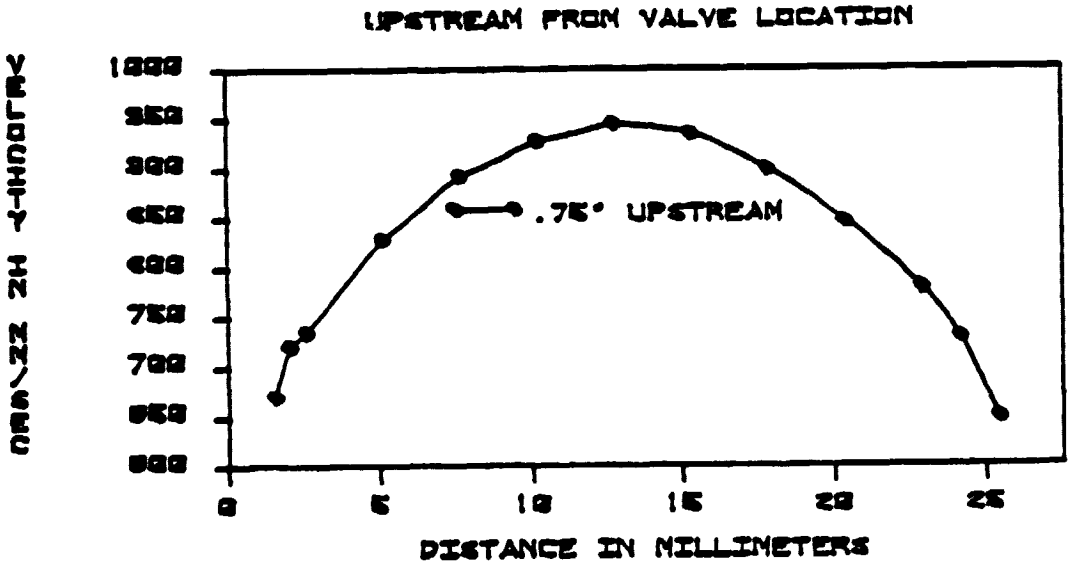


Fig. 6.

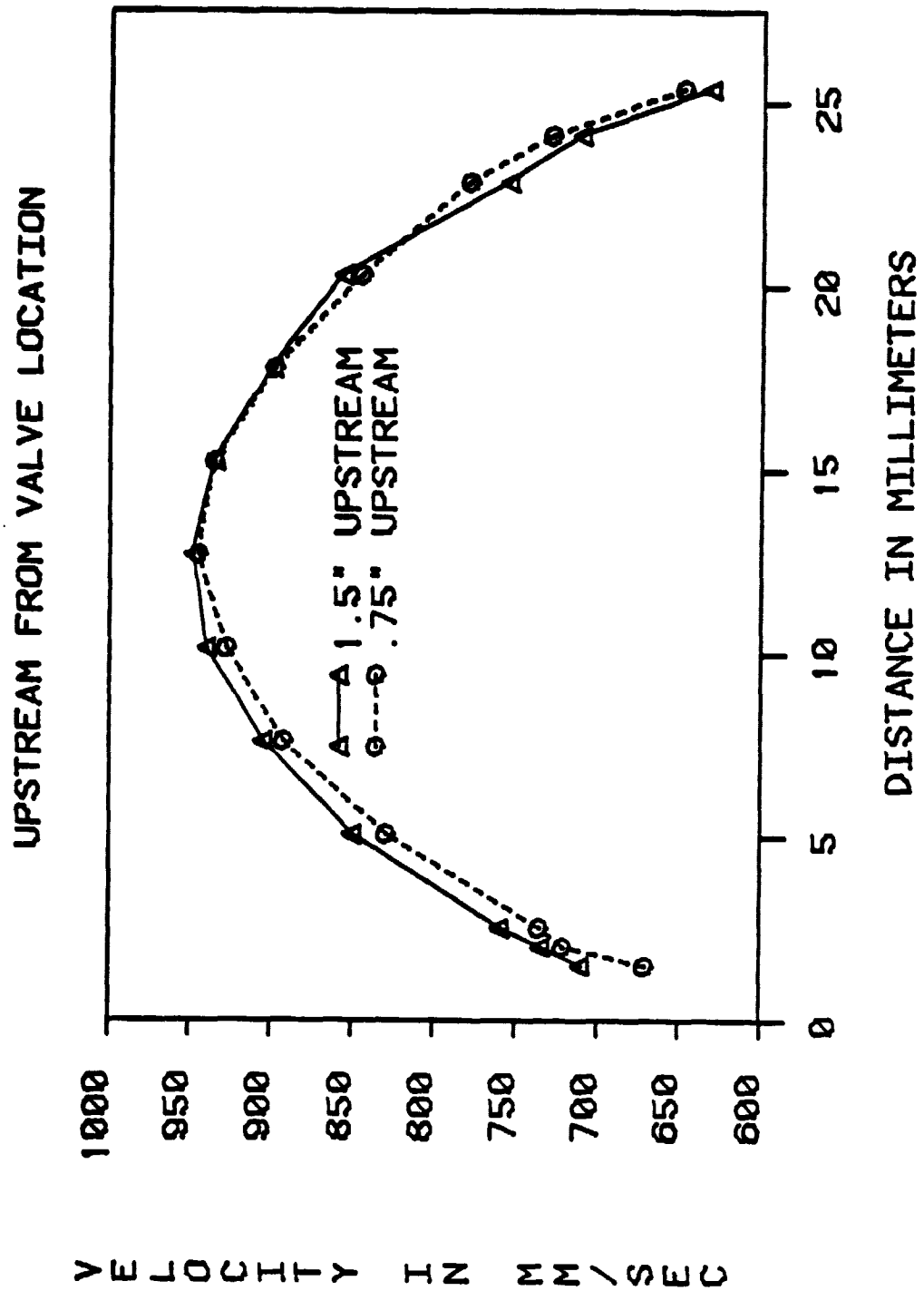


Fig. 7.

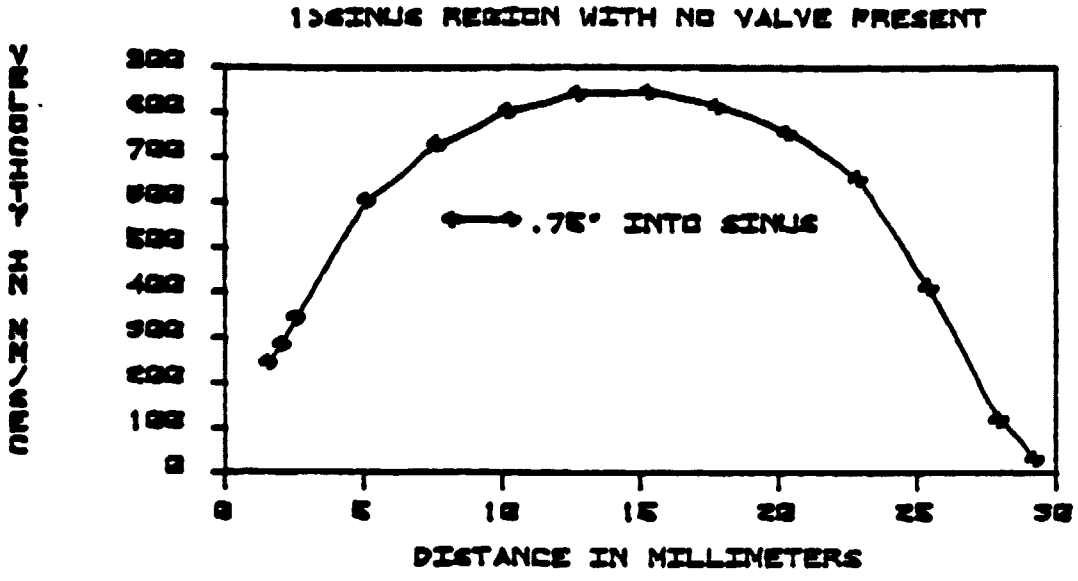


Fig. 8.

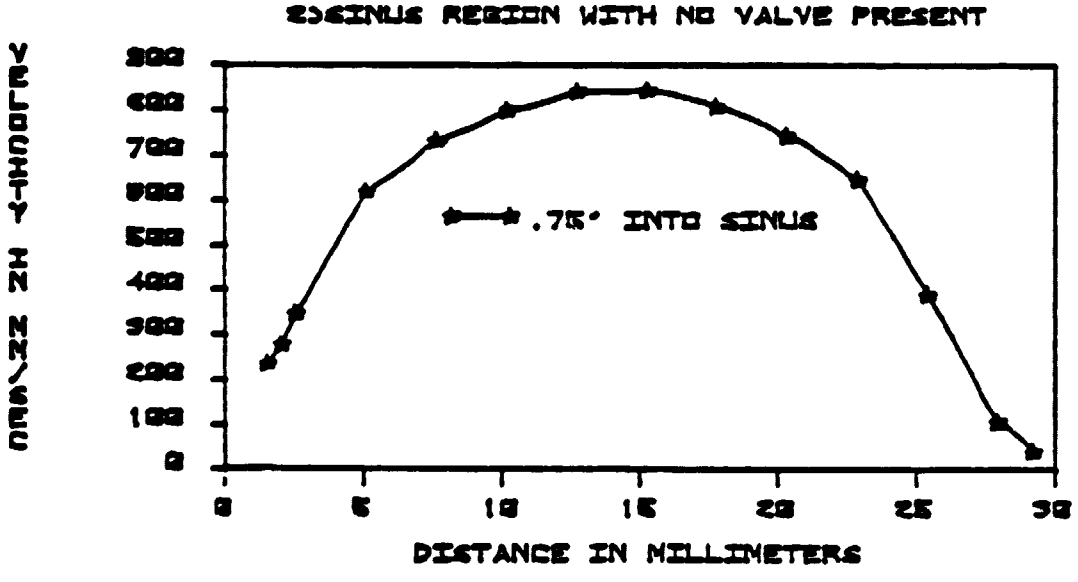


Fig. 9.

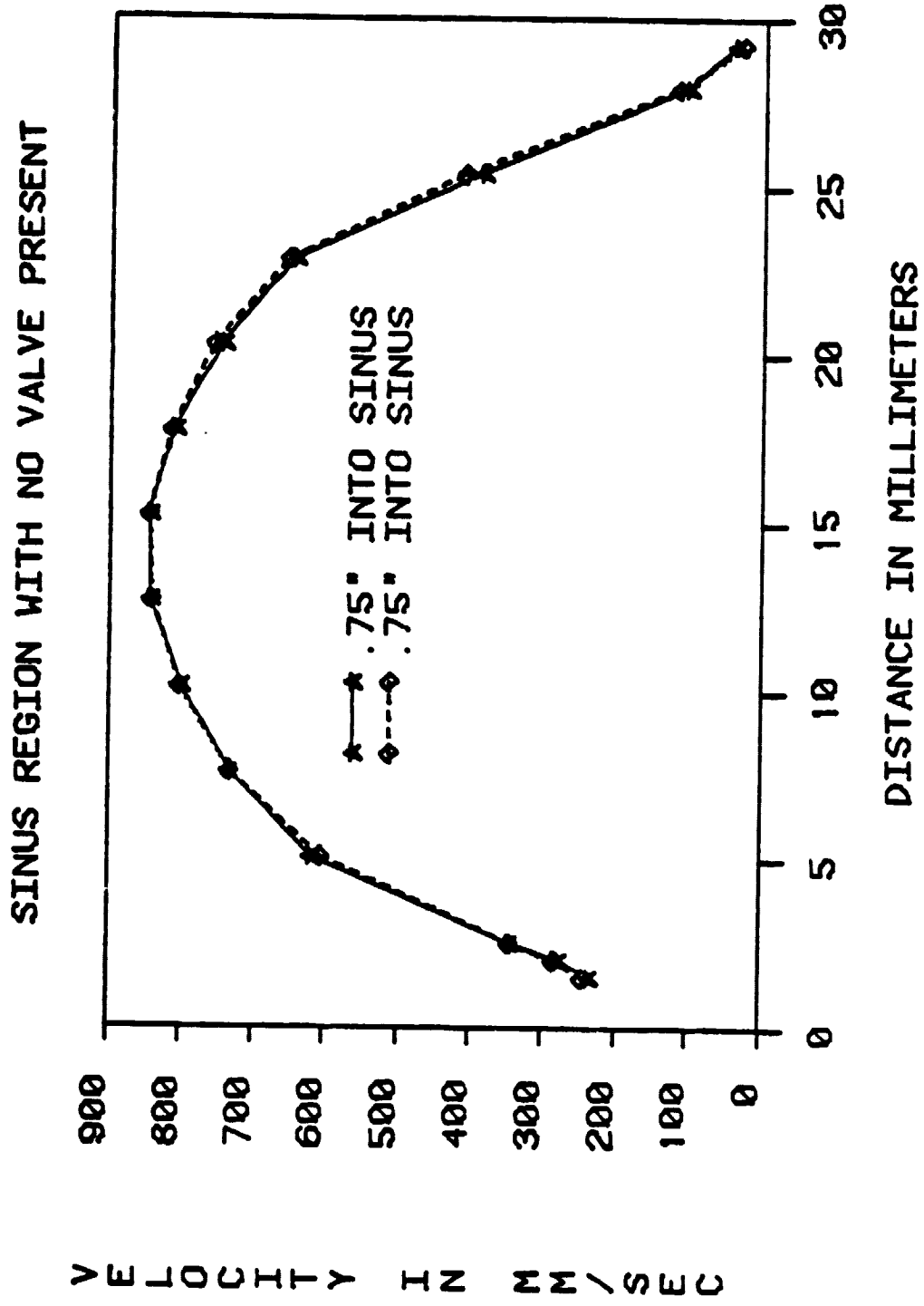


Fig. 10.

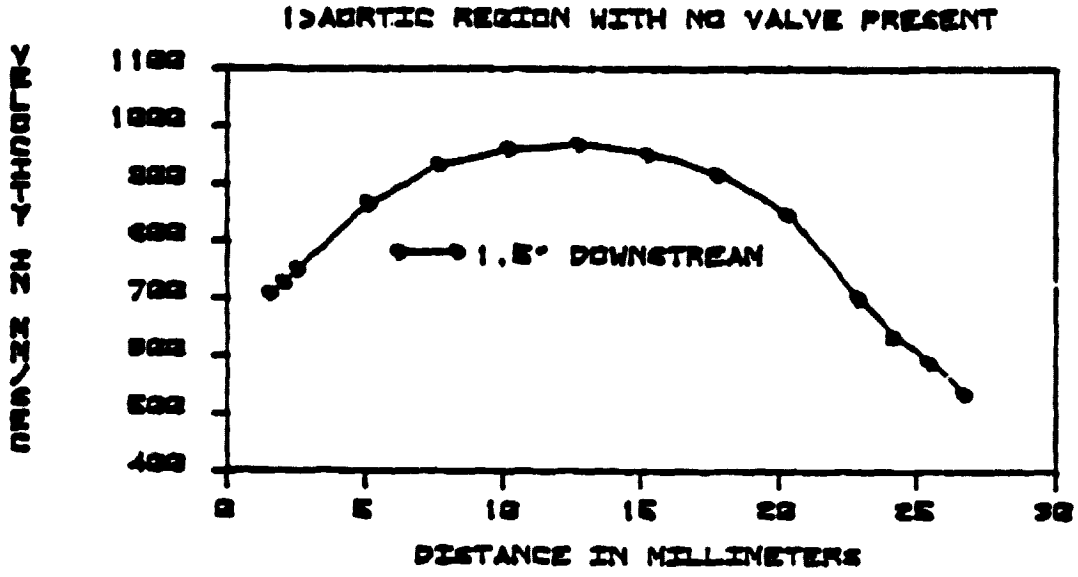


Fig. 11.

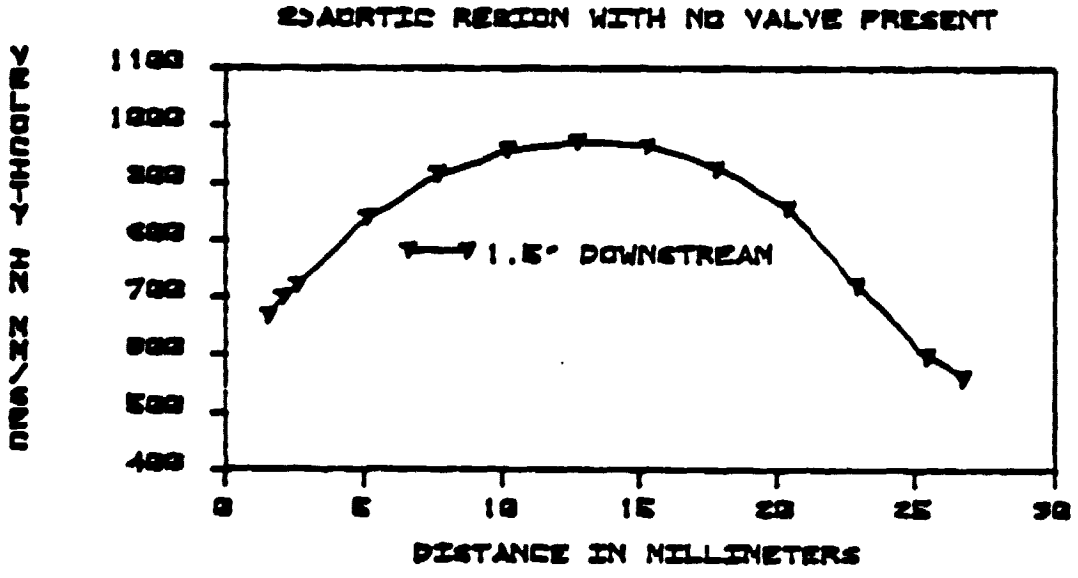


Fig. 12.

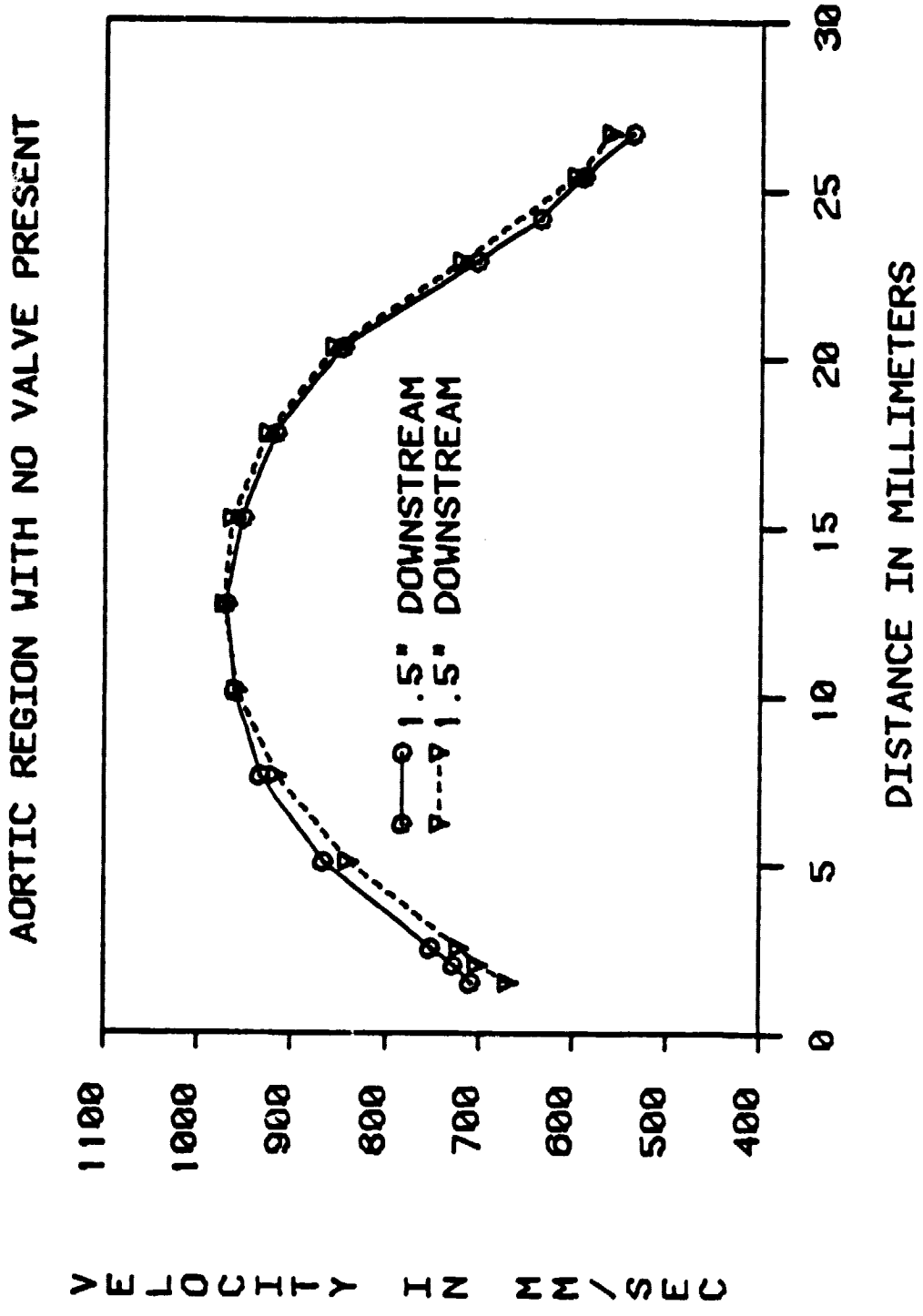


Fig. 13.

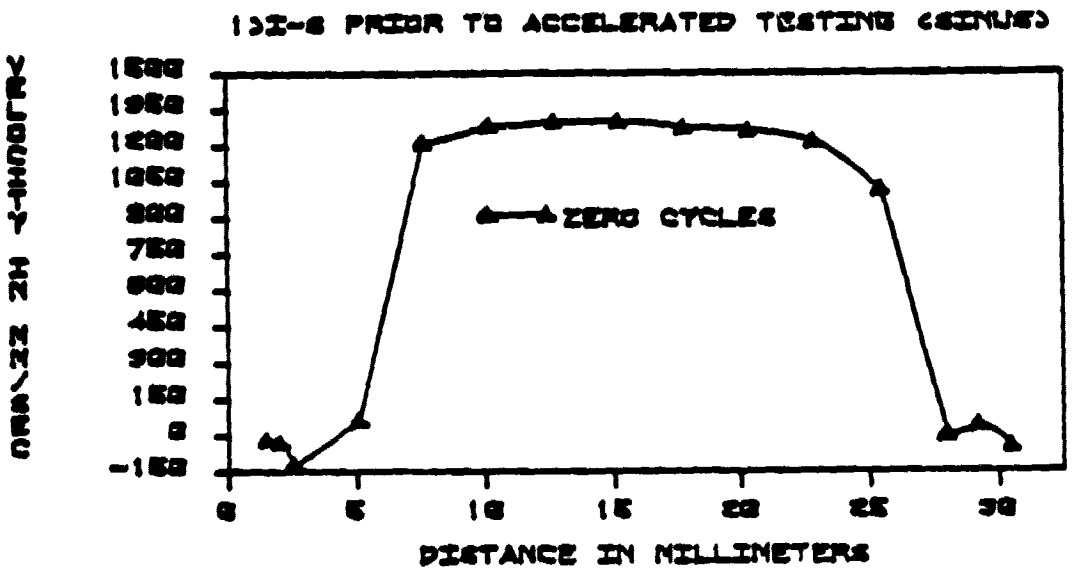


Fig. 14.

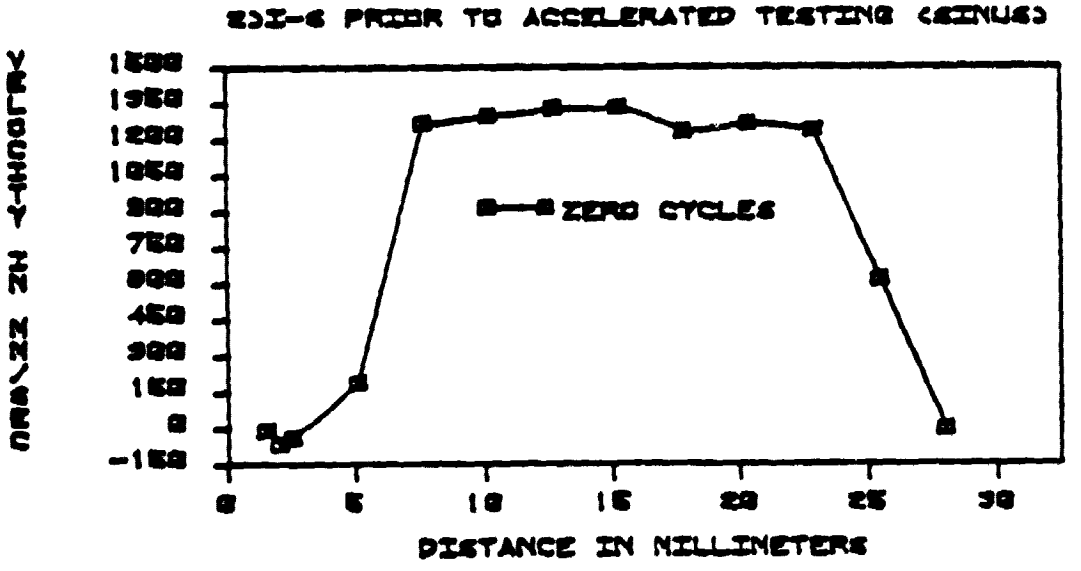


Fig. 15.

ORIGINAL PAGE IS
OF POOR QUALITY

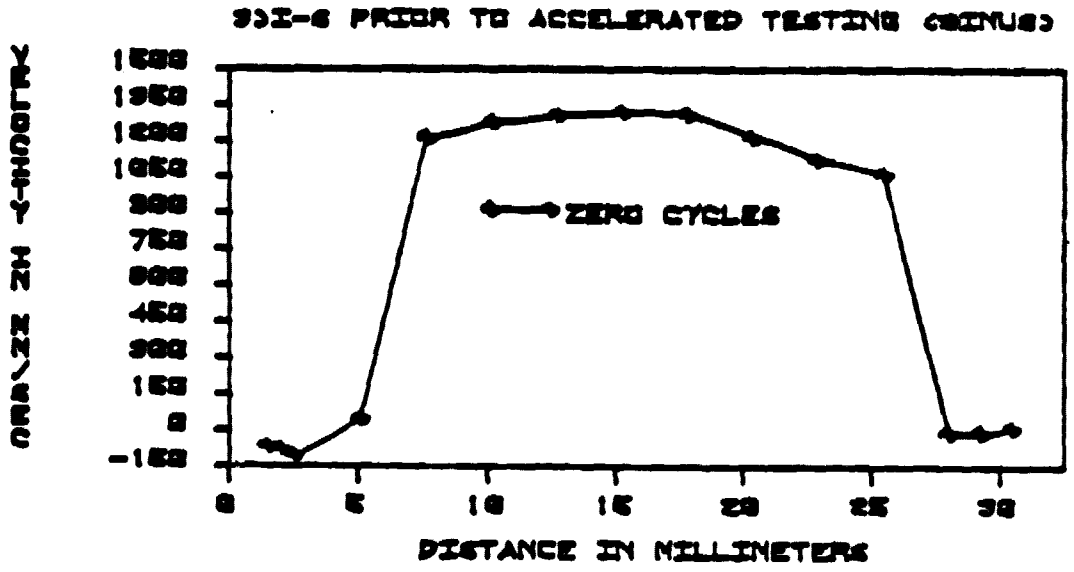


Fig. 16.

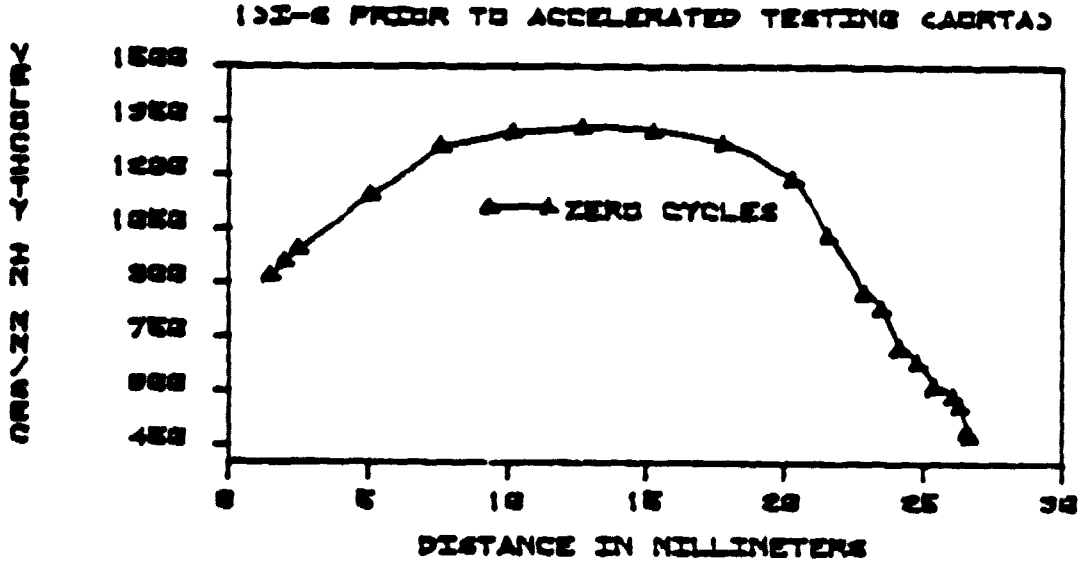


Fig. 17.

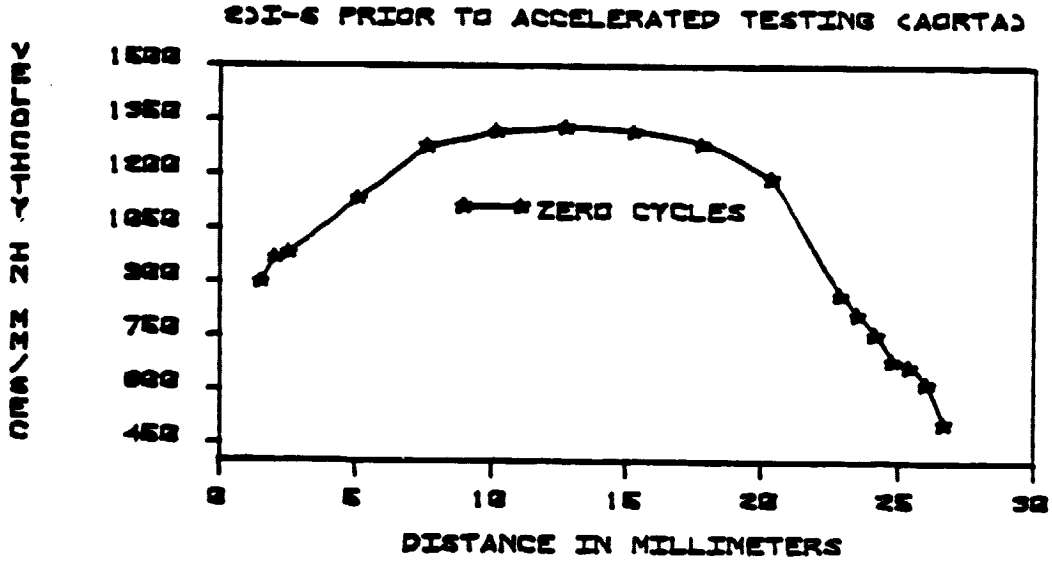


Fig. 18.

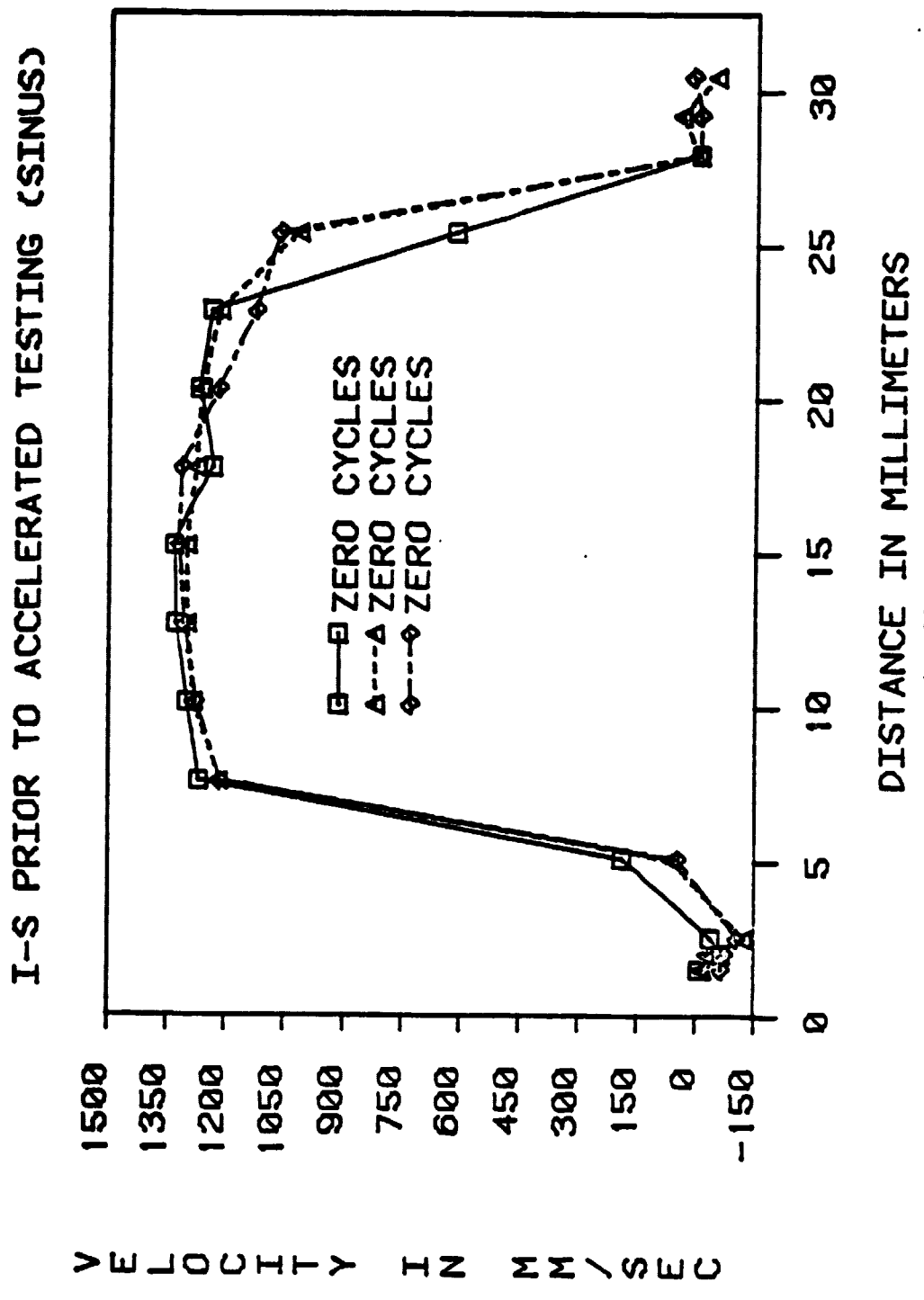


Fig. 19a.

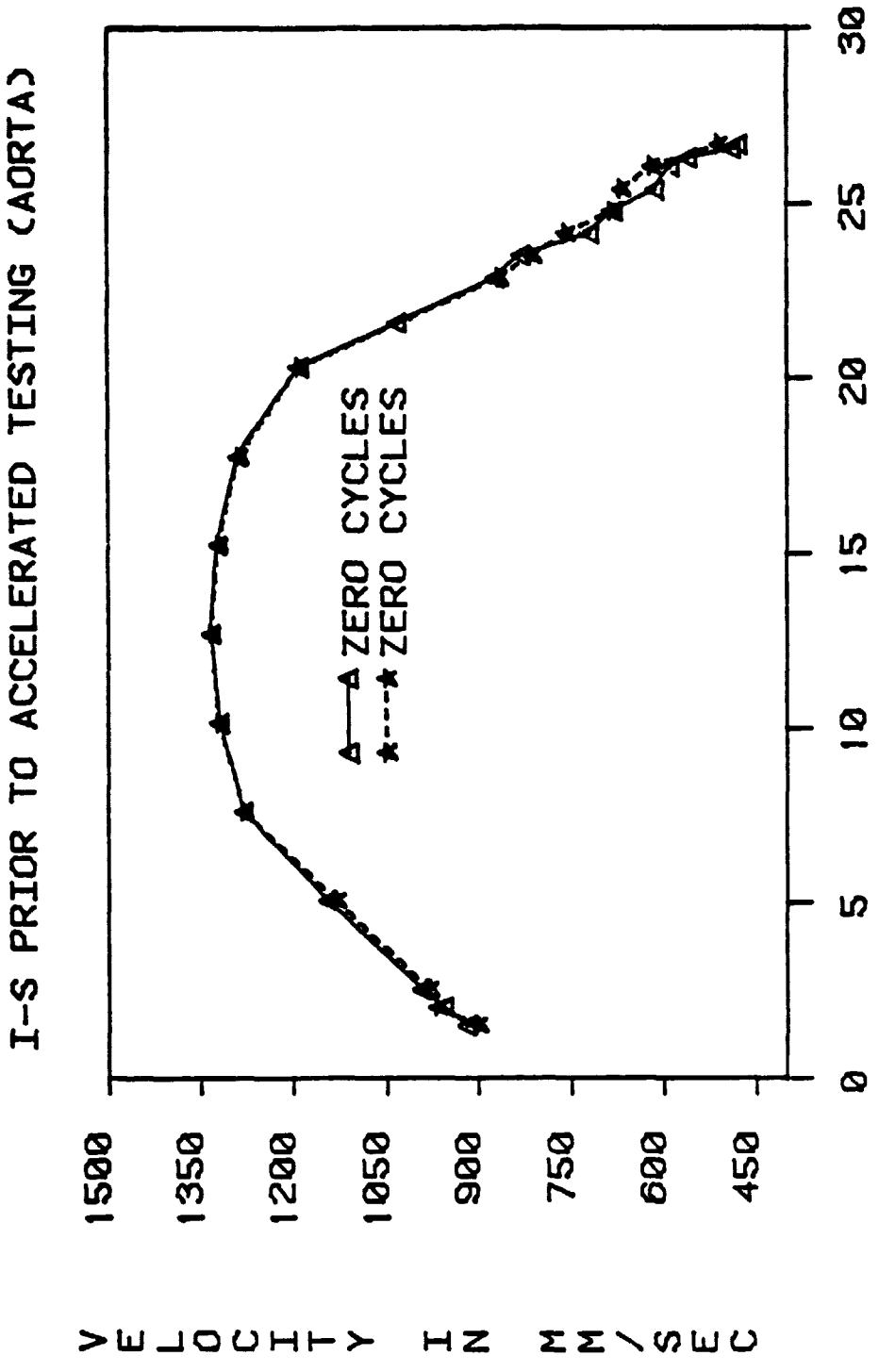


Fig. 19b.

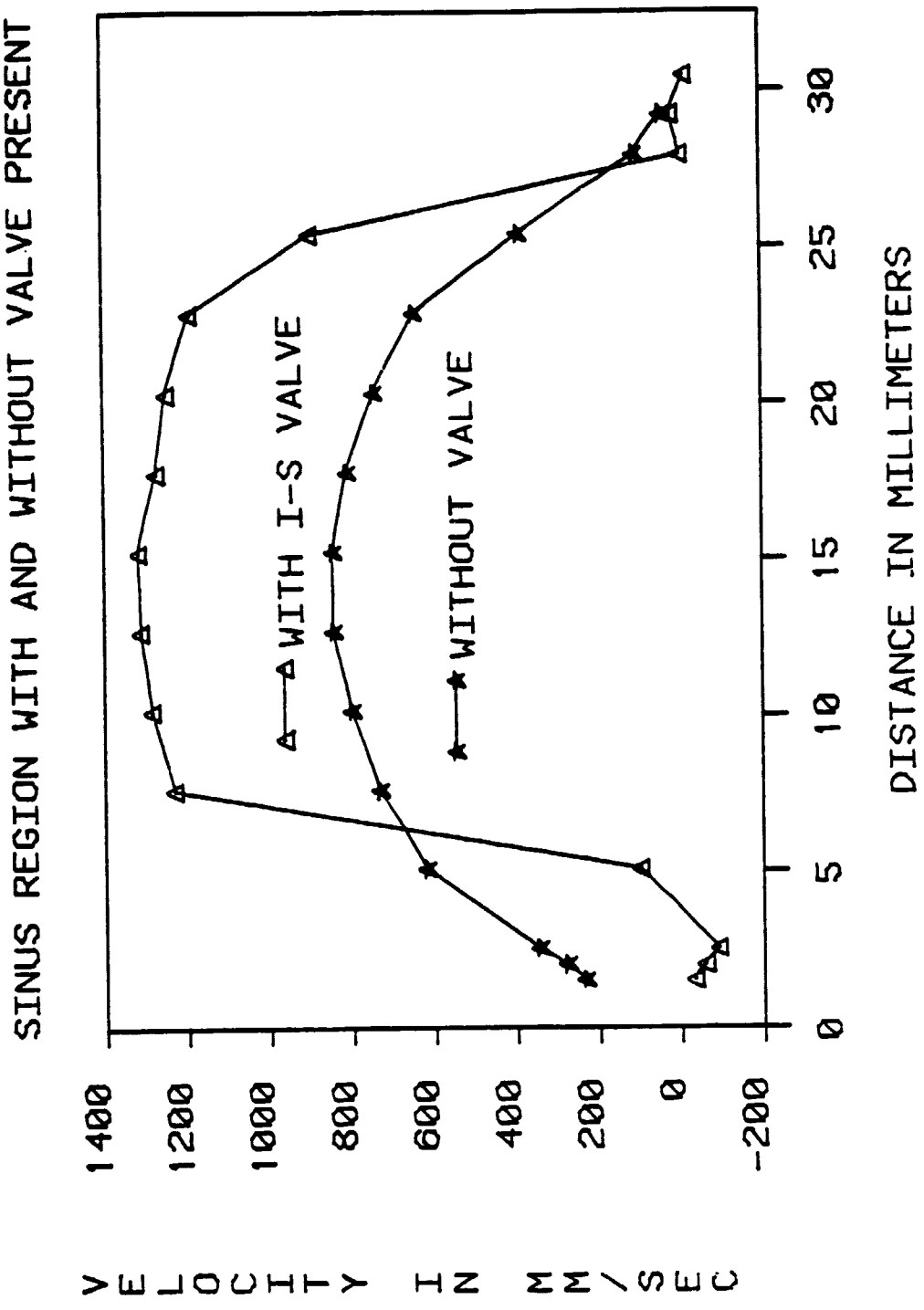


Fig. 20.

ever the Reynolds no. is too large (Re>20,000). In Fig. 19a the indication is one of turbulent flow with flow reversals (negative velocities) occurring near the walls.[47] These flow reversals occur behind the leaflets and close to the walls. When air bubbles are allowed to infiltrate the system a swirling action can be seen behind the leaflets, qualitatively verifying the area of flow reversals. This seems logical because there exists very high velocity flows in the orifice, which continue out to the leaflets' edge. This continuation turns into an overflow at the end of the valve, and progresses behind the leaflets. The region behind the leaflets, however, is one of very low pressures in comparison to what is seen in the orifice. This causes the swirling action to be present as long as the flow through the valve continues. In the aortic region (Fig. 19b), the shape of the velocity profiles look very similar to those without a valve present (Fig. 13). The peak velocities do look somewhat different, which is accounted for by the fact that the high velocity turbulent flow from the sinus is dumping into the smaller aortic region. No other residual effects exist at this point, since all velocities are positive (Fig. 19b).

The I-S valve was then removed and the C-E calve put in its place. Since both valves have the same mounting diameter, the housing did not have to be altered. The data from the measurements made in both the sinus and aortic regions is contained in Figs. 21-25, with the overlays in Figs. 26 & 27. This is the initial flow evaluation prior to any accelerated testing. Again,

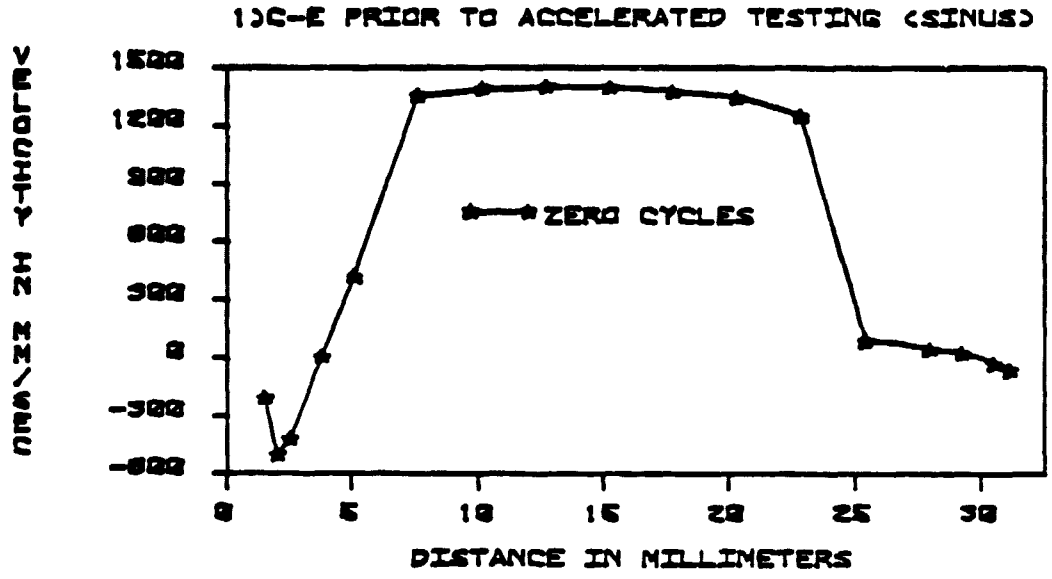


Fig. 21.

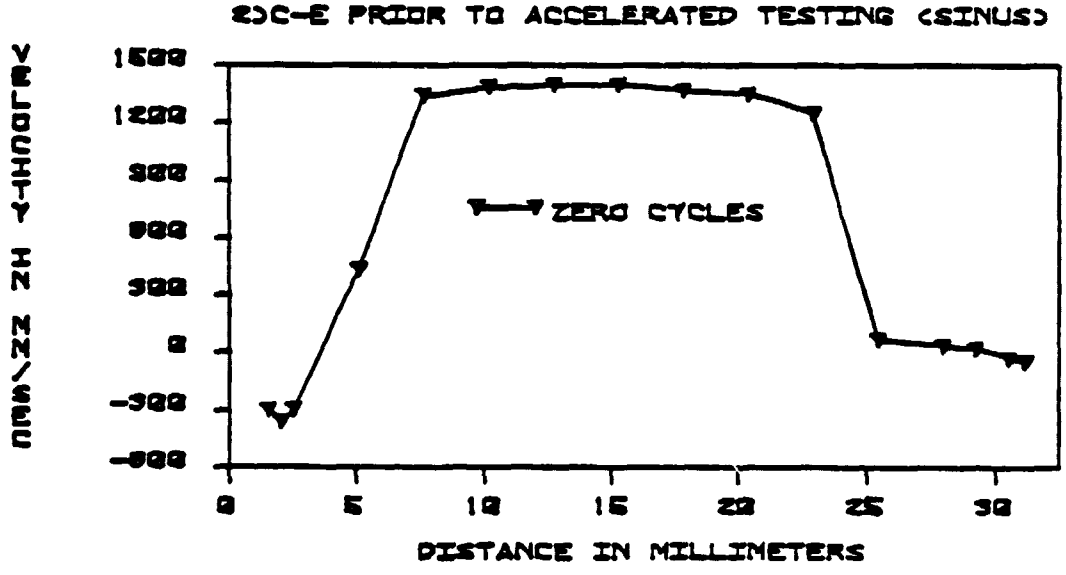


Fig. 22.

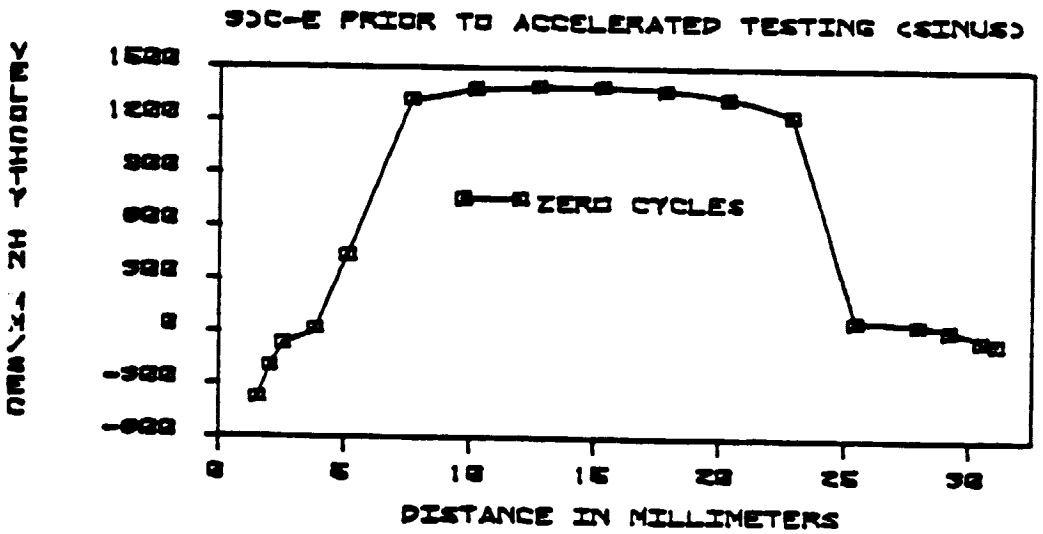


Fig. 23.

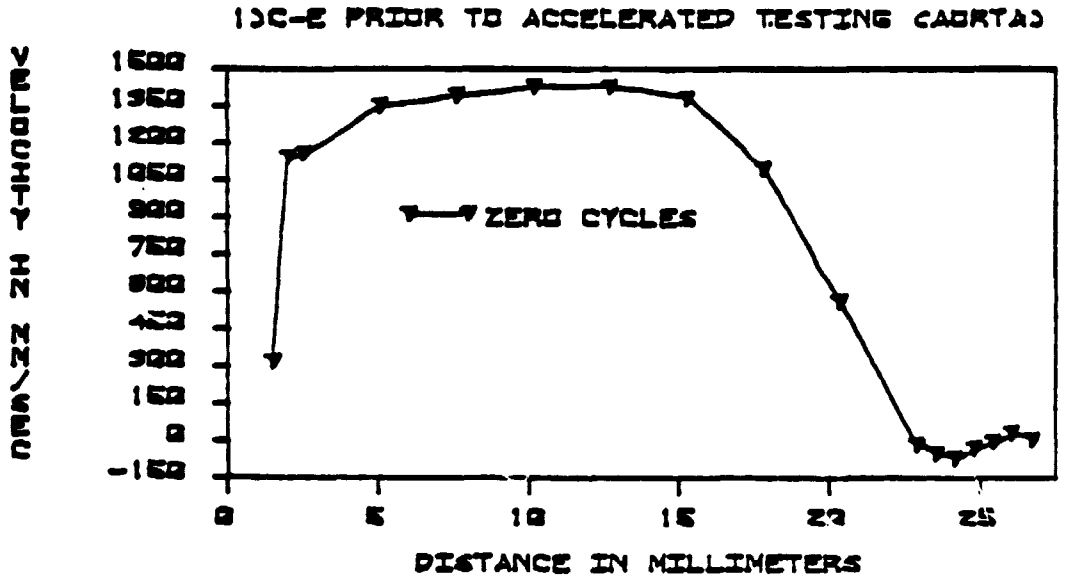


Fig. 24.

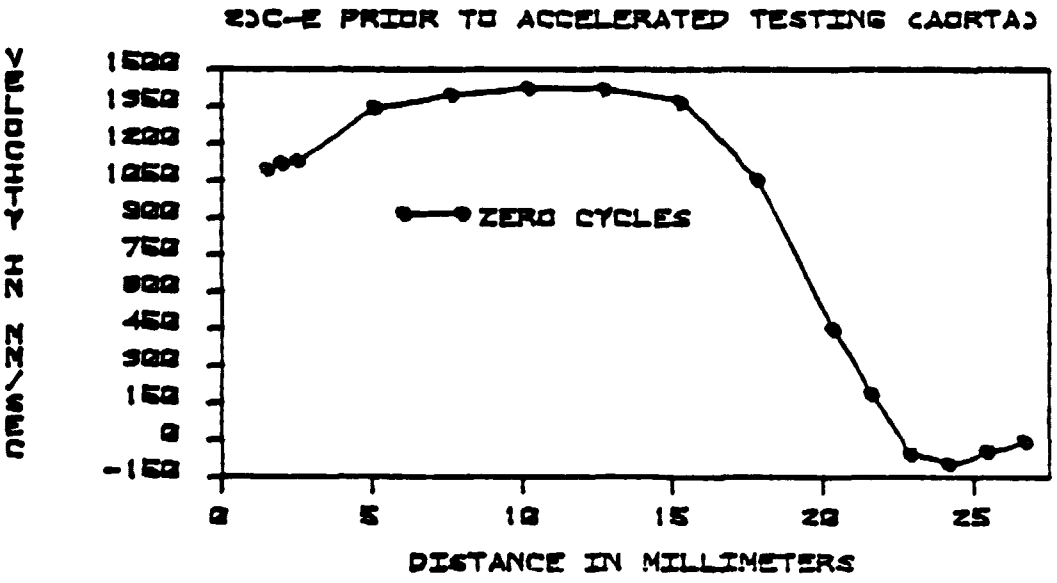


Fig. 25.

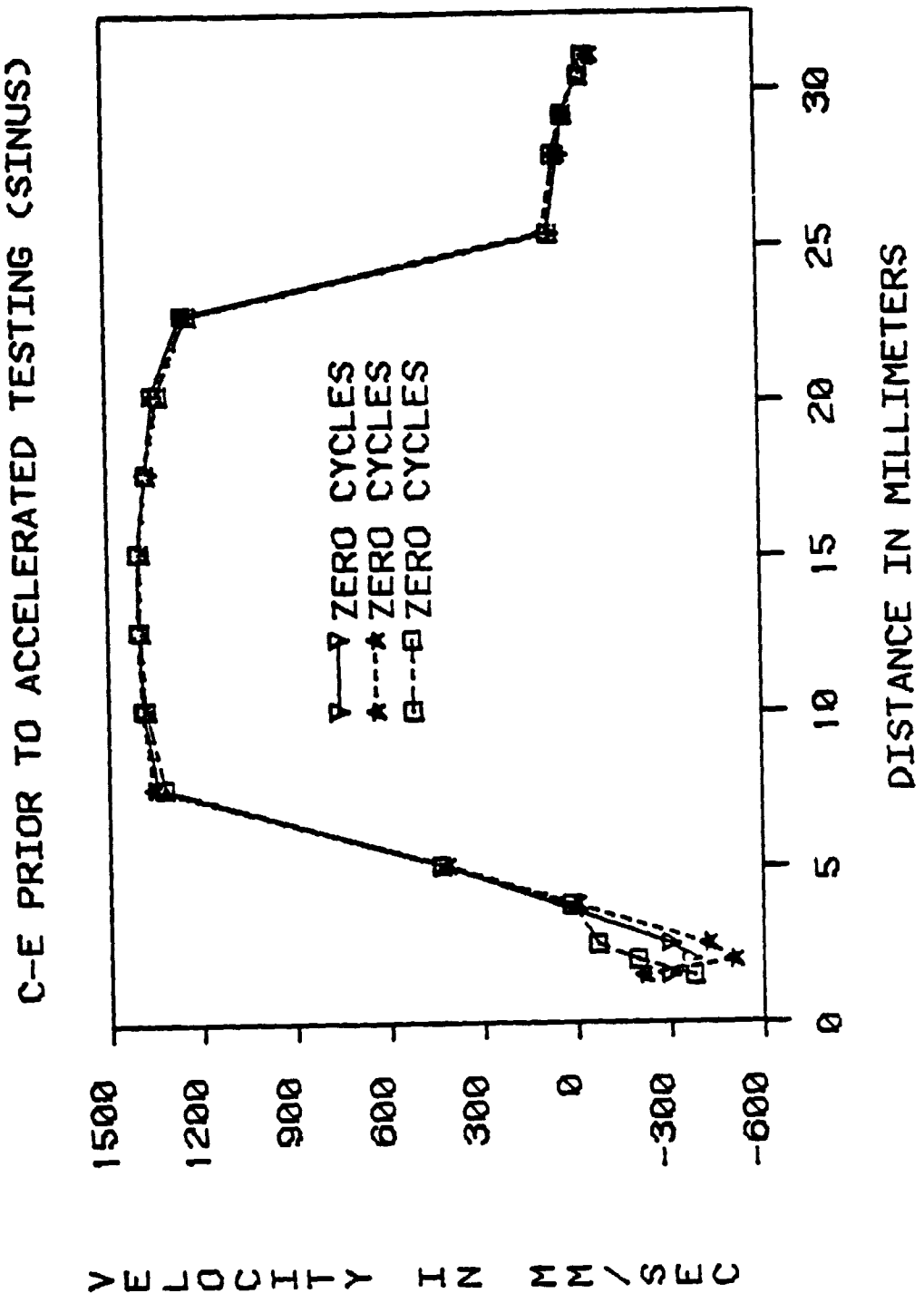


Fig. 26.

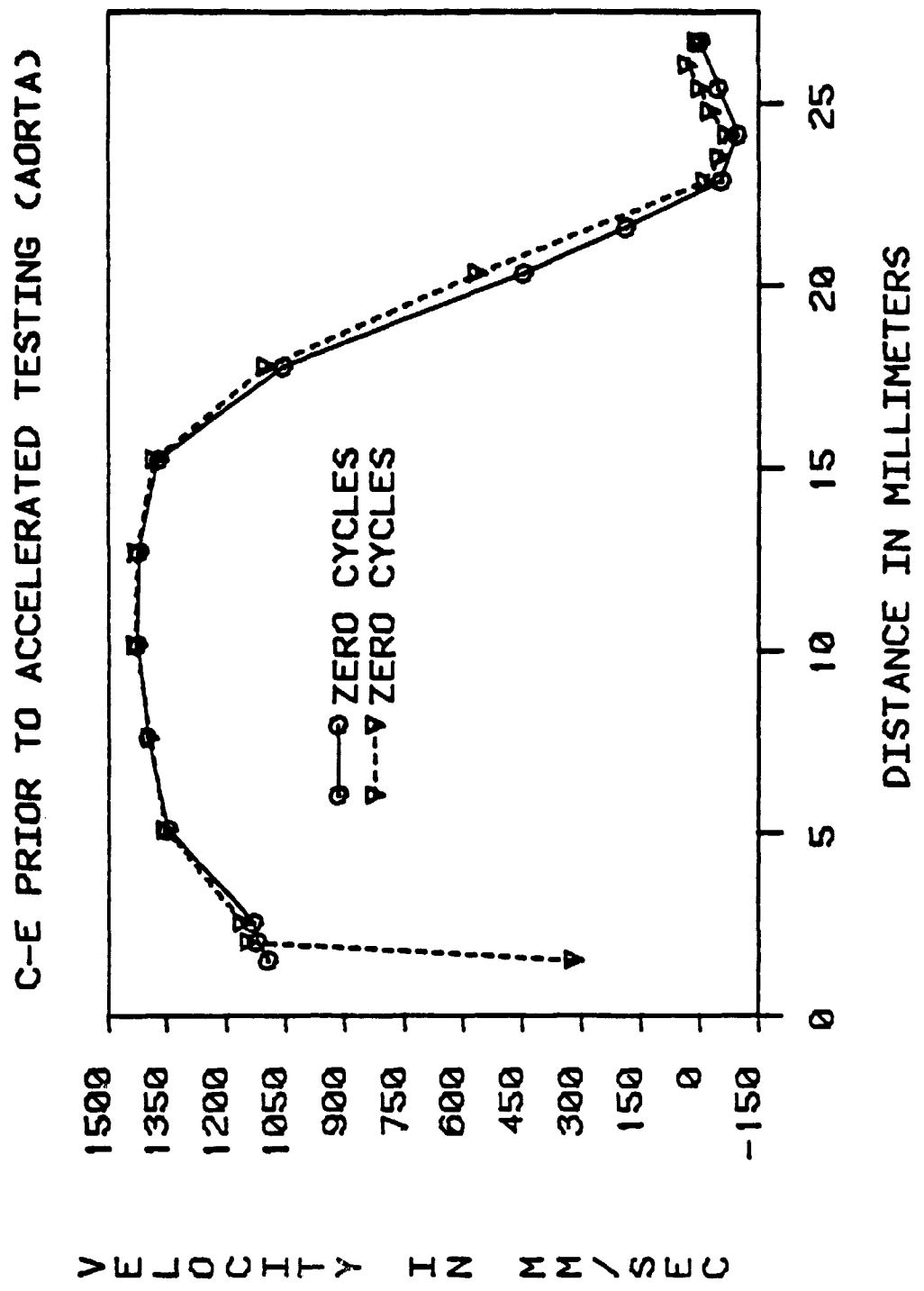


Fig. 27.

in the sinus region what is observed is quite similar to what was seen with the I-S valve. The indication of turbulent flow with flow reversals near the walls is present in Fig. 26. Nevertheless, the magnitude of both the peak velocities and the negative velocities is greater for the C-E valve in comparison with the I-S valve. The data indicates that the high velocity flow area is somewhat smaller with the C-E valve. This would account for the larger magnitudes since the constriction would cause higher pressures through the channel leading to larger velocities. The aortic region shows a different behavior than that which has been seen previously (Fig. 27). The profiles exhibit a certain amount of negative flow towards the outer wall. The existence of these residual effects from the sinus region might be explained in a few different ways. The fact that the flow reversals were only seen on one side indicates that the valve leaflets do not open symmetrically, a fairly common problem with bioprostheses. Another factor that may have contributed to the flow reversals could be the fluttering of the outer wall leaflet. Leaflet flutter was present with the C-E valve, much more so then was observed with the I-S valve.

After initial flow characterization, the valves were documented and photographed using a Pentax 35 mm. camera with three extender tubes, and then placed into the accelerated tester. The valves were also viewed under optical microscopes to determine their condition. It was found that the leaflets were in good shape, but had become a little dirty while in the flow chamber

(Figs. 28 & 29). The dirt did not appear to cause any damage to the tissue and when the valves were operated in the accelerated tester, the dirt was agitated off completely. The accelerated tester was run at the speed of 1300 R.P.M. using the saline solution. Dr.Shlomo Gabbay, from the Albert Einstein College of Medicine, helped design the accelerated tester, and maintains that the system can be operated at speeds of at least 1600 and even possibly 1800 R.P.M.[48] Some of the heart valve manufacturers seem to feel this rate is too high, even when maintaining physiologic closing pressures. In fact, Dr. Gabbay has noted in a paper which is in publication at this time, that when operating at these high rates in vitro many different types of leaflet tears have been observed.[48] Most of these tears seem to have some correlation with what is seen clinically, however Dr. Gabbay does admit that a few of these tears are unique to the accelerated tester and have no clinical correlation.[48] The accelerated tester operating at 1300 R.P.M. still opens and closes the valves at approximately 18x the normal rate. The temperature inside the system was kept at 37 degrees celsius (body temperature), while closing pressures were maintained within the physiologic range for both valves. The physiologic range is considered to be between 60 and 100 mm.Hg pressure.[48,49] Closing pressures at the beginning of the first accelerated test interval were approximately 60 mm.Hg for the I-S valve (Fig. 30) and 80 mm.Hg for the C-E valve (Fig. 31). For the first accelerated test interval, the plan was to run the system through

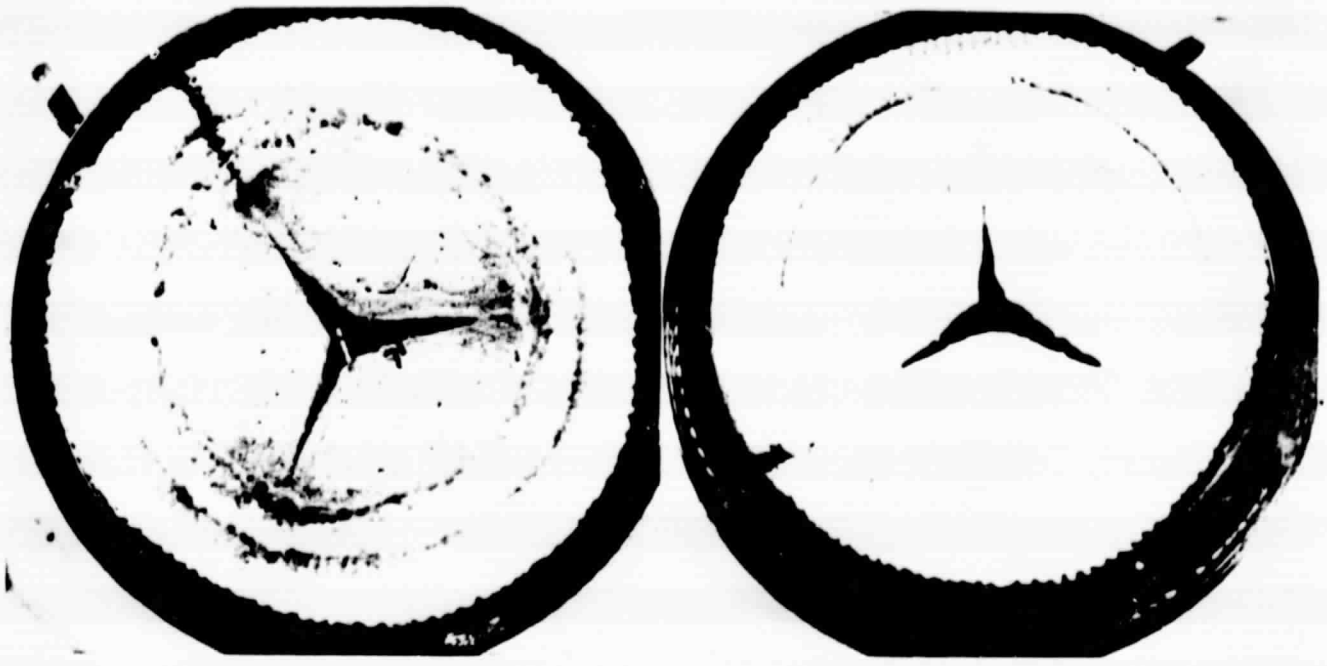

Figs. 28. I-S Valve prior to Accelerated Testing (Inflow and Outflow Sides).

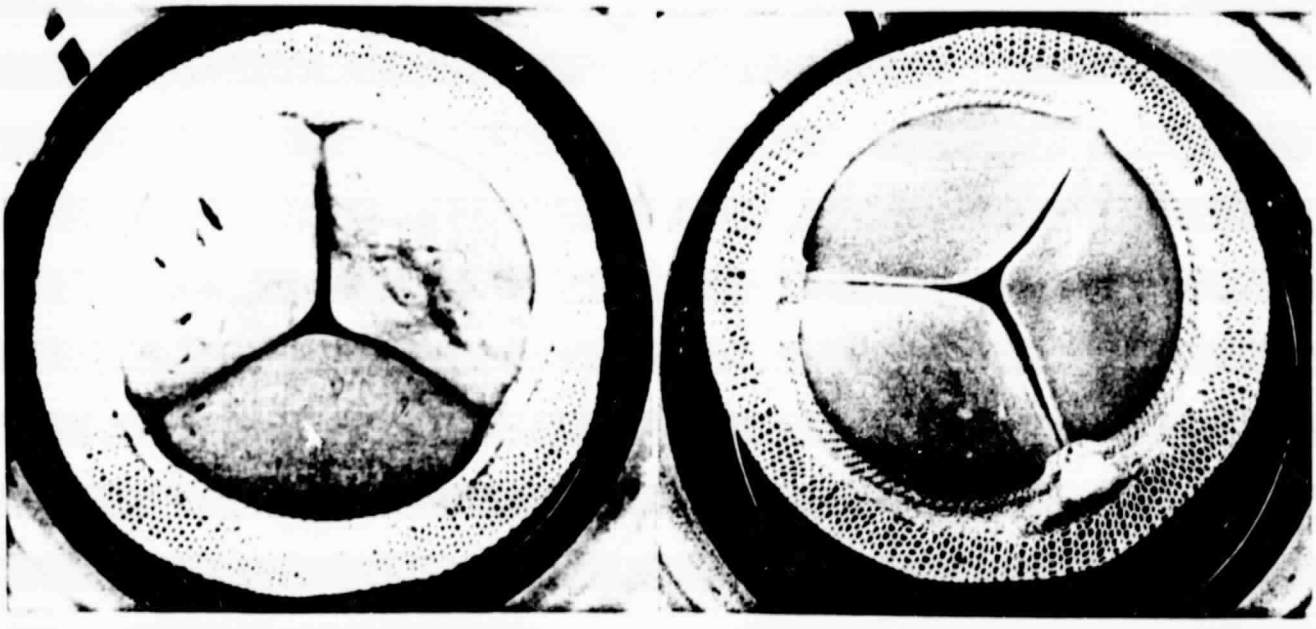

Figs. 29. C-E Valve prior to Accelerated Testing (Inflow and Outflow Sides).

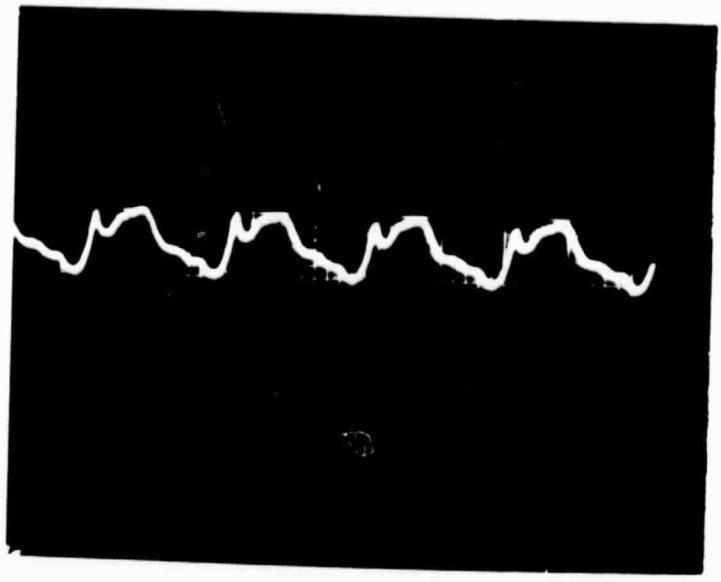

Fig. 31. Closing Pressure on the C-E Valve at the Beginning of the First Accelerated Test Interval

10 million cycles. However, a tear was noted on the I-S valve after 9.38 million cycles. The first interval was stopped at this point and the closing pressures were again recorded at 60 and 70 mm.Hg (Figs. 32 & 33). In Figs. 34 & 35 a complete tear can be seen in the lower right hand corner of one leaflet, while a second tear is about to occur in the upper middle section of another leaflet. The position of the I-S valve had shifted slightly in the chamber just prior to this tearing. This shift in position caused no change in the operation of the valve, still a correlation between the tear and the position shift may, in fact, exist. However, Dr. Gabbay has just completed a fatigue study on 10 I-S valves of the same type, and he stated that initial failures were recognized in over half of his test valves in as early as 3 million to 15 million cycles. Some complete failures even occurred prior to 8 million cycles.[48] The C-E valve appeared to be operating at full capacity with no apparent difficulties at this time (Figs. 36 & 37).

After documentation, the valves were placed back into the aortic flow chamber for the next L.D.A. evaluation. In Figs. 38-41 the profiles are given for the I-S valve after 9.38 million cycles in both the sinus and aortic regions. The overlays (Figs. 42 & 43) show a great amount of reproducibility. In comparison with the profile shapes of Figs. 19a & 19b, those in Figs. 42 & 43 do look very similar. This is quite interesting because it demonstrates the fact that even with basically two tears present in the leaflets of the I-S valve,

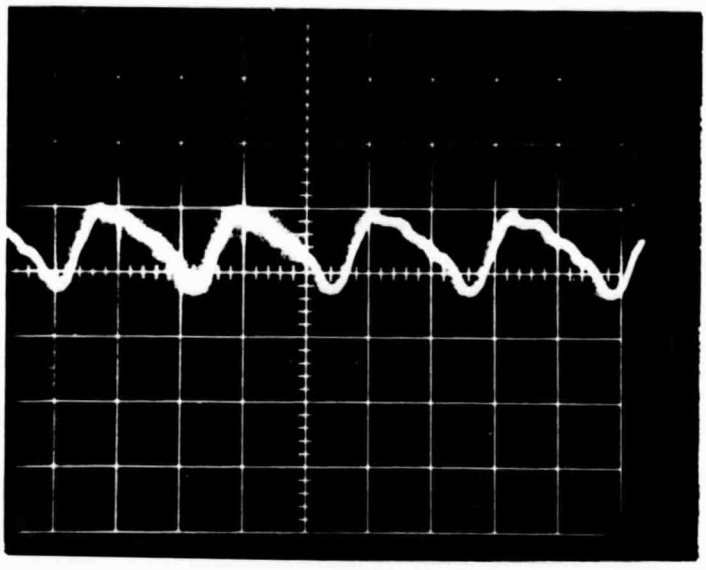

Fig. 32. Closing Pressure on the J-B Valve at the End of the First Accelerated Test Interval.

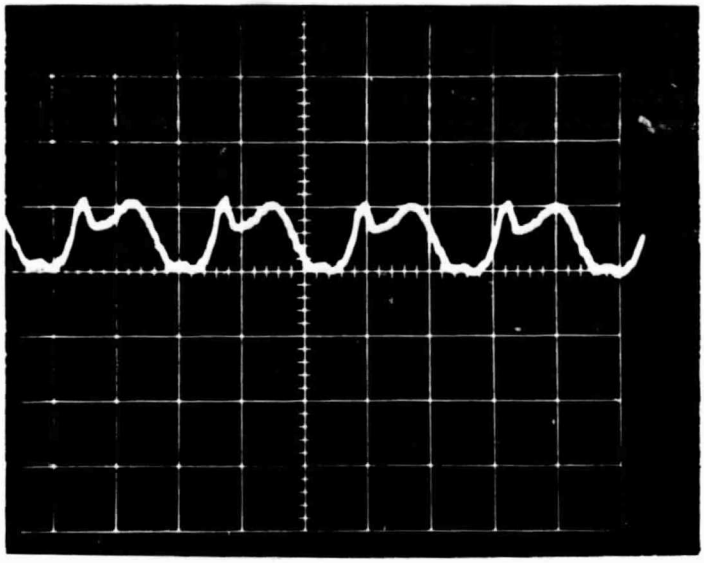

Fig. 33. Closing Pressure on the C-E Valve at the End of the First Accelerated Test Interval.

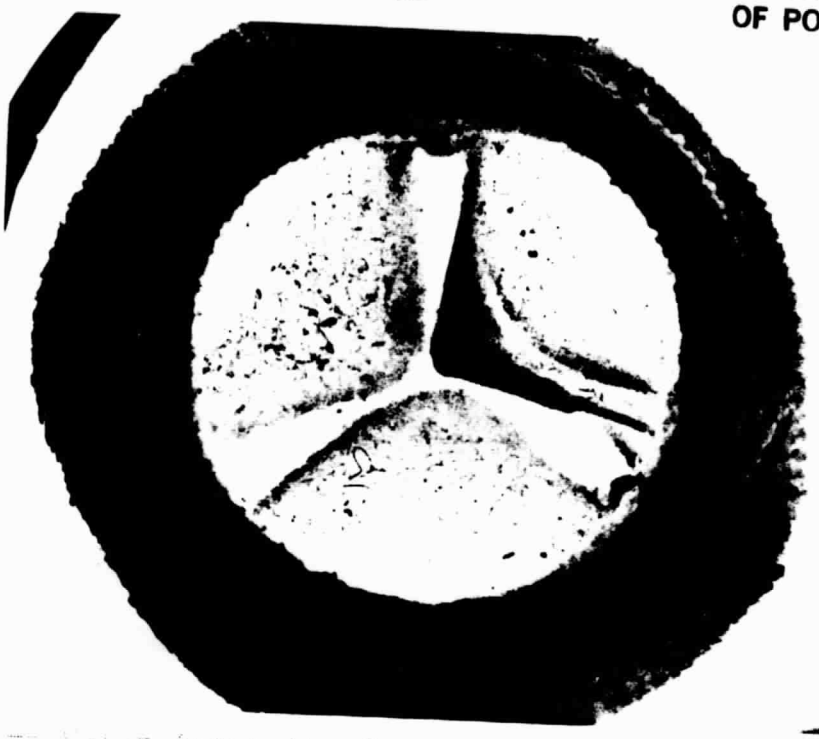

Fig. 34. [illegible] Valve After the First Accelerated Test Interval (Inflow Side).

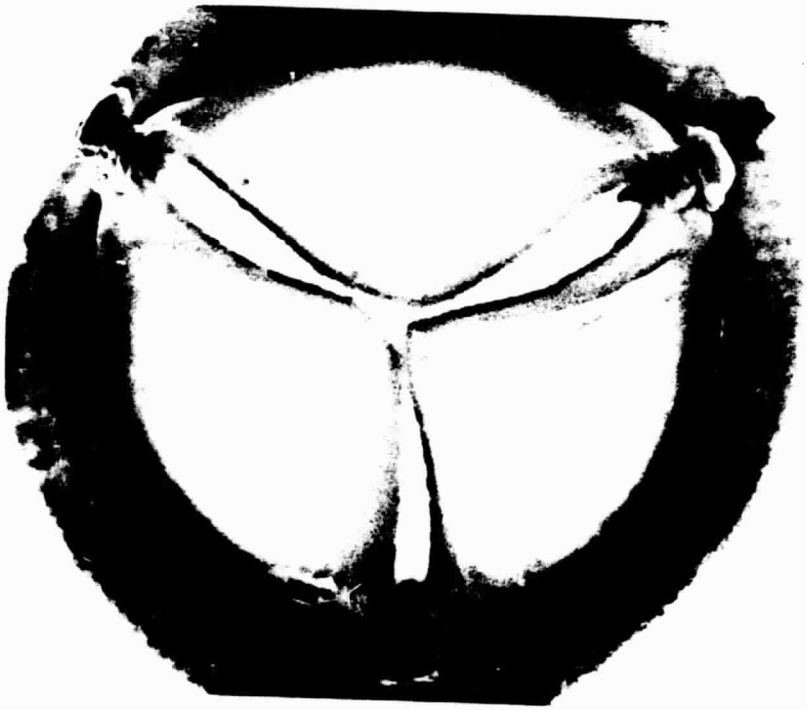

Fig. 35. 1-S Valve After the First Accelerated Test Interval (Outflow Side).

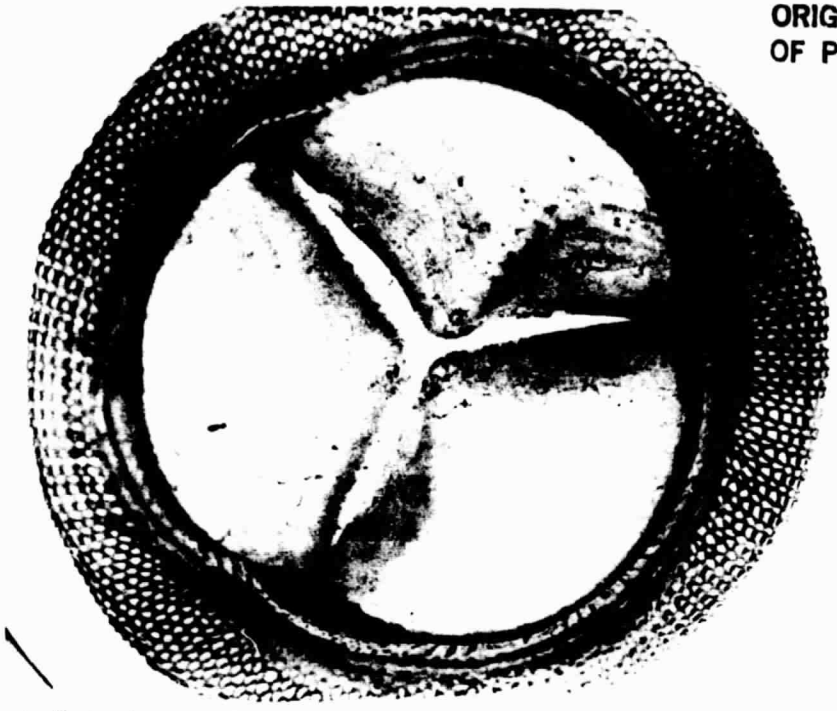

Fig. 36. C-E Valve After the First Accelerated Test Interval (Inflow Side).

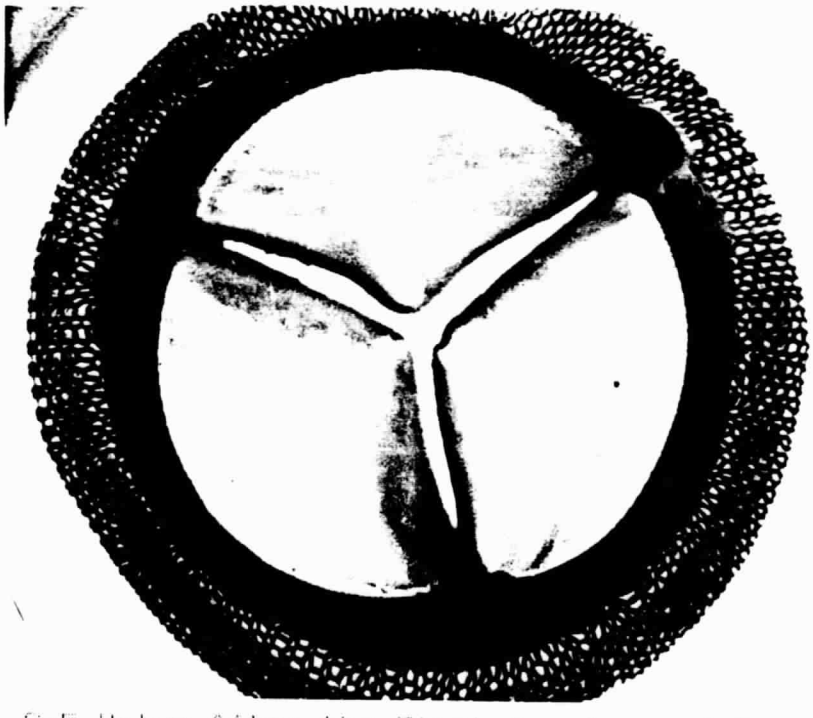

Fig. 37. C-E Valve After the First Accelerated Test Interval (Outflow Side).

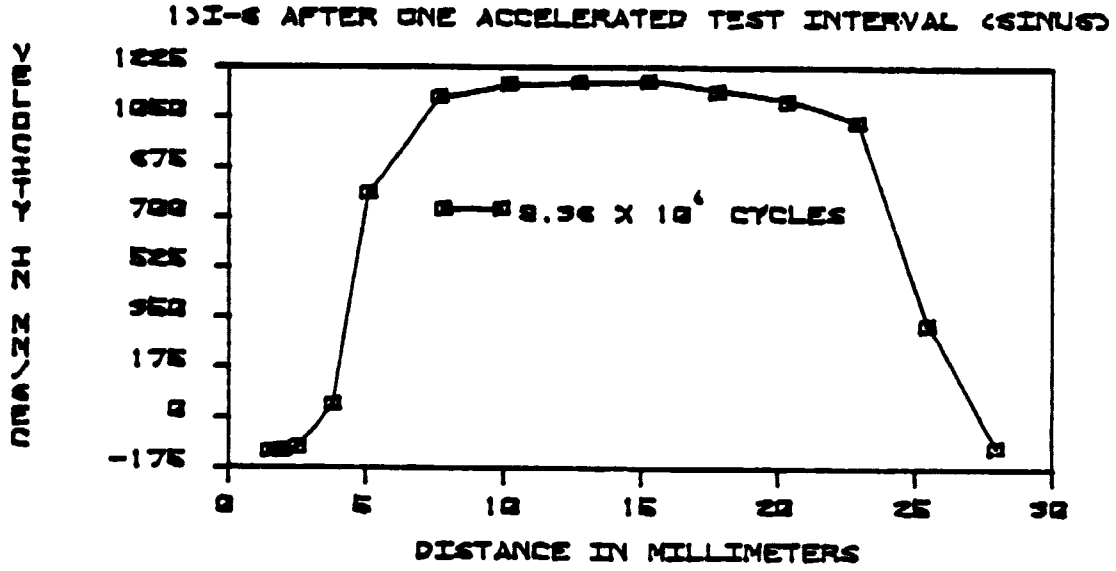


Fig. 38.

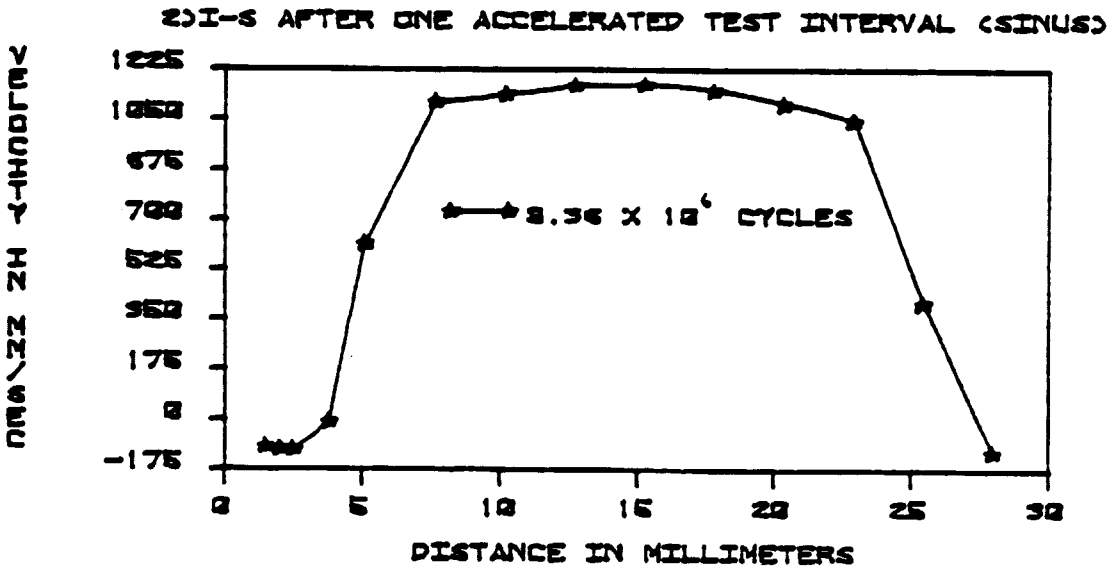


Fig. 39.

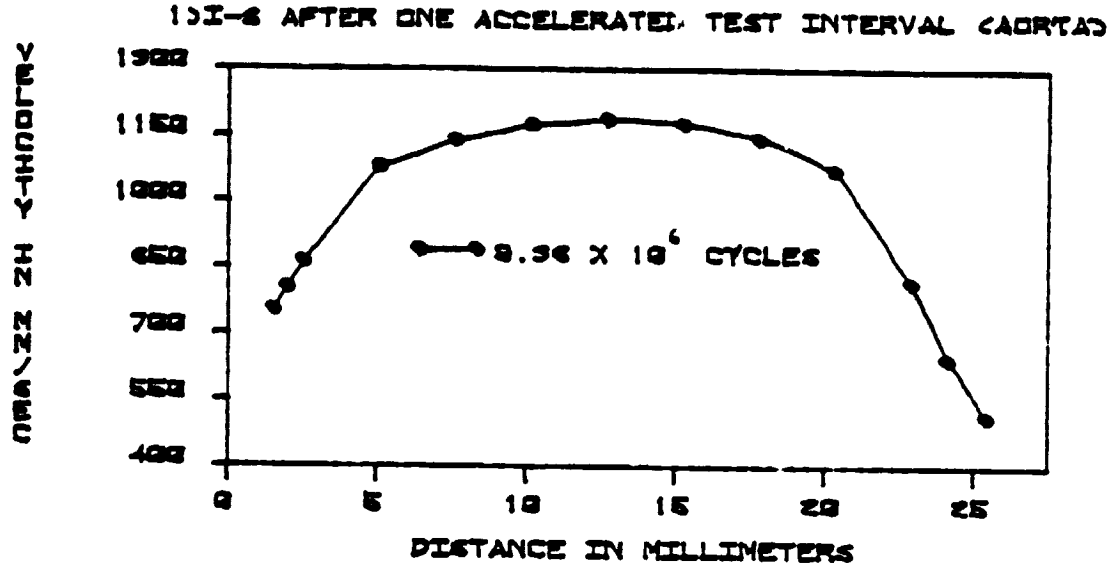


Fig. 40.

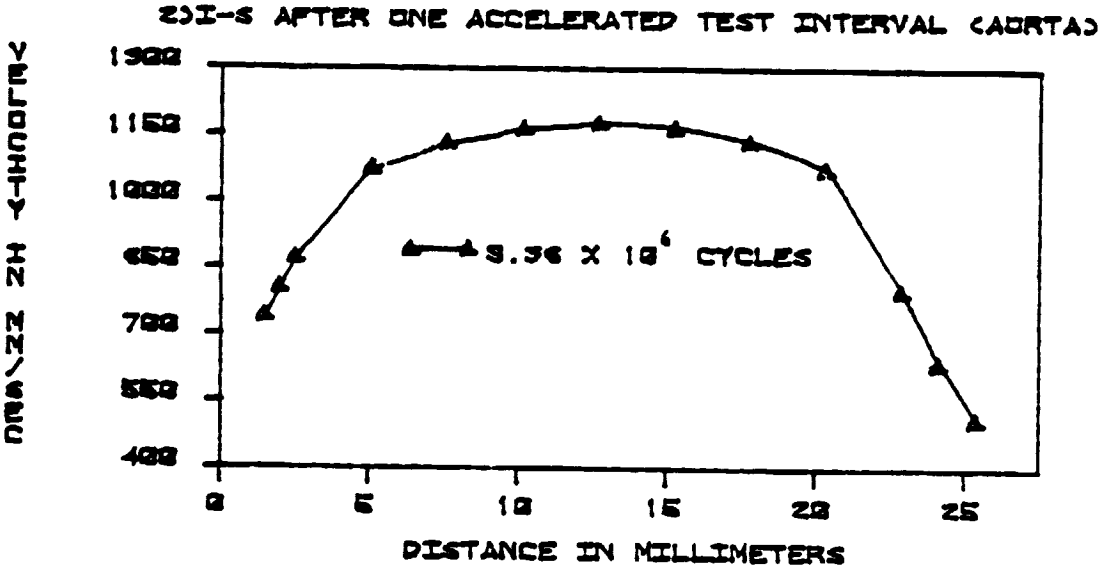


Fig. 41.

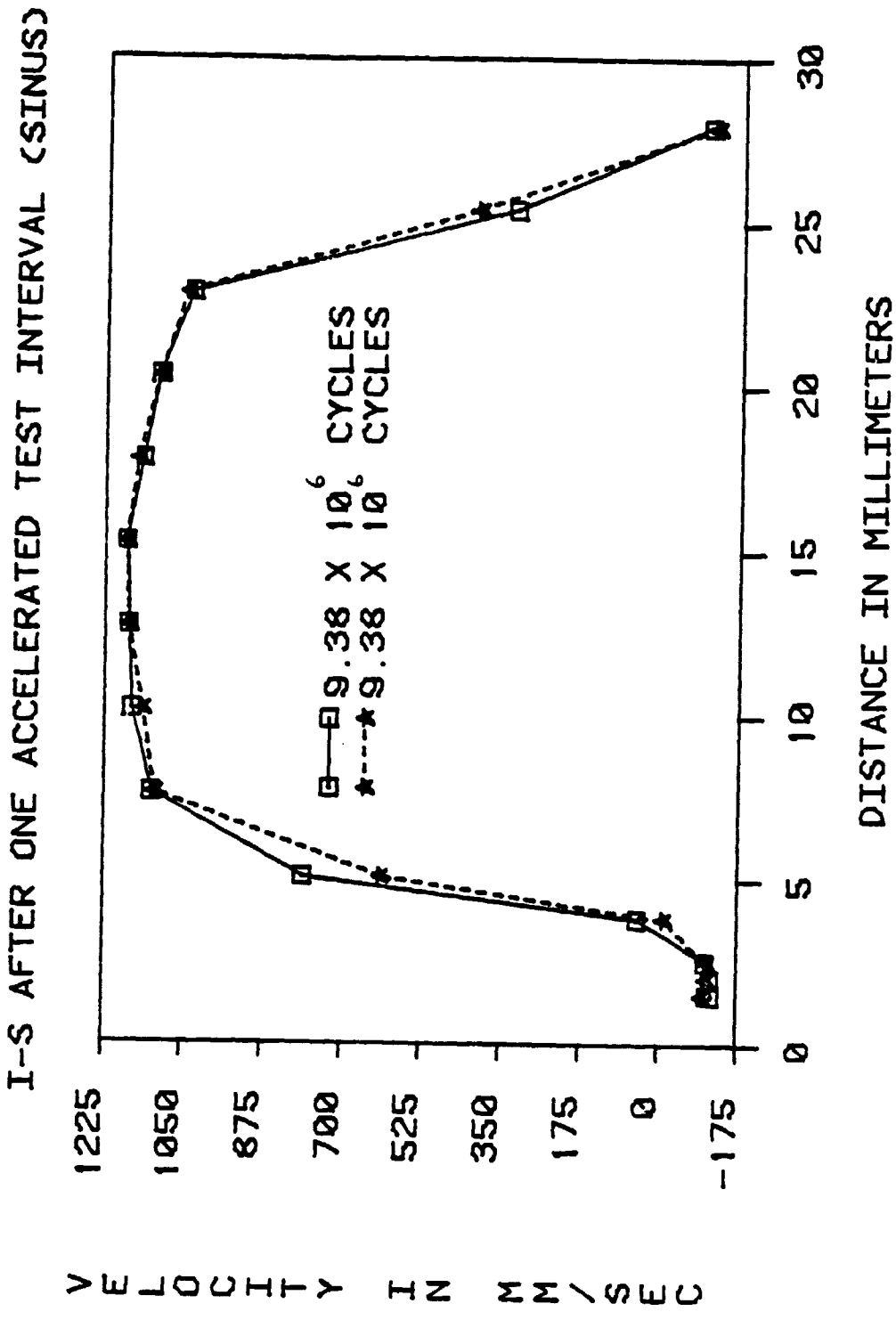


Fig. 42.

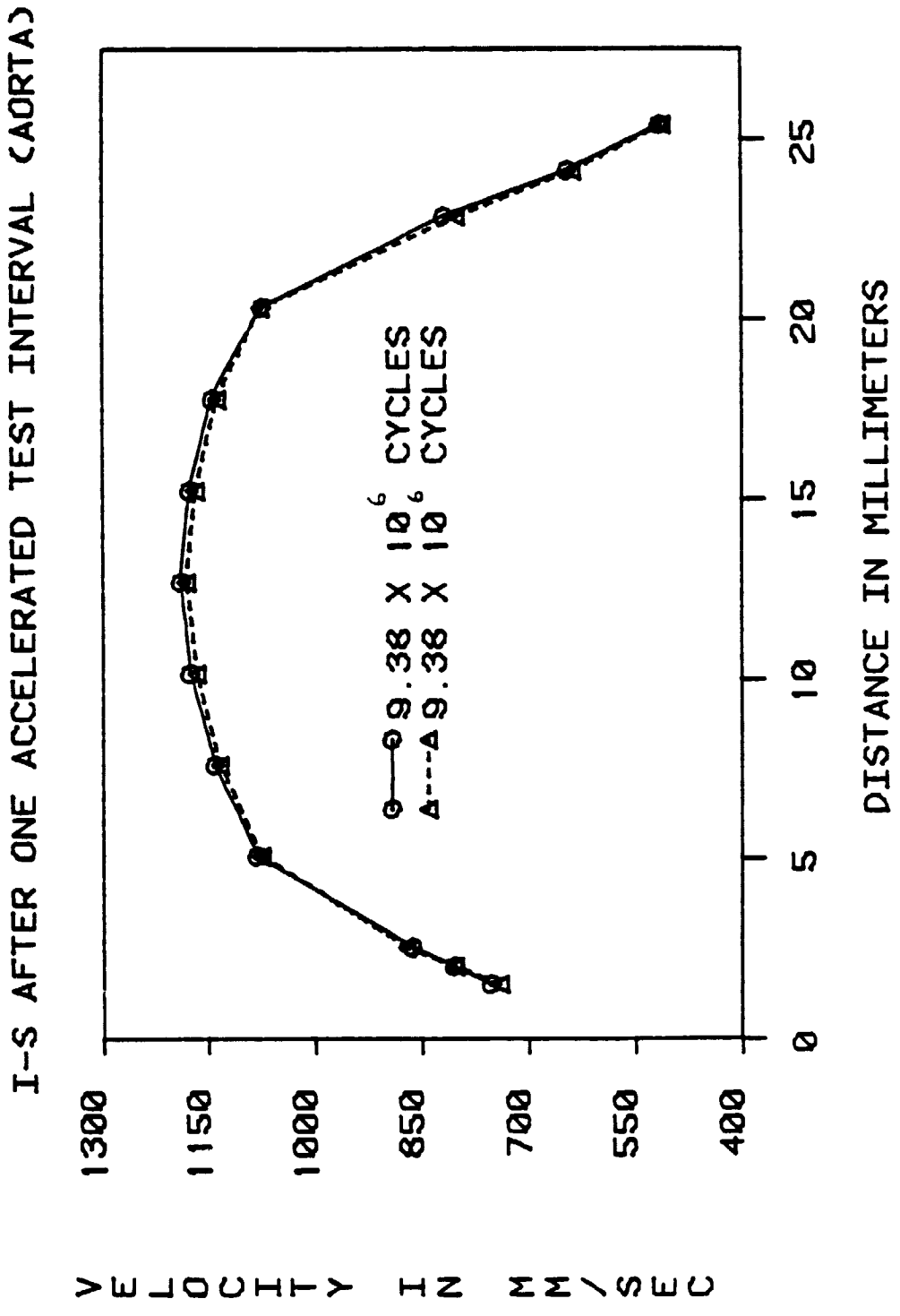


Fig. 43.

the valve was still operating successfully under steady flow conditions. This refers back to the discussion of the advantages of bioprostheses over the totally artificial ones. The point of interest being that the failure of bioprostheses usually progresses slowly, thereby reducing the risk of sudden death and allowing the time necessary to make corrections. In the case of the totally artificial valves, failure is almost always catastrophic and leads to immediate patient death.

The C-E valve also underwent L.D.A. evaluation after the first accelerated test interval (Figs. 44-47). When comparing the overlays of Fig. 26 with 48, the shapes do look similar but Fig. 48's profiles appear somewhat smoother. Part of that might be due to the fact that measurements taken for Fig. 48 were not as close to the inner wall. At both of the walls the velocity obviously drops to zero; this is preceeded by a decrease in the magnitude of the velocity at points very close to the walls. Also the leaflets did not appear to be fluttering as much as before, which might account for the lower magnitude negative velocities in Fig. 48 and the nonexistent negative velocities in Fig. 49. In the overlay in Fig. 49 the profiles which were measured under the same conditions do not demonstrate reproducibility of data. They do show some similarities through the channel up until the near vicinity of the outer wall; close to the outer wall there does exist large unexplainable variances.

At this point the investigation of the I-S valve was complete. The valve had been taken to initial failure in the

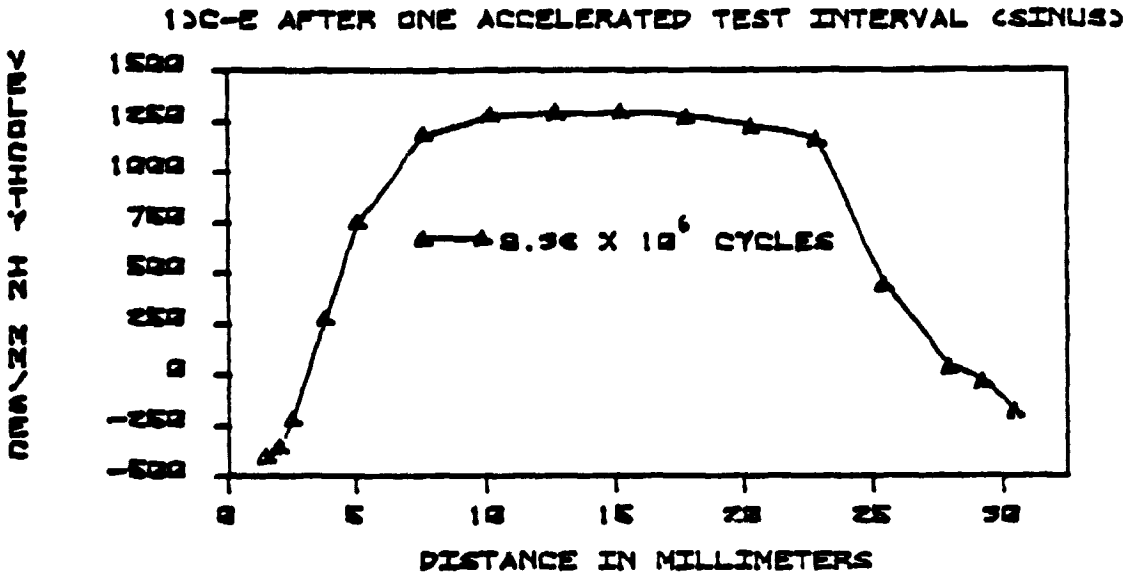


Fig. 44.

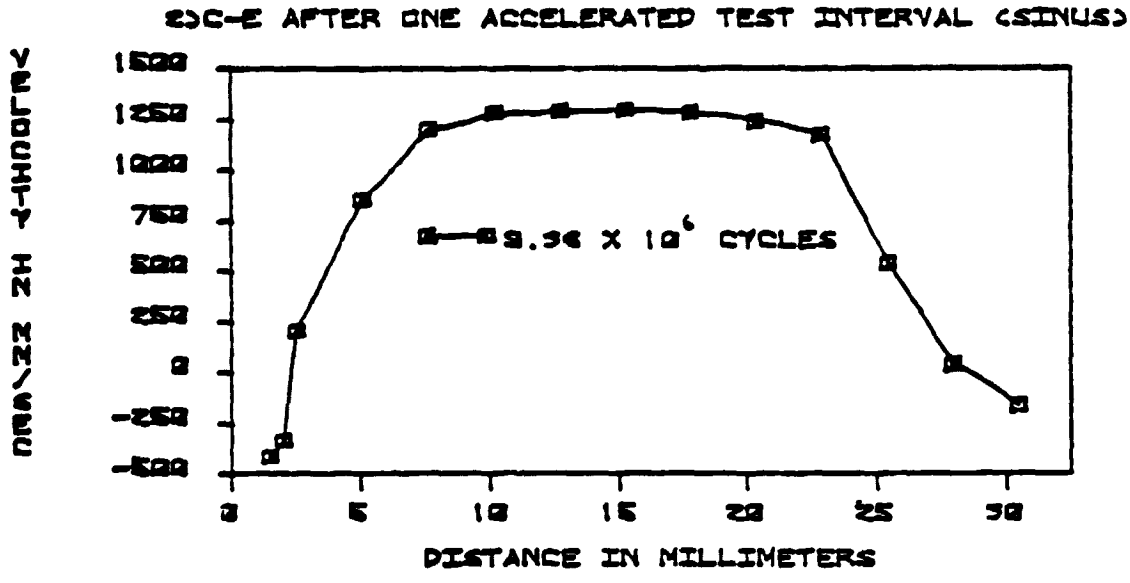


Fig. 45.

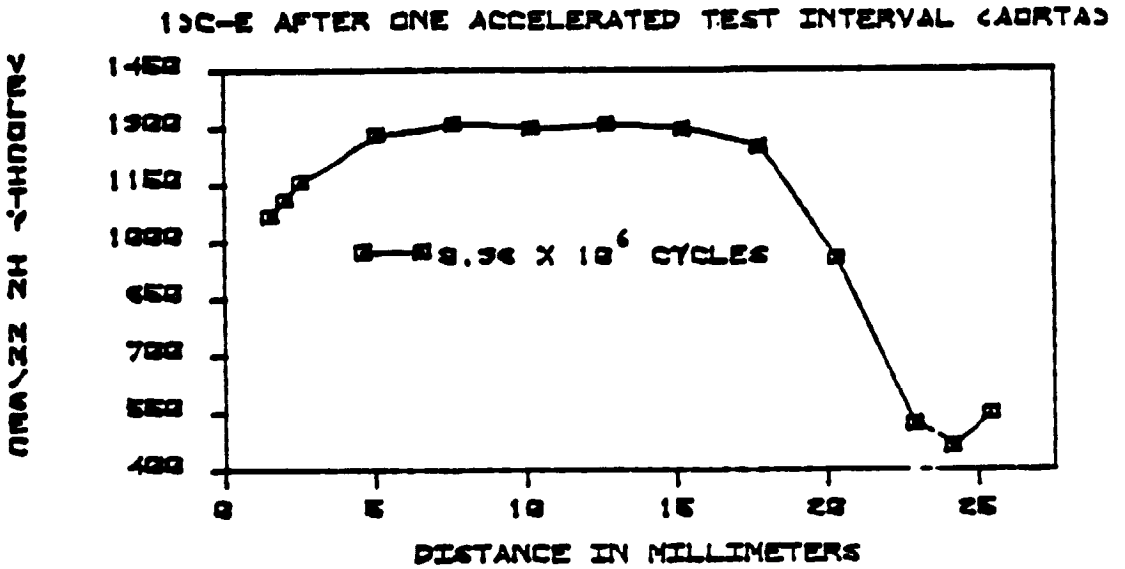


Fig. 46.

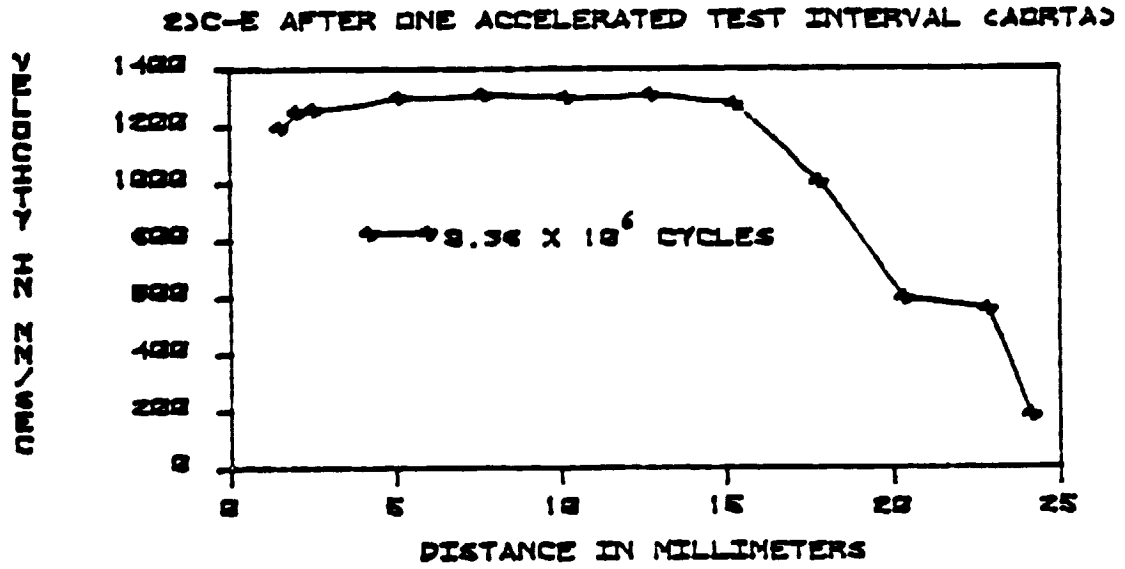


Fig. 47.

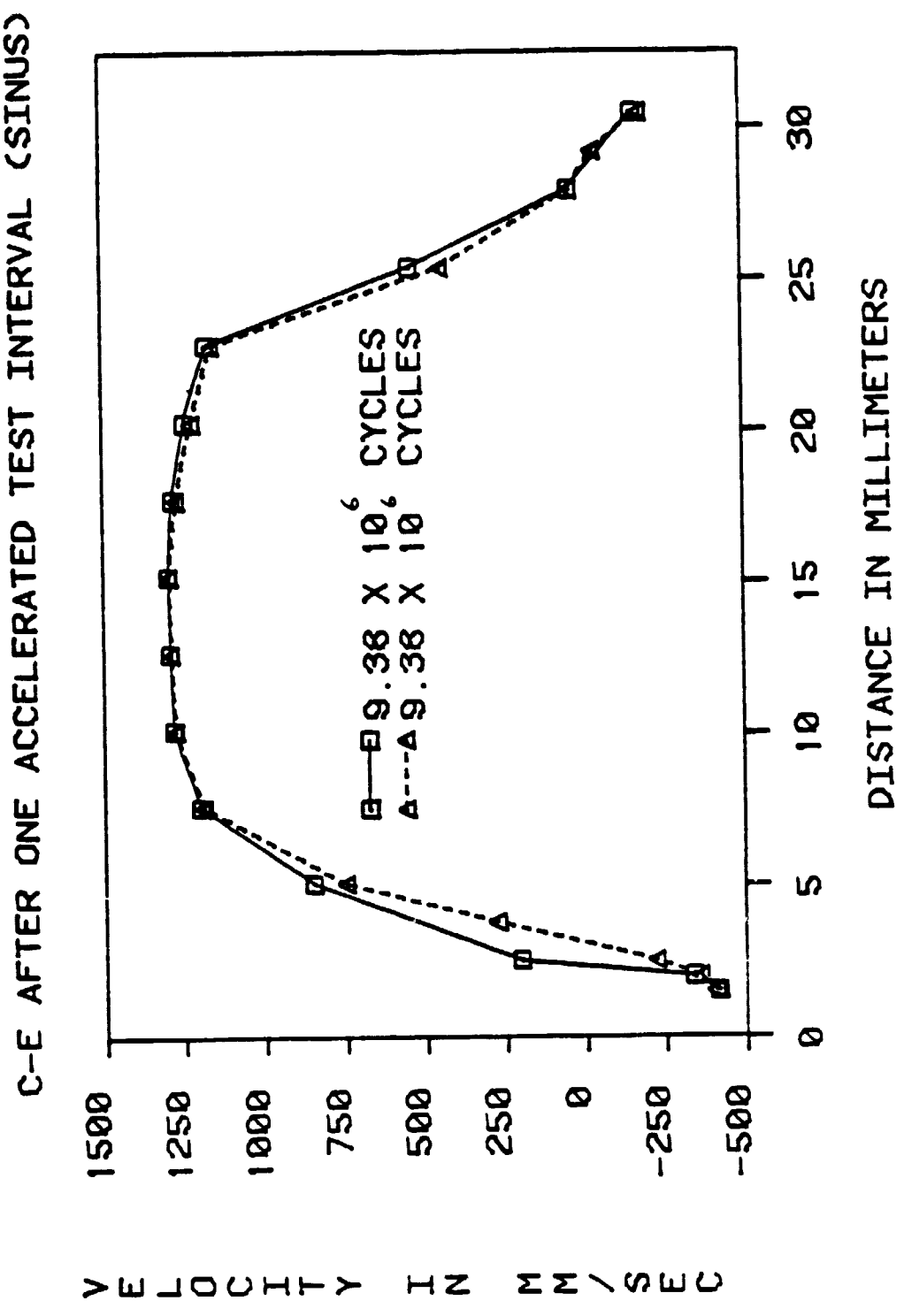


Fig. 48.

ORIGINAL PAGE IS
OF POOR QUALITY

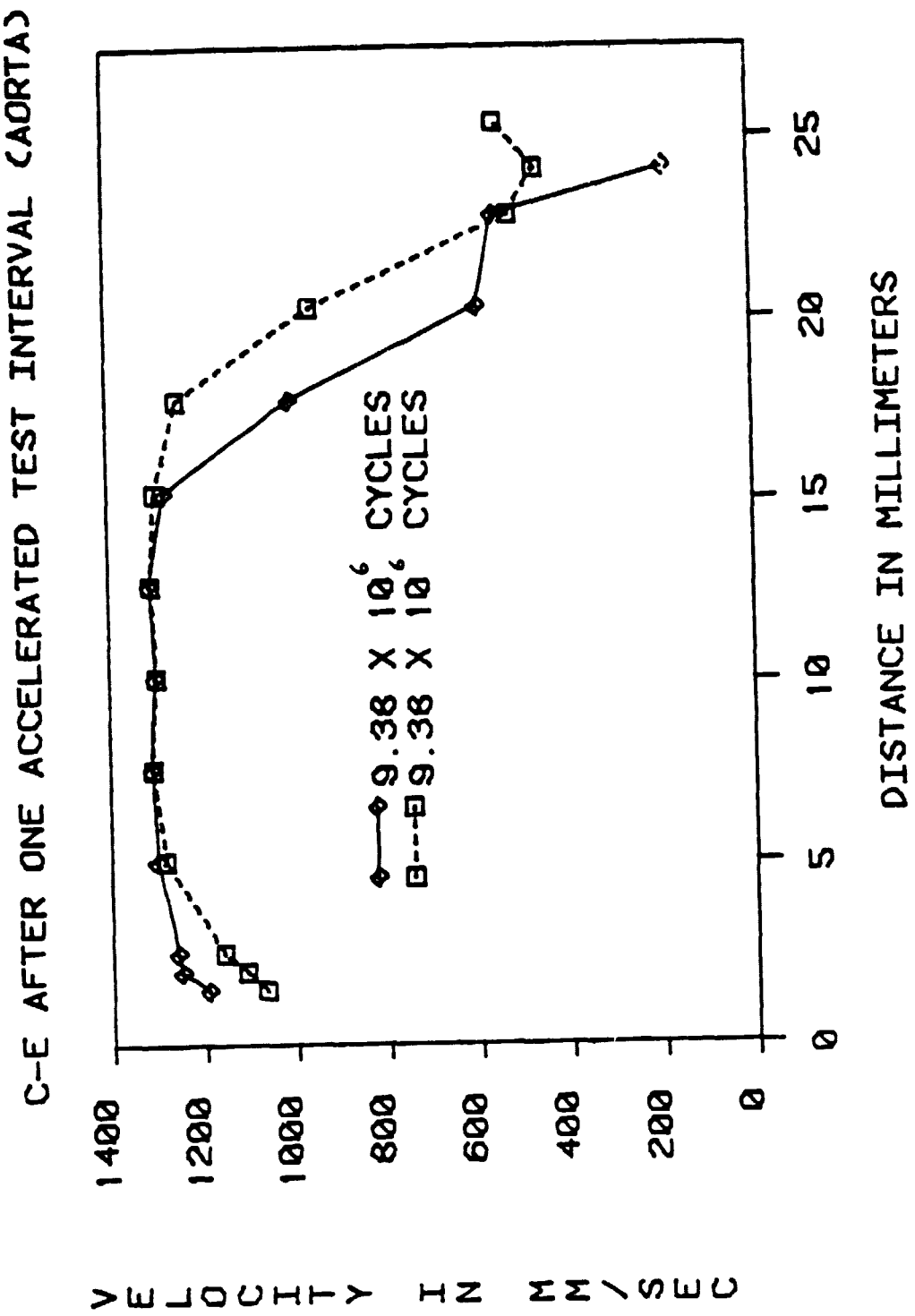


Fig. 49.

accelerated tester. It was placed back into a container filled with saline for storage. The study continued using the C-E valve. The next step was to place the C-E valve back into the accelerated tester for another interval of cycles. Since each accelerated test chamber holds two valves, another valve was needed to run opposite the C-E valve. A ball and cage valve was chosen mainly out of the curiosity to see this type of valve in operation. There seemed to be a fair amount of vibration in the system due to the opening and closing of the ball and cage valve. This became apparent when making the closing pressure measurements on the tissue valve. Small variations appeared in the peak values, but none exceeded the 100 mm.Hg physiologic limit. Multiple photographs were taken to guarantee this fact (Figs. 50-52). The closing pressure for the C-E valve was in the range of 80 to 90 mm.Hg. The accelerated test continued to run smoothly up through approximately 20 million cycles on the C-E valve. At that point, a few areas of thinning at the upper part of the prong were noted, where the tissue is sutured in place. The decision was made to allow the system to keep running until a tear in one or more leaflets could be discerned. At 23.91 million cycles a tear became evident in one leaflet at the region of thinning. Closing pressure measurements were again made indicating an 85 mm.Hg closing pressure (Fig. 53), and then the valve was removed for visual inspection. This type of tear was found to be somewhat common both clinically and also as a result of fatigue testing.[13,44,48,50]

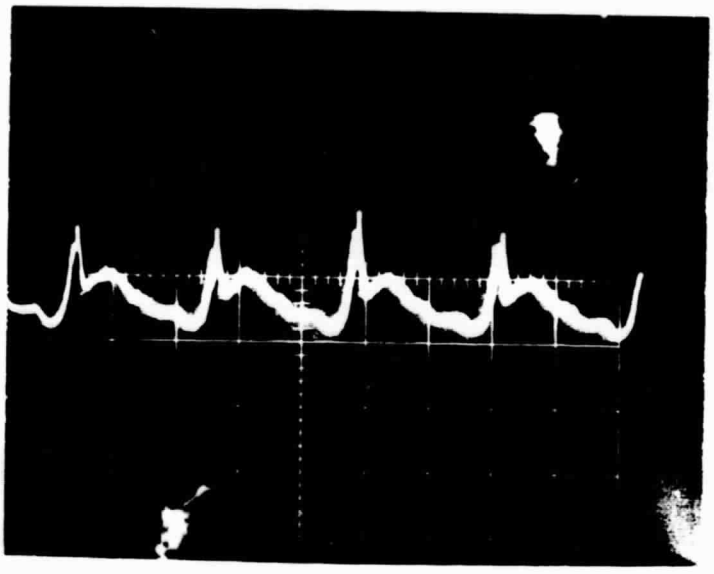

Fig. 50. Closing Pressure on the C-E Valve at the Beginning of the Second Accelerated Test Interval.

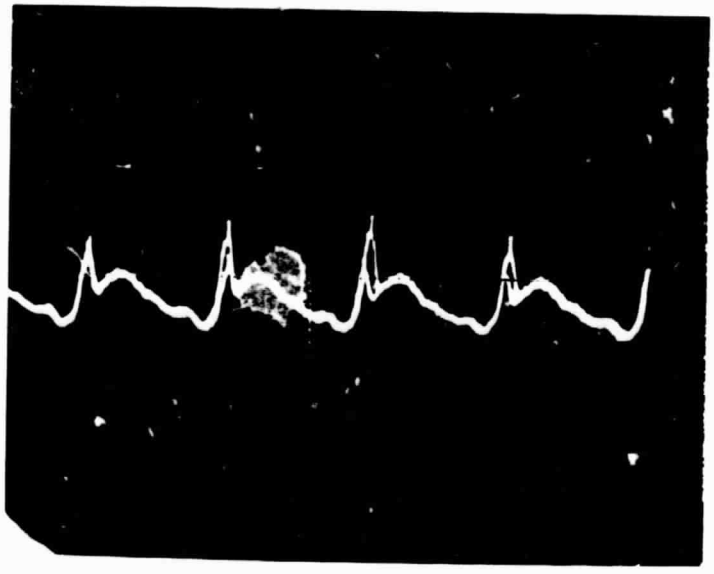

Fig. 51. Closing Pressure on the C-E Valve at the Beginning of the Second Accelerated Test Interval.

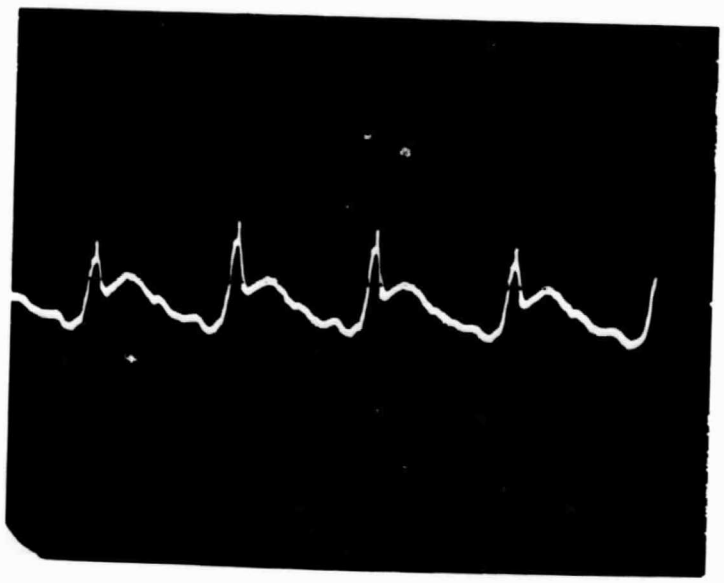

fig. 52. Closing Pressure on the C-E Valve at the Beginning of the Second Accelerated Test Interval.

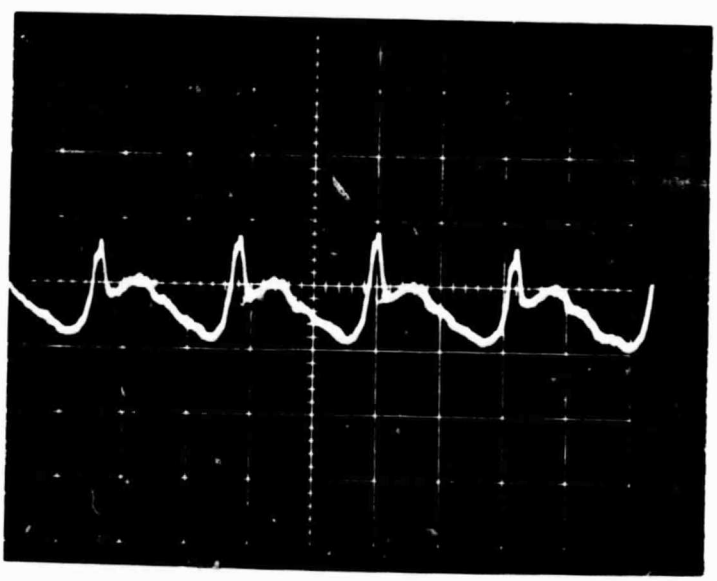

fig. 53. Closing Pressure on the C-E Valve at the End of the Second Accelerated Test Interval.

The region of failure may not be easily seen in the photographs (Figs. 54, 55), so a schematic drawing has been added for clarification (Fig. 56).[48] As was true with the I-S valve, the C-E valve was still operating successfully with one tear present and two others about to occur. The evidence for this claim is contained in Figs. 57-62. The sinus region profiles in Fig. 61 are very similar in shape and peak velocities to the previous set in Fig. 48. The profiles in the aortic region (Fig. 62) look even better then those seen in Fig. 49, and again no residual effects from the sinus region are present, in the form of flow reversals.

The final data analysis comes from comparative velocity profiles at various accelerated test intervals overlayed onto one another (Figs. 63-66). These final profiles were obtained through averaging all of the corresponding data points, and thus they should be the most accurate. In Fig. 63 the profiles of the I-S valve resemble each other in shape but are noticeably different in peak velocity. This is also found to be true in Fig. 64. When looking at the C-E valve data (Figs. 65 & 66), the same result is seen. The peak velocities show a marked difference for either the I-S or C-E valve with zero cycles as compared to the same valve with 9.38 or 23.91 million cycles on it. This difference always takes the shape of a decrease in peak velocity with fatigue. If one looks closely at the sinus region data for both valves (Figs. 63 & 65), even though the shapes do resemble each other, there is a definite difference in the width

Figs. 54. & 55. C-E Valve After the Second Accelerated Test Interval (Inflow and Outflow Sides).

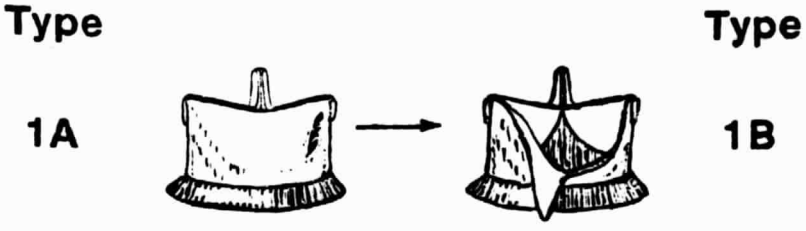


Fig. 56. Schematic Drawing of the Initial Failure of the C-E Valve (1A) and Predicted Complete Rupture (1B). (S. Gabbay, et al., J. Thorac. Cardiovasc. Surg., In Press).

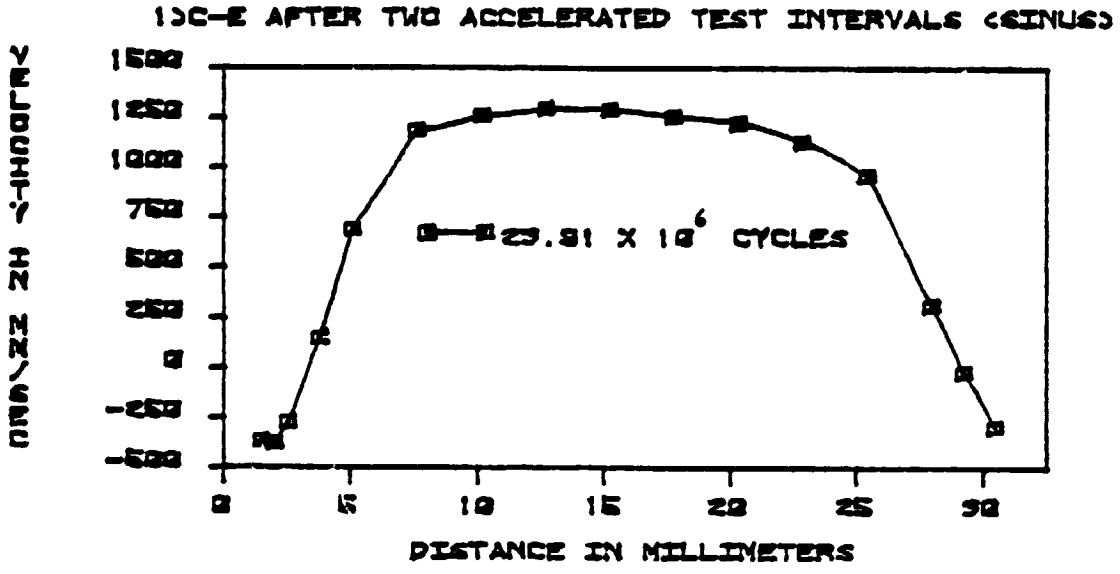


Fig. 57.

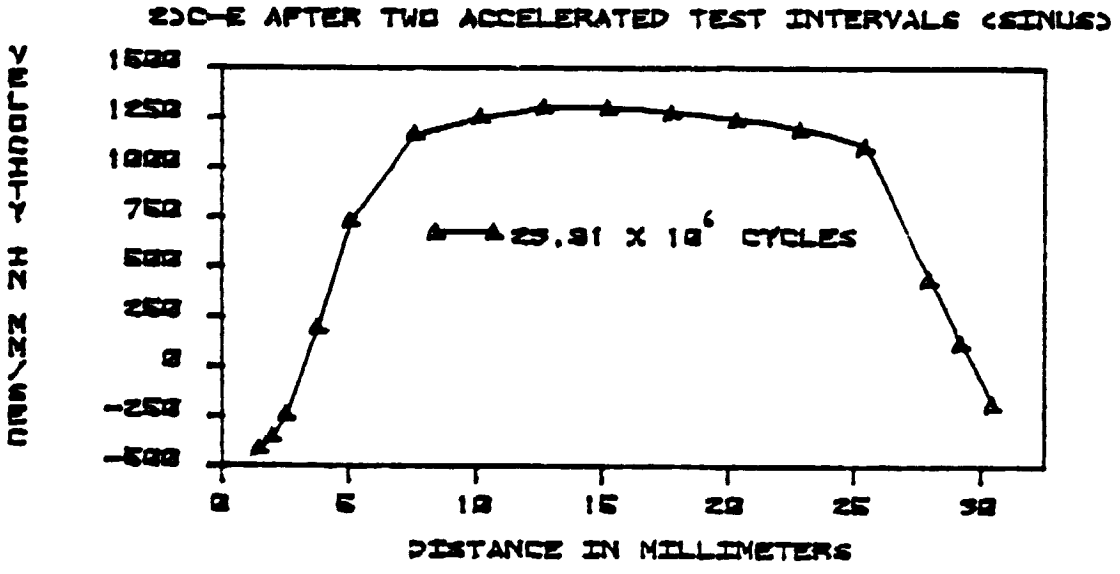


Fig. 58.

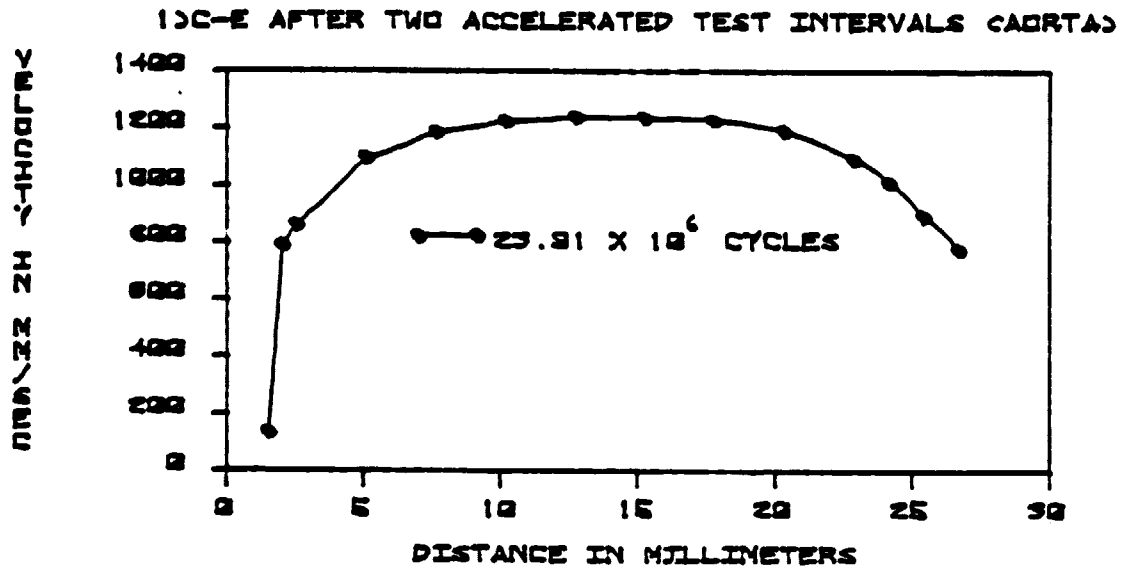


Fig. 59.

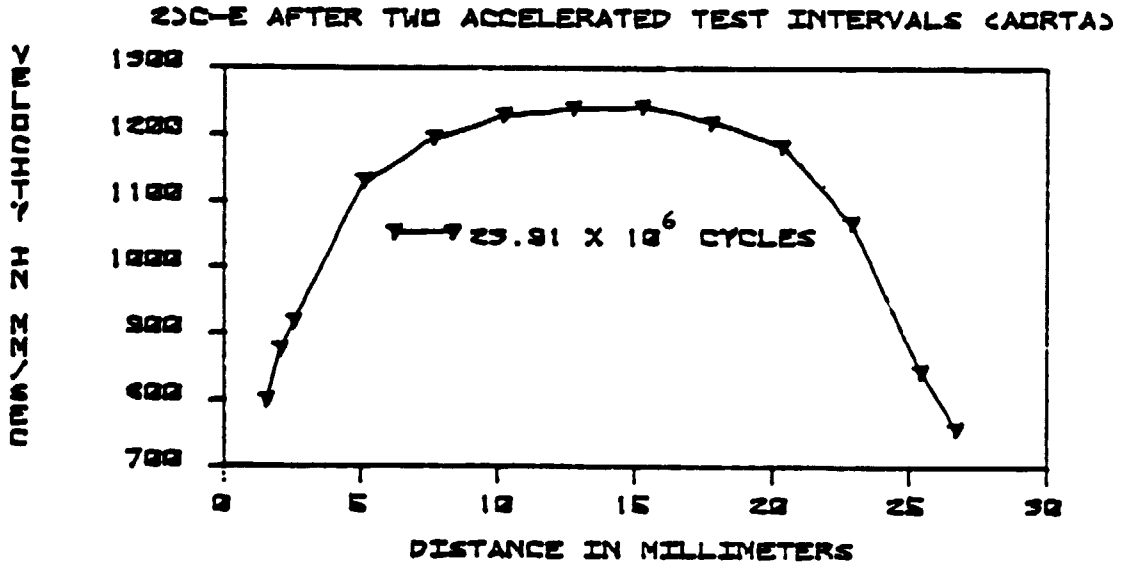


Fig. 60.

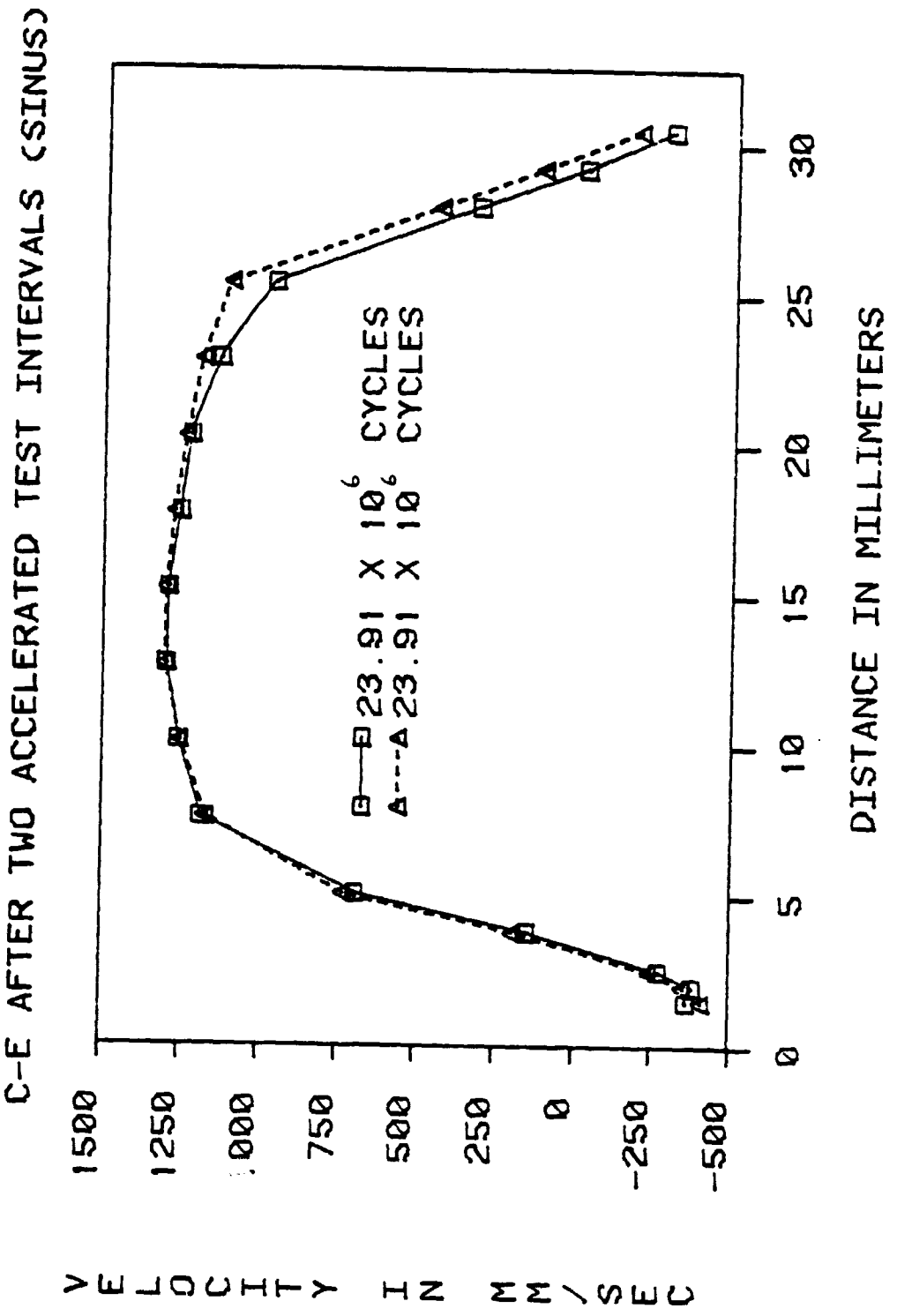


Fig. 61.

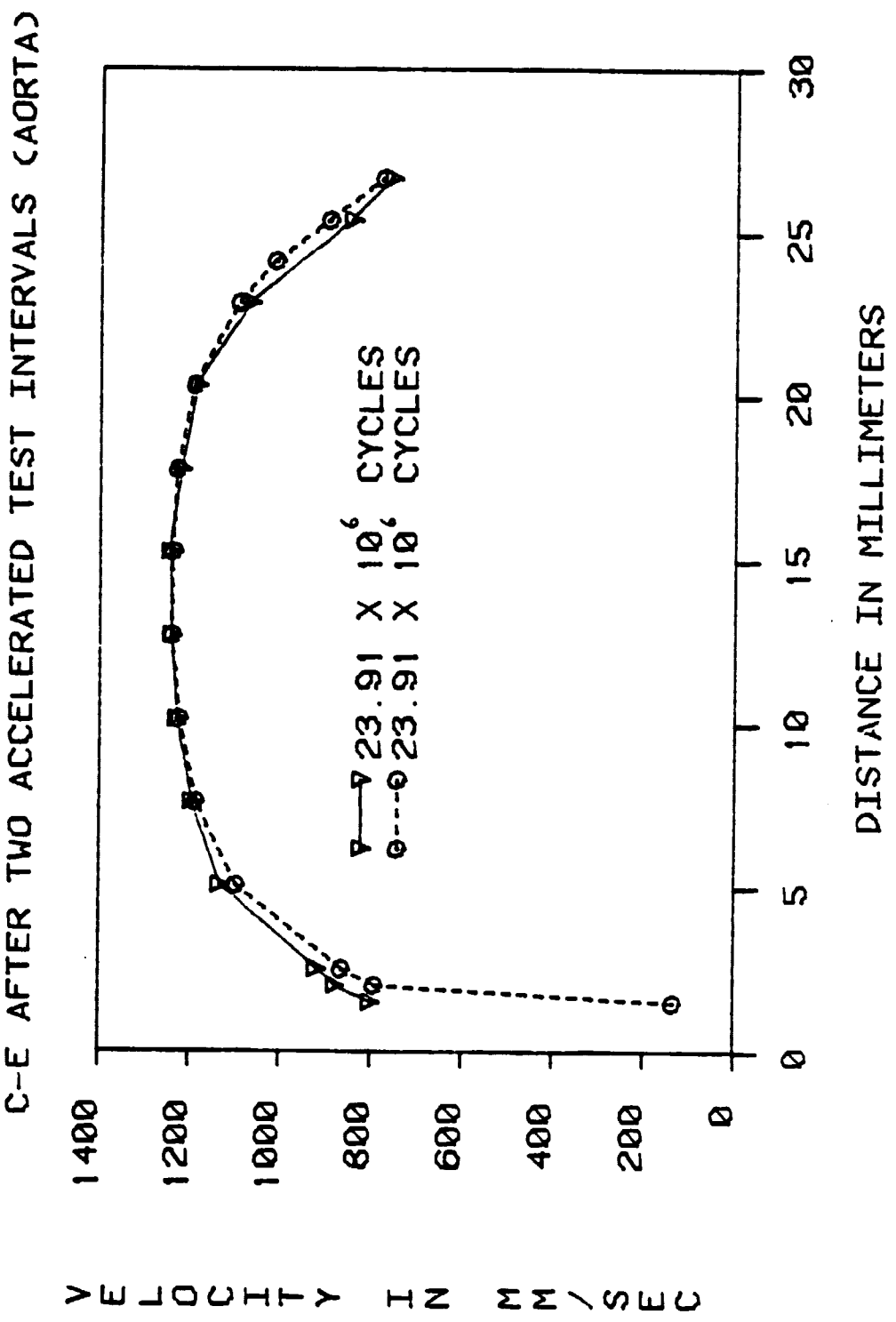


Fig. 62.

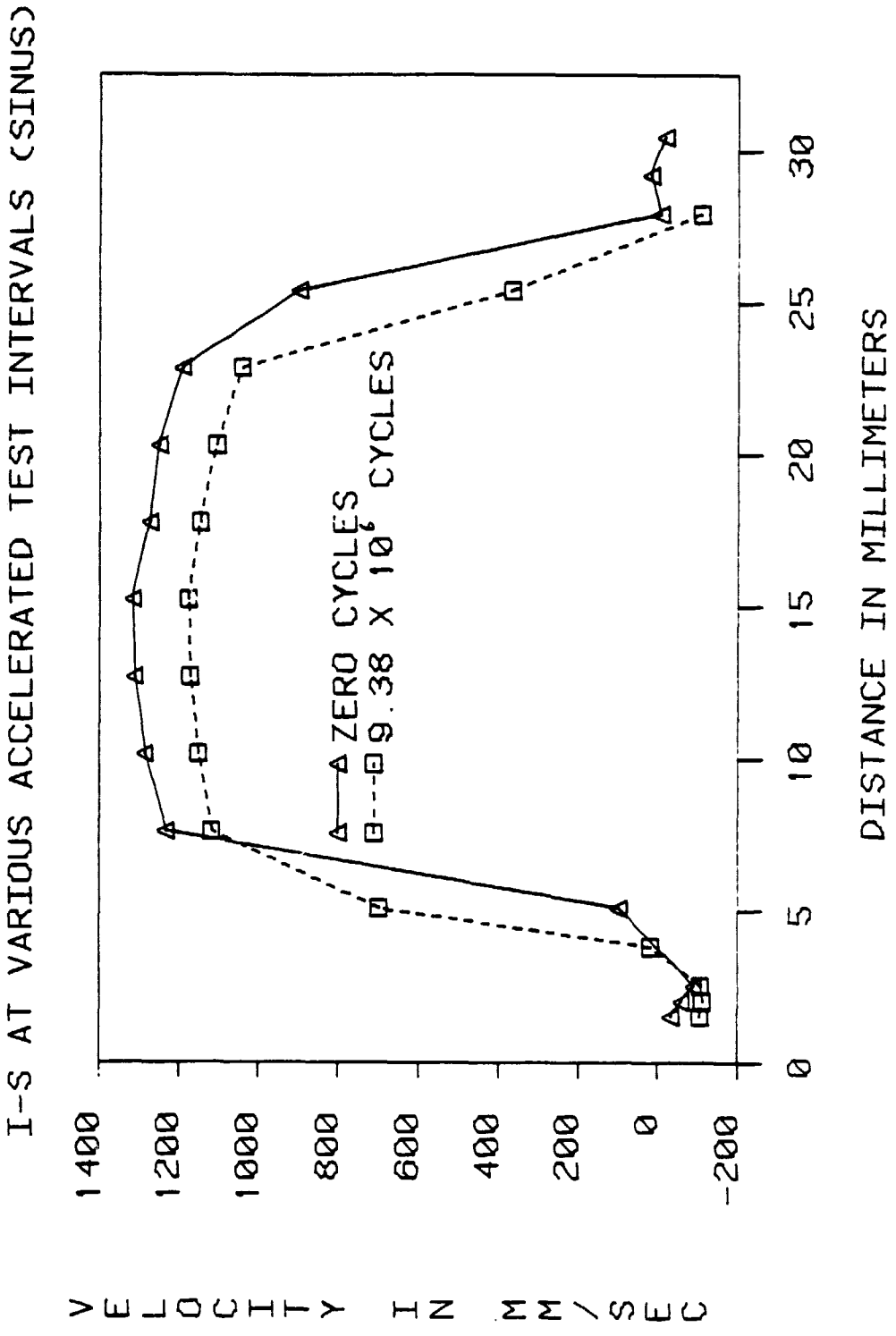


Fig. 63.

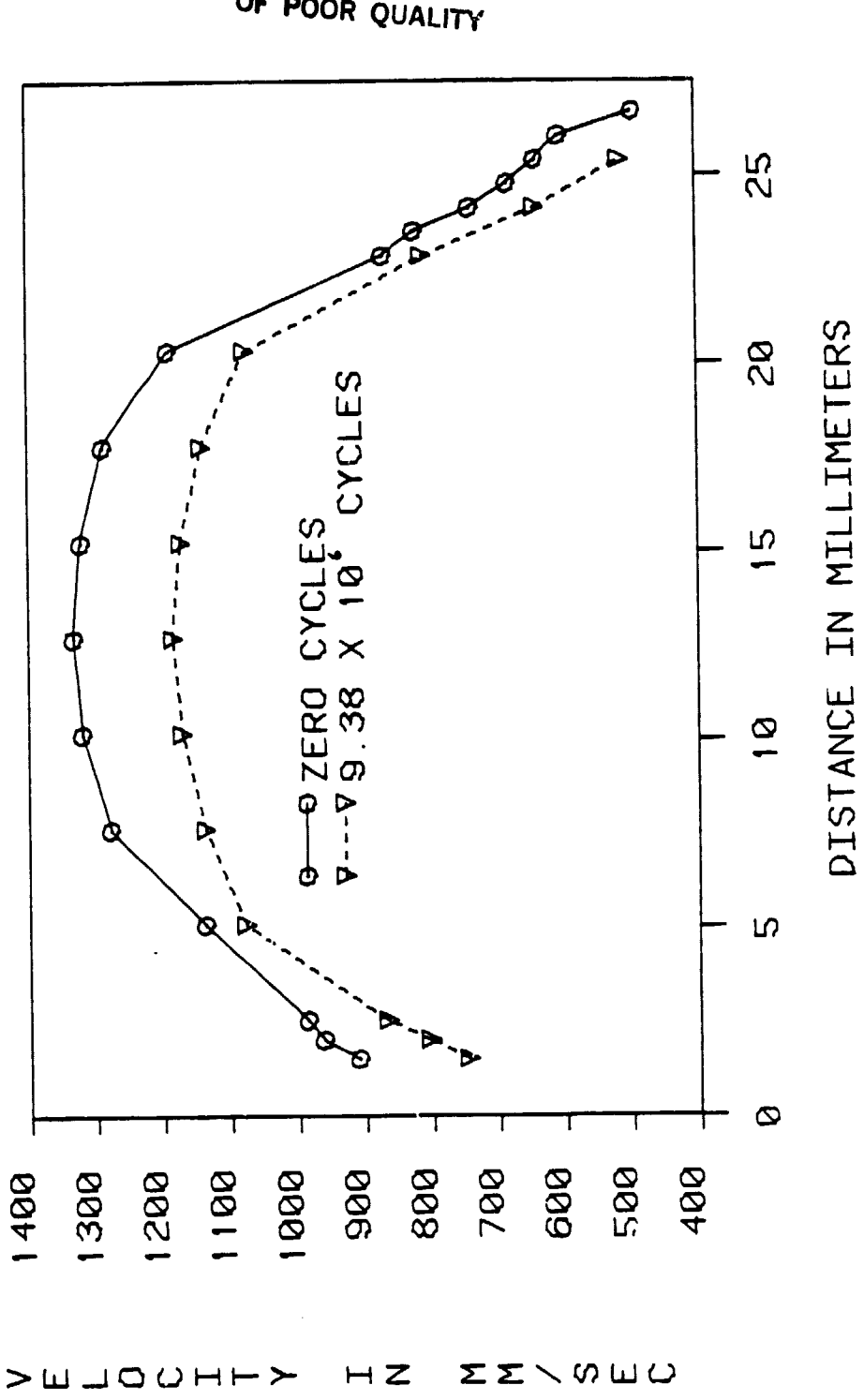


Fig. 64.

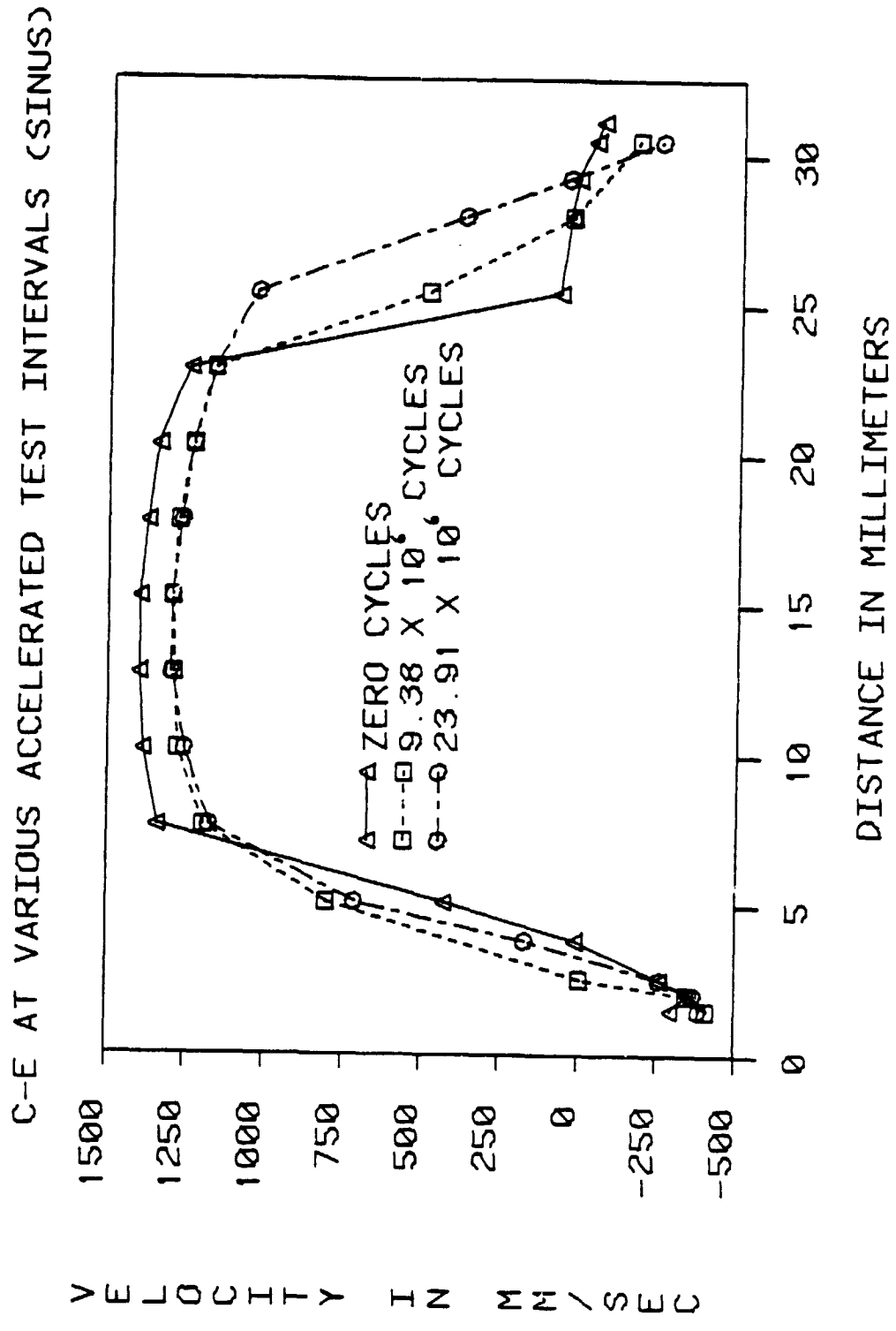


Fig. 65.

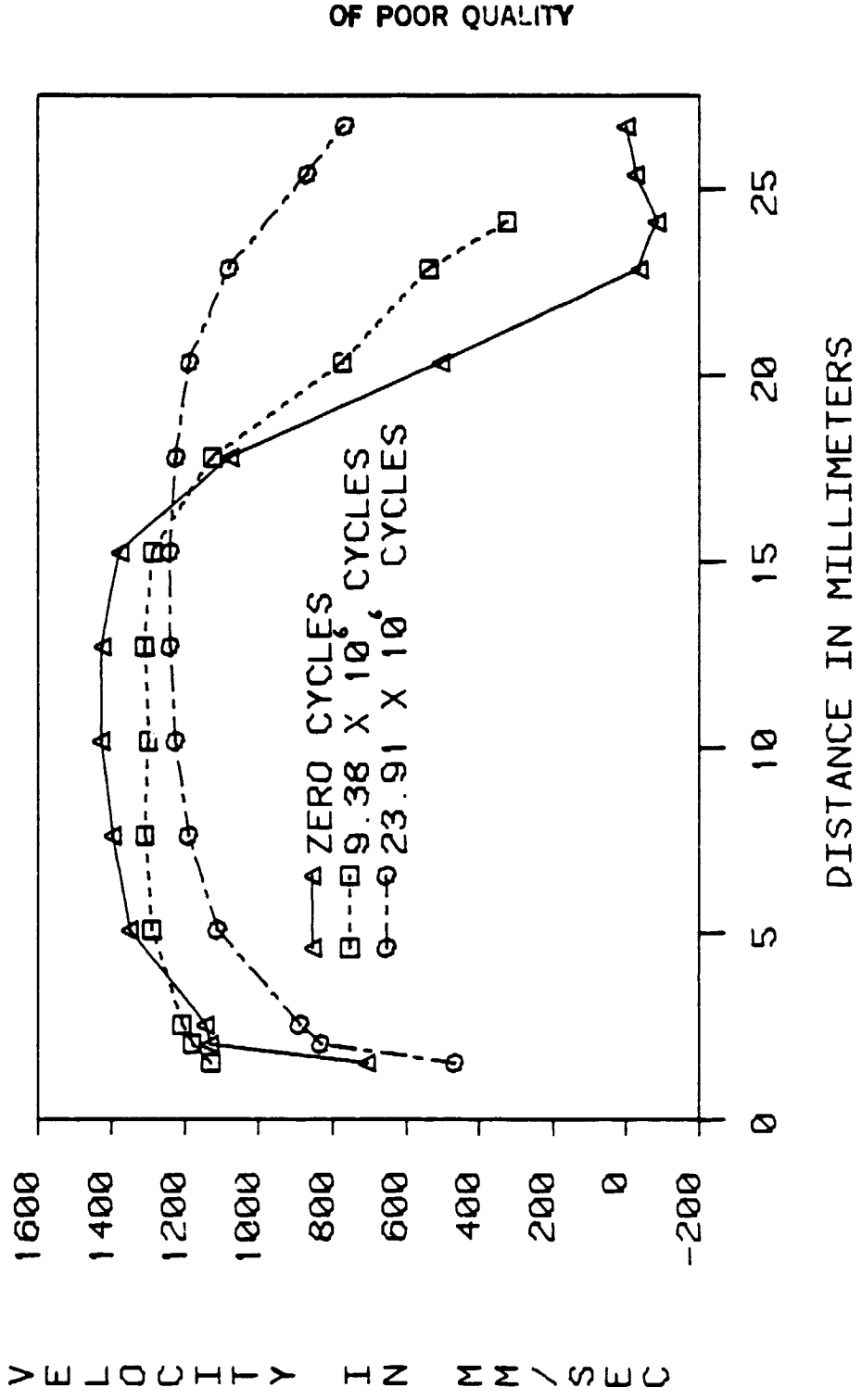


Fig. 66.

of the profiles. The profiles from the fatigued valves are wider, indicating in essence a larger flow area. This of course would go hand in hand with a drop in peak velocity. As the cross-sectional flow area becomes larger, the internal pressure differential in the system will become smaller. This drop in the pressure differential causes the fluid velocities to also be reduced. One other point that comes to mind from the C-E valve data (Figs. 65 & 66) is that the profiles obtained after the second accelerated test interval look somewhat similar to the ones obtained after the first interval. This could be an indication that the major changes which take place in the valve occur after the first few million cycles.

In terms of time frames, Dr. Gabbay states that at accelerated rates of 1800 R.P.M. and closing pressures of 70 to 80 mm.Hg, there exists a 12 to 1 ratio between time to failure in the Shelhigh F.T.S. #2 and the time to failure in vivo.[48] He also states that at 1000 R.P.M. with closing pressures in the same range, the ratio drops to 4 or 6 to 1.[48] At a 1300 R.P.M. rate with closing pressures ranging from 60 to 85 mm.Hg, an estimate of the ratio between the onset of failure in the fatigue tester and what is seen clinically should be about 7 or 8 to 1. Since the initial failure of the I-S valve occurred at approximately 9.4 million cycles in the fatigue tester, the same type of failure should have occurred at about 75 million cycles in a patient. Remembering that 40 million cycles corresponds to one year's worth of use, signs of initial failure in a patient

should have occurred just prior to two years of implantation. The C-E valve would not have shown signs of initial failure until about 190 million cycles, corresponding to just under 5 years of implantation.

# CONCLUSIONS

The purpose of this project was to assess the durability of certain bioprostheses through the use of a study which combined L.D.A. measurements with accelerated testing. An attempt was made to correlate information obtained through the use of these two research tools. The results of this study indicate that the hydrodynamic performance does, in fact, change with fatigue (time in use). The major change that occurred was a drop in the peak flow velocity due to an increase in the high velocity cross-sectional flow area. It seems that the collagen fibers in the pericardial tissue undergo a rearrangement of some type, as can be seen by the thinning areas in the leaflets.[51,52] Tissue does not work harden like a metal, but instead becomes more flaccid in certain areas. This flaccidity leads to tears, which were apparent at approximately 9.4 million cycles for the Ionescu-Shiley valve and at about 24 million cycles for the Carpentier-Edwards valve. The corresponding implantation time to initial failure was approximately 2 and 5 years for the Ionescu-Shiley and Carpentier-Edwards valves respectively.

The characteristic peak flow velocity change is easily identifiable by L.D.A., but L.D.A. can only be done in vitro. There is a technique used, however, for the investigation of stenotic vessels in vivo called Doppler Ultrasound. This technique is used to measure peak blood flow velocities. If Doppler Ultrasound could be used at specified time intervals in the near vicinity but downstream from a tissue valve, it might be possible to monitor the functioning of the tissue

valve in vivo over time. At this point, there does exist another biological problem which has not been addressed, called calcification. Basically, this is the deposition of lime salts in the tissue of the bioprostheses. This causes the tissue to become rigid and the valve to become stenotic.[53-55] However, those involved in the field of bioprostheses seem to believe that the calcification problem will be overcome in the near future, through different tissue stabilizing methods.[56] Therefore, Doppler Ultrasound may become a feasible technique for monitoring the function of bioprostheses over time in vivo.

BIBLIOGRAPHY

1. C.R. Lam, H.H. Aram, and E.R. Munnell, Surgery, Gynecology and Obstetrics, 94, 129, (1952).

2. C.A. Hufnagel, Bull Georgetown Univ. Med. Cent., 4, 128, (1951).

3. J.M. Campbell, J. Thorac. Cardiovasc. Surg., 19, 312, (1950).

4. J.B. Williams: U.S. Patent No. 19323, February 9, (1858).

5. E.A. Lefrak and A. Starr, Cardiac Valve Prostheses, (Appleton-Cent.-Crofts, New York, 1979), 3-32.

6. A. Carpentier, Medical Instumentation, 2, 98, (1977).

7. A. Carpentier and C. Dubost, in Biological Tissue in Heart Valve Replacement, edited by M.I. Ionescu, (Butterworth and Co., London, 1971), 515-541.

8. N. Zuhdi, et al., Ann. Thorac. Surg., 17, 479, (1974).

9. L.R. Sauvage, Med. Instrum., 2, 107, (1977).

10. E. Zerbini and L.B. Puig, in Biological Tissue in Heart Valve Replacement, edited by M.I. Ionescu, (Butterworth and Co., London, 1971), 255-298.

11. R.E. Clark, et al., Ann. Thorac. Surg., 26, 323, (1978).

12. A. Carpentier, in Biological Tissue in Heart Valve Replacement, edited by M.I. Ionescu, (Butterworth and Co., London, 1971), 49-82.

13. T.L. Spray and W.C. Roberts, Am. J. Cardiol., 40, 319, (1977).

14. N.D. Broom, J. Biomechanics, 10, 707, (1977).

15. L.E. Housman, et al., J. Thorac. Cardiovasc. Surg., 76, 212, (1978).

16. A. Carpentier, et al., J. Thorac. Cardiovasc. Surg., 68, 771, (1974).

17. F.J. Thomson and B.G. Barratt-Boyes, J. Thorac. Cardiovasc. Surg., 74, 317, (1977).

18. R.L. Reis, et al., J. Thorac. Cardiovasc. Surg., 62, 683, (1971).

19. W.D. Hancock, Med. Instum., 2, 102, (1977).

20. W.W. Angell, J.D. Angell, and J.C. Kosek, in Tissue Heart Valves, edited by M.I. Ionescu, (Butterworth and Co., London, 1979), 91-124.

21. J.T. Wright, in Tissue Heart Valves, edited by M.I. Ionescu, (Butterworth and Co., London, 1979), 31-37.

22. W.G. Rainer, et al., Med. Instrum., 2, 104, (1977).

23. N.D. Broom, J. Thorac. Cardiovasc. Surg., 76, 202, (1978).

24. W.G. Rainer, et al., Ann. Thorac. Surg., 28, 274, (1979).

25. R.E. Clark and W.M. Swanson, J. Thorac. Cardiovasc. Surg., 78, 277, (1979).

26. G.P. Steinmetz, Jr., et al., J. Thorac. Cardiovasc. Surg., 47, 186, (1964).

27. D.S. Luciano, A.J. Vander, and J.H. Sherman, Human Function and Structure, (McGraw-Hill, New York, 1978), 374-394.

28. R.E. Clark, et al., Surg. Forum, 26, 242, (1975).

29. A.P. Yoganathan, et al., Med. & Biol. Eng. & Comput., 17, 38, (1979).

30. K.B. Chandran, et al., Med. & Biol. Eng. & Comp., 21, 529, (1983).

31. W.M. Phillips, et al., Trans. Am. Soc. Artif. Intern. Organs, 26, 43, (1980).

32. A.P. Yoganathan, W.H. Corcoran, and E.C. Harrison, J. Biomechanics, 12, 135, (1979).

33. A.P. Yoganathan, Ph.D. Thesis, California Institute of Technology, Pasadena, 1978.

34. C.B. Wisman, et al., Trans. Am. Soc. Artif. Intern. Organs, 28, 164, (1982).

35. L.E. Drain, The Laser Doppler Technique, (John Wiley & Sons Ltd., New York, 1980), 1-38, 85-118, 168-170.

36. F. Durst, A. Melling, and J.H. Whitelaw, Principles and Practices of Laser-Doppler Anemometry, (Academic Press Inc., New York, 1976), 1-55, 108-124.

37. B.M. Watrasiewicz and M.J. Rudd, Laser Doppler Measurements, Butterworth and Co., London, 1976), 1-31, 37-47.

38. A.P. Yoganathan, W.H. Corcoran, and E.C. Harrison, J. Bioeng., 2, 369, (1978).

39. G.J. Tortora and N.P. Anagnostakos, Principles of Anatomy and Physiology, (Canfield Press, San Francisco, 1978), 443-461.

40. S. Gabbay, et al., Circulation, 60, 62, (1979).

41. R.M. Becker, et al., J. Thorac. Cardiovasc. Surg., 80, 613, (1980).

42. S. Gabbay, et al., J. Thorac. Cardiovasc. Surg., 76, 771, (1978).

43. A.P. Tandon, et al., Ann. Thorac. Surg., 26, 149, (1977).

44. M.I. Ionescu, et al., in Cardiac Bioprostheses, edited by L.H. Cohn and V. Gallucci, (Yorke Med. Books, New York, 1982), 42.

45. M.I. Ionescu, A.P. Tandon, and D.A. Mary, J. Thorac. Cardiovasc. Surg., 73, 31, (1977).

46. D.N. Ross, Circulation, 45, 1259, (1972).

47. S. Eskinazi, Principles of Fluid Mechanics, (Allyn and Bacon, Inc., Boston, 1968), 369-371, 404-408, 413-416.

48. S. Gabbay, et al., J. Thorac. Cardiovasc. Surg., In Press.

49. S. Gabbay, Verbal Communications, January, 1984.

50. M.C. Fishbein, et al., Am. J. Cardiol., 40, 331, (1977).

51. N.D. Broom and F.J. Thomson, Thorax, 34, 166, (1979).

52. N.D. Broom, J. Thorac. Cardiovasc. Surg., 75, 121, (1978).

53. V.J. Ferrans, et al., Am. J. Cardiol., 43, 721, (1980).

54. J.P. Marbarger, Jr. and R.E. Clark, Ann. Thorac. Surg., 34, 22, (1982).

55. J.J. Lamberti, et al., Ann. Thorac. Surg., 28, 28, (1979).

56. E.P. Mueller, Personal Communications, January, 1984.